อภินันทนาการ

สัญญาเลขที่ R2557C095

สำนักหอสมุด

รายงานวิจัยฉบับสมบูรณ์

แบบจำลองคณิตศาสตร์สำหรับโรคอหิวาและการศึกษาการควบคุมการแพร่ระบาด

ดร.ชัยรัตน์ มดนาค

ภาควิชาคณิตศาสตร์ คณะวิทยาศาสตร์

สำนักหอสมุด มหาวิทยาลัยนเรศวร
วันลงทะเบียน 15 มิ.ย. 2559
เลขทะเบียน 16986444
เลขเรียกหนังสือ
ว RA 644 .C3 ด4245 2558

กองทุนวิจัยมหาวิทยาลัยนเรศวร

บทคัดย่อ

งานวิจัยฉบับนี้ได้ศึกษาเกี่ยวกับ การสร้างแบบจำลองทางคณิตศาสตร์เพื่อศึกษาการแพร่ระบาดของโรคอหิวาตกโรค และการควบคุมการระบาดโดยใช้วัคซีน การบำบัดน้ำเสีย และการรักษาเบื้องต้นด้วยยาหรือกระบวนทางการแพทย์ ซึ่งผลการศึกษาถูกนำเสนอโดยใช้ผลเฉลยเชิงตัวเลขเพื่อการเปรียบเทียบ และการทดสอบความมีเสถียรภาพของจุดวิกฤติของการเกิดการระบาดได้ นำเสนอในรูปแบบของทฤษฎีด้วยเช่นเดียวกัน ทฤษฎีทางด้าน Optimal Control Theory ถูกใช้สำหรับการหาค่าความเหมาะสมของการรักษา

คำสำคัญ : โรคอหิวา การรักษาด้วยการฉีดวัคซีน การหาค่าเหมาะสม การควบคุมโรค

Abstract

The use of cholera vaccines has been increasingly recognized as an effective control measures in cholera endemic counties. In this paper, we present and analyze a cholera epidemiological model with control measures incorporated. Equilibrium analysis is conducted in the case with constant controls for both epidemic and endemic dynamics. Optimal control theory is applied to seek cost-effective solution of multiple time-dependent intervention strategies against cholera outbreaks.

Keyword: Cholera model, Disease control, Stability, Optimal control

Executive Summary

1. ความสำคัญและที่มาของปัญหาที่ทำการวิจัย

โรคอหิวาเป็นโรคร้ายแรง ผู้ติดเชื้อที่ปราศจากการรักษาอย่างถูกต้อง สามารถเสียชีวิตได้อย่างเฉียบพลัน การระบาดของโรคอหิวาเกิดได้หลายสาเหตุ อย่างเช่น การดื่มน้ำที่ปนเปื้อนเชื้อแบคทีเรียสายพันธ์ Vibrio Cholerae หรืออาหารดิบๆสุกๆซึ่งมีเชื้อแบคทีเรียสายพันธ์นี้ปนเปื้อน ส่วนการแพร่ระบาดของโรคจากคนสู่คนไม่ค่อยพบเห็นมากนัก

ไม่นานมานี้ เราจะเห็นว่ายังมีข่าวการแพร่ระบาดของโรคนี้ทั่วโลก และจะเห็นว่าจำนวนครั้งที่เกิดเพิ่มมากขึ้นทุกๆปี ครั้งล่าสุดในปี 2010-2011 ในประเทศ Haiti เป็นการกลับมาระบาดครั้งยิ่งใหญ่ของโรคนี้อีกครั้งในยุคสมัยใหม่นี้ และเป็นครั้งที่ร้ายแรงที่สุด โดยจากรายงานพบว่า มีผู้ติดเชื้อมากกว่า 530,000 ราย และเสียชีวิตมากกว่า 7,000 ราย [1] การระบาดของโรคครั้งสำคัญๆที่มีผู้เสียชีวิตเป็นจำนวนมากยังพบเห็นได้ในหลายประเทศ อาทิเช่น Sierra Leone ในปี 2012, Nigeria ในปี 2010, Vietnam ในปี 2009, Zimbabwe ในปี 2008 และประเทศอินเดียในปี 2007 สำหรับประเทศไทยยังพบผู้ติดเชื้อโรคอหิวาทุกปี โดยข้อมูลจากสำนักระบาดวิทยา กรมควบคุมโรค พบว่า ตั้งแต่วันที่ 1 มกราคม – 18 กันยายน 2555 ได้รับรายงานผู้ป่วยยืนยันอหิวาตกโรค จำนวน 29 ราย โดยมีรายงานจาก 10 จังหวัด ได้แก่ จังหวัดตาก 13 ราย ยะลา 5 ราย กรุงเทพ 4 ราย เชียงใหม่ ประจวบคีรีขันธ์ ตราด สุพรรณบุรี นครราชสีมา ภูเก็ต ระนอง จังหวัดละ 1 ราย [2]

มีการศึกษาโดยใช้แบบจำลองคณิตศาสตร์มากมายสำหรับโรคอหิวา เพื่อทำความเข้าใจเกี่ยวกับโรค พฤติกรรมของการแพร่ระบาดของโรค รวมทั้งการควบคุมการแพร่ระบาด ในปี 2009 Mukandavire [3] เสนอแบบจำลองทางคณิตศาสตร์ที่ไม่ซับซ้อนมากนัก ง่ายต่อการเข้าใจ และมีความซับซ้อนในการหาผลเฉลยทางตัวเลขน้อย ซึ่งเป็นแบบจำลองที่ผู้จัยมากมายนำไปต่อยอด โดยที่โมเดลคือ

$$\frac{dS}{dt} = \mu N - \beta_e S \frac{B}{k+B} - \beta_h SI - \mu S$$

$$\frac{dI}{dt} = \beta_e S \frac{B}{k+B} + \beta_h SI - (\gamma + \mu) I$$

$$\frac{dR}{dt} = \gamma I - \mu R$$

$$\frac{dB}{dt} = \varepsilon I - \delta B$$

โดยที่ S คือ กลุ่มสุ่มเสี่ยงของผู้ติดเชื่อ I คือ กลุ่มผู้ติดเชื้อ R คือ กลุ่มผู้ที่ได้รับการรักษาหายแล้ว และ B คือ กลุ่มประชากรของแบคทีเรีย โดยที่พารามิเตอร์อื่นๆคือค่าคงตัวต่างๆ

2. วัตถุประสงค์

เพื่อสร้างแบบจำลองทางคณิตศาสตร์ในการอธิบายการระบาดของโรคอหิวา และศึกษาการควบคุมการแพร่ระบาดโดยศึกษาแนวทางการป้องกันและรักษา รวมทั้งพิจารณาแนวทางที่เหมาะสมต่อการรักษาในสถานการณ์ต่างๆกันไป

3. ระเบียบวิธีวิจัย

3.1 ศึกษาแบบจำลองทางคณิตศาสตร์ต้นแบบที่นำเสนอโดย Mukandavire

3.2 ศึกษาแบบจำลองทางคณิตศาสตร์อื่นๆที่เกี่ยวข้องกับโรคอหิวาเพื่อเป็นประโยชน์ต่อการขยายโมเดล

3.3 สร้างแบบจำลองทางคณิตศาสตร์ขั้นสูงสำหรับโรคอหิวา

3.4 ตรวจสอบความถูกต้องของโมเดล

3.5 ศึกษาความเป็นไปได้ในการขยายแบบจำลองทางคณิตศาสตร์เพื่องานวิจัยในอนาคตและการประยุกต์ใช้

3.6 สรุปและเขียนงานวิจัย เพื่อตีพิมพ์ในวารสารและรายงานไปยังเจ้าของทุนวิจัย

4. แผนการดำเนินงานวิจัย

กิจกรรม	เดือนที่											
	1	2	3	4	5	6	7	8	9	10	11	12
1. ศึกษาแบบจำลองทางคณิตศาสตร์ต้นแบบที่นำเสนอโดย Mukandavire												
2. ศึกษาแบบจำลองทางคณิตศาสตร์อื่นๆที่เกี่ยวข้องกับโรคอหิวาเพื่อเป็นประโยชน์ต่อการขยายโมเดล												

3. สร้างแบบจำลองทางคณิตศาสตร์ขั้นสูงสำหรับโรคอหิวา และตรวจสอบความถูกต้อง												
4. ศึกษาความเป็นไปได้ในการขยายแบบจำลองทางคณิตศาสตร์เพื่องานวิจัยในอนาคตและการประยุกต์ใช้												
5. สรุปและเขียนงานวิจัย เพื่อตีพิมพ์ในวารสารและรายงานไปยังเจ้าของทุนวิจัย												

5. ตัวชี้วัดเพื่อการเมินผลสำเร็จของโครงการ

5.1 ตีพิมพ์ในวารสารระดับนานาชาติที่มีค่า Impact Factor จำนวน 1 เรื่อง

เนื้อหางานวิจัย

(ดูรายระเอียดทั้งหมดดังเอกสารแนบหน้าถัดไป)

LIST OF CONTENTS

1 Introduction 1

2 Basic Concepts 5
2.1 A Mathematical model with immigrants 10
2.1.1 Mathematical model 10
2.2 Optimal control study. 22
2.2.1 The Basic Problem and Necessary Conditions 22
2.2.2 Pontryagin's Maximum Principle 23

3 Methodology and Results 29
3.1 The disease-free equilibrium. 29
3.2 Epidemic Dynamic. 32
3.3 Endemic dynamics. 37
3.4 Optimal Control Study. 47

4 Conclusion 56

References 59

Chapter 1
Introduction

INFECTIOUS AGENT

Cholera is an acute bacterial, intestinal infection caused by toxigenic Vibrio cholerae O-group 1 or O-group 139. Many other serogroups of V. cholerae, with or without the cholera toxin gene (including the nontoxigenic strains of the O1 and O139 serogroups), can cause a choleralike illness. Only toxigenic strains of serogroups O1 and O139 have caused widespread epidemics and are reportable to the World Health Organization (WHO) as "cholera." V. cholerae O1 has 2 biotypes, classical and El Tor, and each biotype has 2 distinct serotypes, Inaba and Ogawa. The symptoms of infection are indistinguishable, although more people infected with the El Tor biotype remain asymptomatic or have only a mild illness. Globally, most cases of cholera are caused by O1 El Tor organisms. In recent years, an El Tor variant that has characteristics of both classical and El Tor biotypes and may be more virulent than older El Tor strains has emerged in Asia and spread to Africa and the Caribbean.

TRANSMISSION

Toxigenic V. cholerae O1 and O139 are free-living bacterial organisms found in fresh and brackish water, often in association with copepods or other zooplankton, shellfish, and aquatic plants. Cholera infections are most commonly acquired from drinking water in which V. cholerae is found naturally or into which it has been introduced from the feces of an infected person. Other common vehicles include contaminated fish and shellfish. Other foods, including produce, are less commonly implicated. Direct transmission from person to person, even to health care workers during epidemics, has been reported but is not frequent.

EPIDEMIOLOGY

Since 1961, the seventh pandemic of cholera, caused by V. cholerae serogroup O1, biotype El Tor, has spread from Indonesia through most of Asia into Eastern Europe and Africa, and from North Africa to the Iberian Peninsula. In 1991, an extensive epidemic began in Peru and spread to neighboring countries in the Western Hemisphere. Although few cases of cholera occur in South or Central America, V. cholerae O1 remains endemic

in much of Africa and South and Southeast Asia. V. cholerae O139 spread rapidly through Asia in the early 1990s but has since remained localized to a few areas in Asia. In October 2010, a cholera epidemic began in Haiti, just 10 months after a devastating earthquake destroyed the Haitian capital of Port-au-Prince and surrounding areas. During the first year of the outbreak, 480,577 cases and 6,673 deaths were reported. In the early weeks of the outbreak, the case-fatality ratio (CFR) was 3% to 4%, but declined after improvements in access to care; the CFR for Haiti was 0.84% in 2011 compared with 2.22% in 2010. In November 2010, cholera was first reported in the neighboring Dominican Republic, with 21,432 cases and 363 deaths reported by December 2011. Cholera is likely to persist in Haiti at endemic levels because of the lack of safe water and sanitation infrastructure, with the potential for localized outbreaks and seasonal spikes in cases associated with heavy rainfall. Sporadic cases associated with travel to or from Hispaniola may continue to occur.

Most cholera cases go unreported. In 2011, 58 countries reported 589,854 cholera cases and 7,816 cholera deaths (CFR, 1.3%) to WHO. The 2011 global cholera case numbers represent an 85% increase from 2010. Since 2010, there has been a geographic shift in cholera incidence from Africa to the Americas as a result of the Haiti outbreak, which accounted for 55% and >57% of all cholera cases reported in 2010 and 2011, respectively. From 2001 through 2009, >90% of cholera cases were reported from Africa, including 98% of cases and 99% of deaths during 2009. Cholera has the potential to emerge in dramatic epidemics, as was seen with the massive outbreaks that affected Zimbabwe in 2008 and 2009, with close to 100,000 cases and >4,000 deaths reported, and with the current epidemic in Haiti, with >500,000 cases and 7,000 deaths reported during 2010 and 2011.

From 1999 through 2011, 86 confirmed cases of cholera in the United States were acquired abroad; of these, 40 were associated with the epidemic in Hispaniola in 2010 and 2011. Travelers who follow the usual tourist itineraries and who observe safe food and water recommendations and hygiene precautions while in countries reporting cholera have virtually no risk. The risk is increased for those who drink untreated water, do not follow proper hygiene recommendations, or eat raw or poorly cooked food, especially seafood, in endemic or outbreak settings. Although rare, 2 cases of cholera have been reported among volunteer US health care workers caring for cholera patients during the peak period of the epidemic in Haiti; recent evidence shows that lack of handwashing supplies at treatment centers may lead to diarrheal illness and other health care–associated infections.

Two reports of cholera have been associated with food served on international flights, most recently in 1992, during the Latin American epidemic, on a flight from Argentina to Los Angeles. CDC consequently advised

the International Air Transport Association that prepackaged oral rehydration salts should be carried on international flights and that certain food items (such as shrimp) prepared in cities with cholera epidemics should not be served. Airline flights have not been implicated in any subsequent cases of cholera.

CLINICAL PRESENTATION

Cholera infection is most often asymptomatic or results in a mild gastroenteritis. Severe cholera is characterized by acute, profuse watery diarrhea, described as "rice-water stools," and often nausea and vomiting, leading to volume depletion. Signs and symptoms include tachycardia, loss of skin turgor, dry mucous membranes, hypotension, and thirst. Additional symptoms, including muscle cramps, are secondary to the resulting electrolyte imbalances. If untreated, rapid loss of body fluids can lead to severe dehydration, hypovolemic shock, and death within hours. With adequate and timely rehydration, CFRs are <1%. Most people infected with toxigenic V. choleraewill be asymptomatic or have mild diarrhea.

DIAGNOSIS

Cholera is confirmed through culture of a stool specimen or rectal swab. Cary-Blair medium can be used for transport, and selective media such as taurocholate-tellurite-gelatin agar and thiosulfate-citrate-bile salts (TCBS) agar may be used for isolation and identification. Reagents for serogrouping V. cholerae isolates are available in all state health department laboratories. Commercially available rapid test kits do not yield an isolate for antimicrobial susceptibility testing and subtyping and should not be used for routine diagnosis. All isolates obtained in the United States should be sent to CDC via state health department laboratories for cholera toxin testing and subtyping. Cholera is a nationally reportable disease.

TREATMENT

Rehydration is the cornerstone of cholera treatment. Oral rehydration solution and, when necessary, intravenous fluids and electrolytes, if administered in a timely manner and in adequate volumes, will reduce CFRs to well under 1%. Antibiotics reduce fluid requirements and duration of illness. Antimicrobial therapy is indicated for moderate and severe cases, which can be treated with doxycycline, tetracycline, erythromycin, azithromycin, or ciprofloxacin. Whenever possible, antimicrobial susceptibility testing should inform treatment choices. Zinc supplementation reduces the severity and duration of cholera and other diarrheal diseases in children in resource-limited areas.

PREVENTION

Safe food and water precautions and frequent handwashing are critical in preventing cholera. Chemoprophylaxis is not indicated.

No cholera vaccine is currently licensed in the United States. Two oral vaccines are prequalified by WHO and are available outside the United States: Dukoral (Crucell, the Netherlands) and Shanchol (Shantha Biotechnics, India). CDC does not recommend cholera vaccines for US travelers because of the low risk of cholera and the unavailability of vaccines in the United States. No country or territory requires vaccination against cholera as a condition for entry.

Further information on Dukoral can be obtained form Crucell(www.crucell.com). Information on Shanchol Further information on Dukoral can be obtained from Crucell (www.crucell.com). Information on Shanchol can be obtained from Shantha Biotechnics (www.shanthabiotech.com).

Chapter 2
Basic Concepts

In this chapter, we will present some interesting mathematical models that describes the cholera dynamics. We will start with an early compartmental model that includes only a few state equations. The more complicated Cholera model then will be studied. Finally, we will present and carefully study a model proposed by Jin Wang and Chairat Modnak. Then, we will extend the model and explore strategies to control an cholera outbreak.

The Basic Model

Kermack and Mckendrick proposed the following model in 1927.

Figure 2.1: The SIR Model

$$\begin{aligned} \frac{dS}{dt} &= -\beta SI \\ \frac{dI}{dt} &= \beta SI - \gamma I \\ \frac{dR}{dt} &= \gamma I \end{aligned}$$

where

- S is the susceptible state.
- I is the infected state.
- R is the recovered state.
- β is the contact rate.
- γ is the recovery rate

The Basic SIS Model

Some diseases confer immunity so recovered individuals gain immunity against the disease. This type of disease can be modelled by SIS type where S and I stand for susceptibles and infectives respectively. Here we proposed a simple model of SIS type that includes births in the susceptible class and deaths from two classes with the rate proportional to each class. Their model is

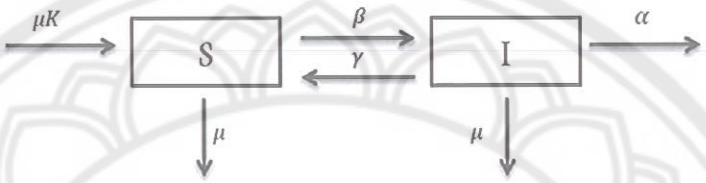

Figure 2.2: The SIS Model

$$\frac{dS}{dt} = -\beta SI + \mu(K - S) + \gamma I$$
$$\frac{dI}{dt} = \beta SI - (\alpha + \mu + \gamma)I$$

where

- S is the susceptible state.
- I is the infected state.
- R is the recovered state.
- K is the recovered state.
- μ is the natural death rate.
- β is the contact rate.
- γ is the recovery rate
- α is the disease-relate death rate form infective class.

The Basic SIR Model

This SIR model was proposed by H.E. Soper. He assumed that the

Figure 2.3: The Basic SIR Model

total population is constant and that the birth rate and death rate are constant. His model is

$$\begin{aligned}\frac{dS}{dt} &= -\beta SI + \mu K \\ \frac{dI}{dt} &= \beta SI - \gamma I \\ \frac{dR}{dt} &= \gamma I - \mu K\end{aligned}$$

where

- S is the susceptible state.
- I is the infected state.
- R is the recovered state.
- K is the birth rate.
- μ is the natural death rate.
- β is the contact rate.
- γ is the recovery rate

The SVIS Model

Let us now consider an SIS type disease when a vaccination program is in effect and there is a constant flow of incoming immigrants. The model is

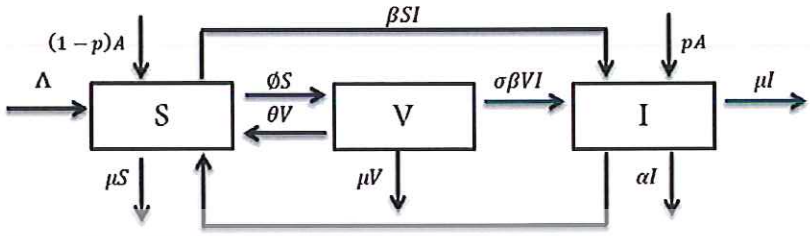

Figure 2.4: The SVIS Model

$$\begin{aligned}
\frac{dS}{dt} &= (1-p)A + \Lambda - \beta SI - (\mu+\phi)S + \gamma I + \theta V \\
\frac{dI}{dt} &= pA + \beta SI + \sigma\beta VI - (\mu+\gamma+\alpha)I \\
\frac{dV}{dt} &= \phi S - \sigma\beta VI - (\mu+\theta)V
\end{aligned}$$

where

- $S(t)$ is the Number of susceptible at time t.
- $I(t)$ is the Number of infected at time t.
- $R(t)$ is the Number of recovered at time t.
- $V(T)$ is the Number of vaccinated individuals at time t.
- A is the Number of immigrants.
- p is the Portion of infectives among immigrants.
- Λ is the birth rate
- μ is the natural death rate.
- β is the contact rate.
- γ is the recovery rate.
- ϕ is the vaccination rate.
- σ is the factor by which the vaccine reduces infection.
- θ is the rate at which the vaccine wears off.
- α is the disease related death rate.
- R_0 is the basic reproductive number.
- R_ϕ is the vaccination reproductive number.

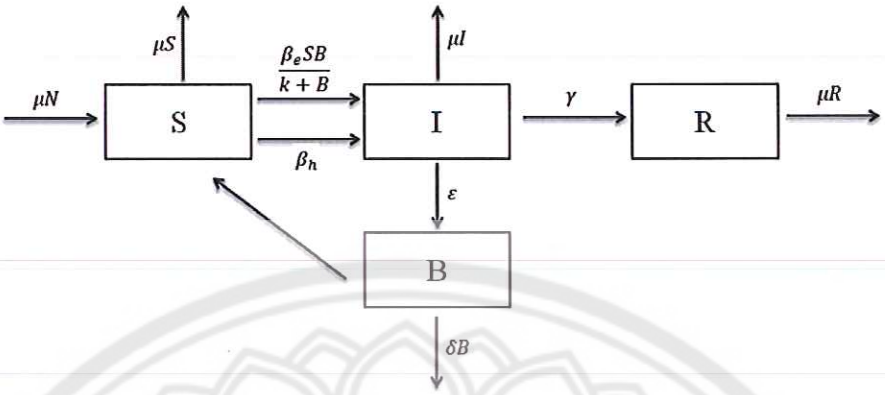

Figure 2.5: The modified SIR Model

The modified SIR model

The modified SIR model propose by Jin Wang and Chairat Modnak.

$$\begin{aligned}
\frac{dS}{dt} &= \mu N - \frac{\beta_e SB}{k+B} - \beta_h SI - \mu S \\
\frac{dI}{dt} &= \frac{\beta_e SB}{k+B} + \beta_h SI - (\gamma + \mu)I \\
\frac{dB}{dt} &= \varepsilon I - \delta B \\
\frac{dR}{dt} &= \gamma I - \mu R
\end{aligned}$$

where

- S is the susceptible state.
- I is the infected state.
- R is the recovered human populatin sets.
- B is the concentration of the vibrios is the envi individualsat time t.
- N is the total population.
- k is the pathogen concentration that yield 50% chance of cholera infection.
- μ is the natural birth and death rate.
- γ is the recovery rate form cholera.
- δ is the death rate of vibrios.
- ε is the rate of human contribution to the environmental vibrios.
- β_e is the rate of ingesting vibrios form the contaminated environment.
- β_h is the rate of through human-to-human.

2.1 A Mathematical model with immigrants

2.1.1 Mathematical model

We recall Jin Wang and Chairat Modnak model that is

$$\begin{aligned}
\frac{dS}{dt} &= \mu N - \frac{\beta_e SB}{k+B} - \beta_h SI - \mu S \\
\frac{dI}{dt} &= \frac{\beta_e SB}{k+B} + \beta_h SI - (\gamma + \mu)I \\
\frac{dB}{dt} &= \varepsilon I - \delta B \\
\frac{dR}{dt} &= \gamma I - \mu R
\end{aligned}$$

where

- S is the susceptible state.
- I is the infected state.
- R is the recovered human populatin sets.
- B is the concentration of the vibrios is the envi individualsat time t.
- N is the total population.
- k is the pathogen concentration that yield 50% chance of cholera infection.
- μ is the natural birth and death rate.
- γ is the recovery rate form cholera.
- δ is the death rate of vibrios.
- ε is the rate of human contribution to the environmental vibrios.
- β_e is the rate of ingesting vibrios form the contaminated environment.
- β_h is the rate of through human-to-human.

We will carry out the numerical simulation. First, we list the values for the various transmission rates in the state equation in Table 1. Particularly, we take the values of μ, β_e and β_h from Zimbabwean cholera data, their values are thus specific to Zimbabwe and may be different for other cholera endemic places. We also set the initial infection number $I(0) = 1000$ and the entire period of time $T = 100$ days.

Parameter	Symbol	Value
Total population	N	10,0000
Natural human birth and death rate	μ	$(43.5yr)^{-1}$
Concentration of V.*cholera* in environment	κ	10^6 cells/ml
Rate of recovery from cholera	γ	$(5day)^{-1}$
Rate of human contribution to V. *cholerae*	ξ	10 cells/ml-day
Death rate of vibrios in the environment	δ	$(30day)^{-1}$
Ingestion rate from the environment	β_e	0.075/day
Ingestion rate through human-human interaction	β_h	0.00011/day

Table 2.1: Cholera model parameters and values [9].

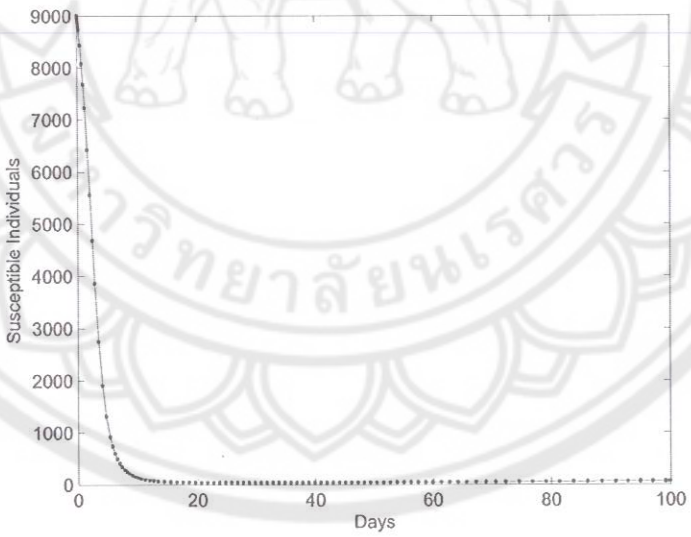

Figure 2.6: Susceptible Individuals

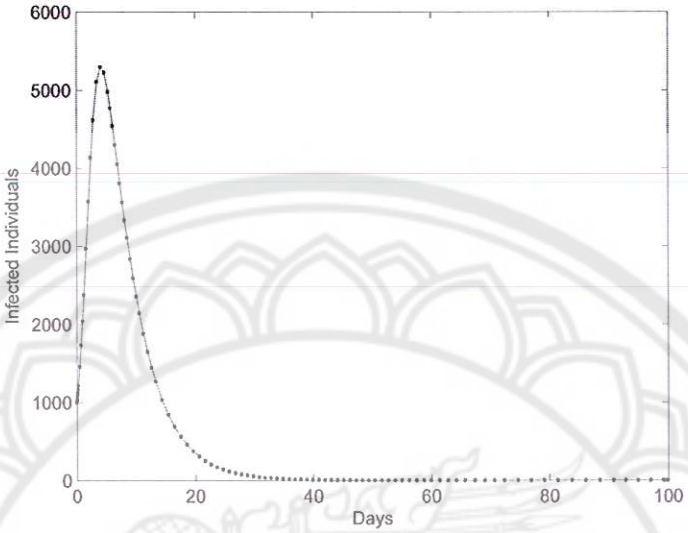

Figure 2.7: Infected Individuals

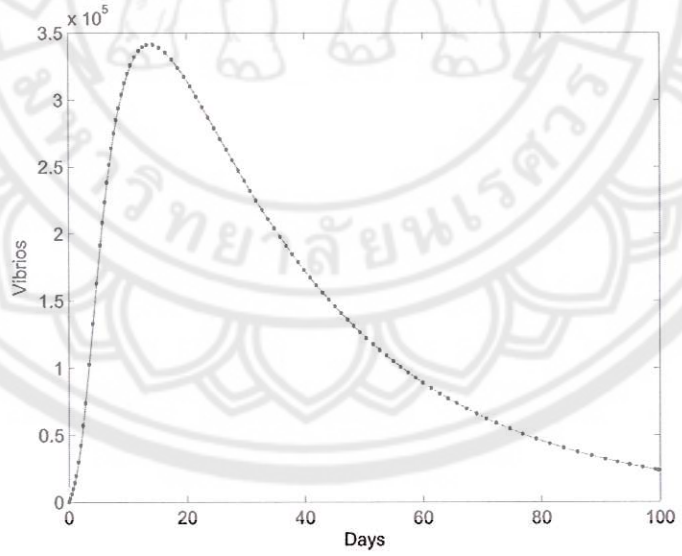

Figure 2.8: Vibrios

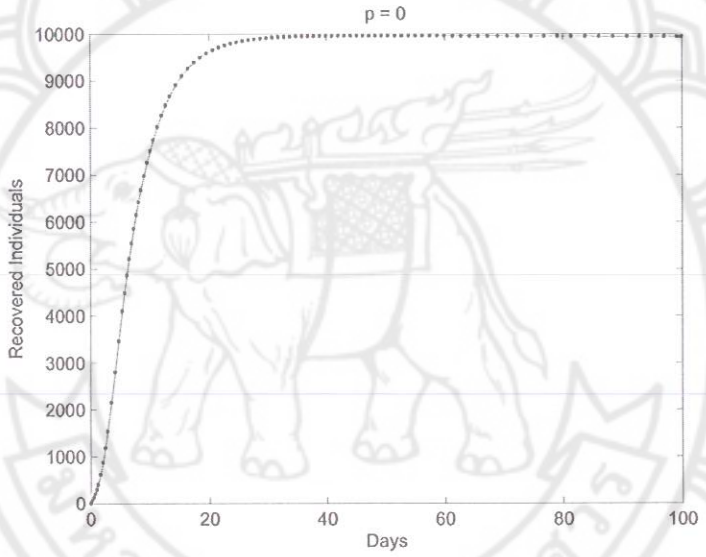

Figure 2.9: Recovered Individuals

Now we modify this model by adding immigrants to the susceptible state, S(t), and there is a constant incoming flow of immigrant where some portion of immigrants,p,is infective.
The system of differential equations of the model becomes

$$\begin{aligned}
\frac{dS}{dt} &= \mu(1-p)A + \mu N - \frac{\beta_e SB}{k+B} - \beta_h SI - \mu S \\
\frac{dI}{dt} &= \mu(pA) + \frac{\beta_e SB}{k+B} + \beta_h SI - (\gamma + \mu)I \\
\frac{dB}{dt} &= \varepsilon I - \delta B \\
\frac{dR}{dt} &= \gamma I - \mu R
\end{aligned}$$

where

- S is the susceptible state.
- I is the infected state.
- R is the recovered human populatin sets.
- B is the concentration of the vibrios in the environment individuals at time t.
- N is the total population.
- A is the number of immigrants.
- p is the portion of infectives among immigrants.
- k is the pathogen concentration that yield 50% chance of cholera infection.
- μ is the natural birth and death rate.
- γ is the recovery rate form cholera.
- δ is the death rate of vibrios.
- ε is the rate of human contribution to the environmental vibrios.
- β_e is the rate of ingesting vibrios form the contaminated environment.
- β_h is the rate of through human-to-human.

Next we will conduct numerical simulations to show what happends to susceptible, infected, vibrios and recovered states for some values of p.

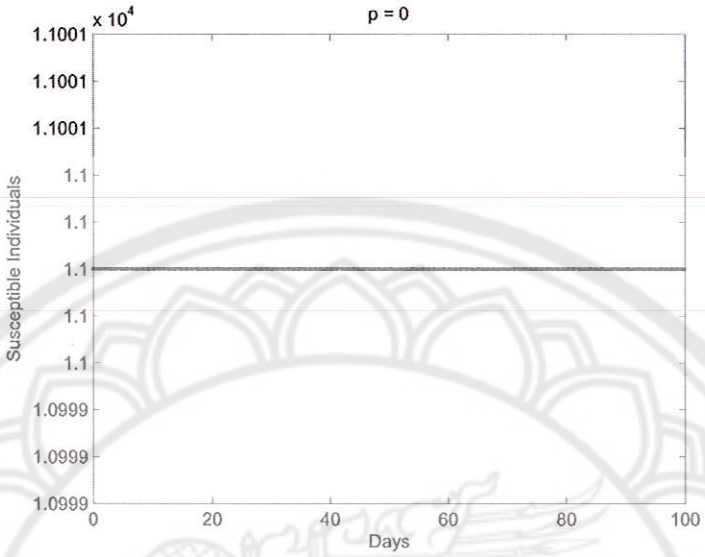

Figure 2.10: Susceptible Individuals

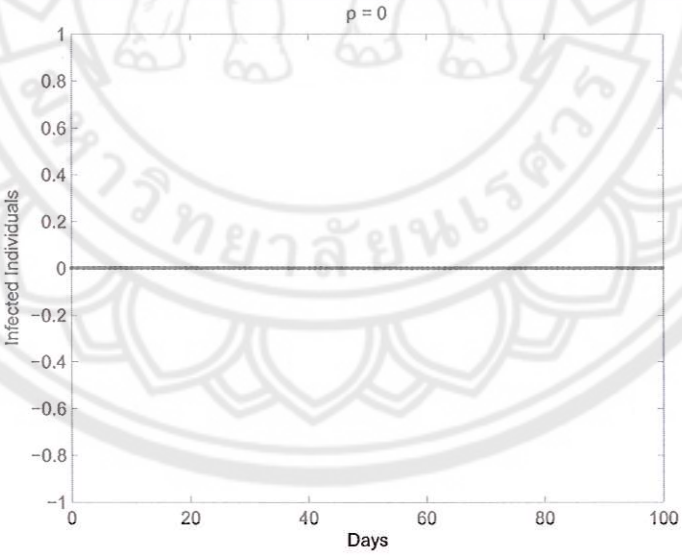

Figure 2.11: Infected Individuals

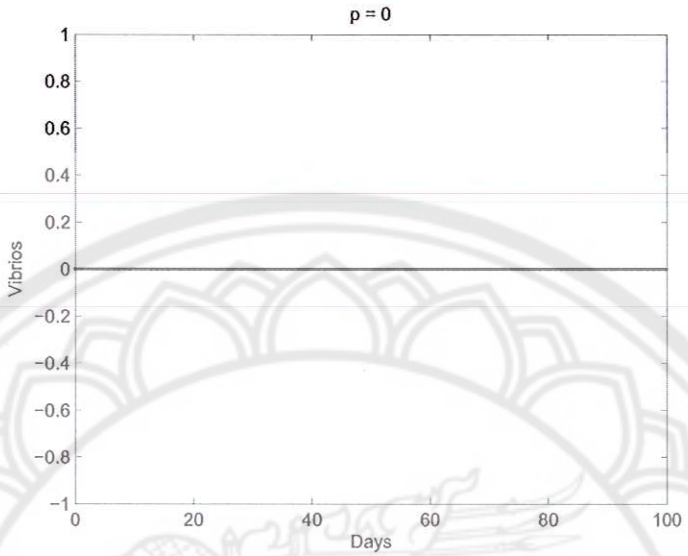

Figure 2.12: Vibrios

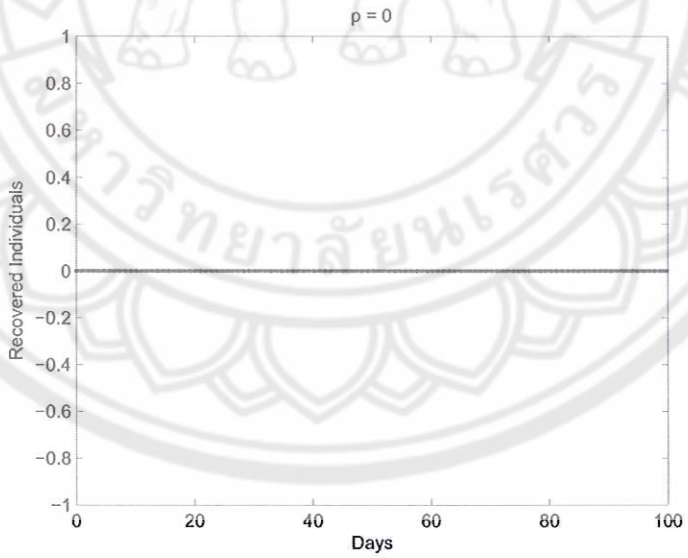

Figure 2.13: Recovered Individuals

The results show that there is no infection when $p = 0$.Therefore there is no spread out of vibrios population. Next we use $p = 0.5$ and the results are showns as follow.

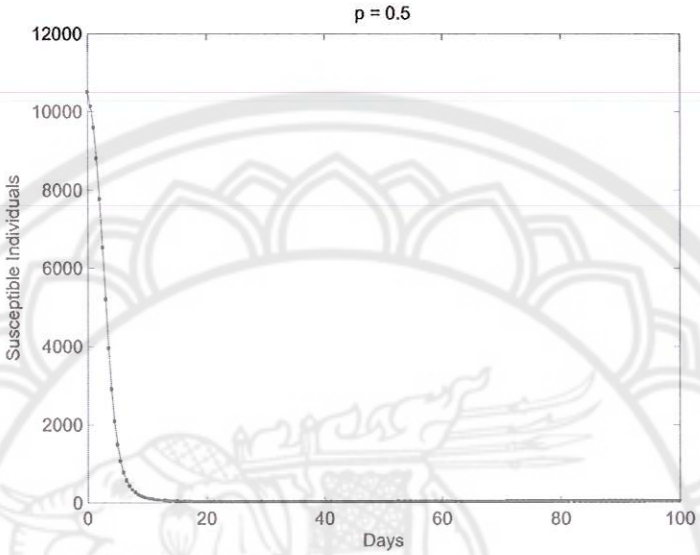

Figure 2.14: Susceptible Individuals

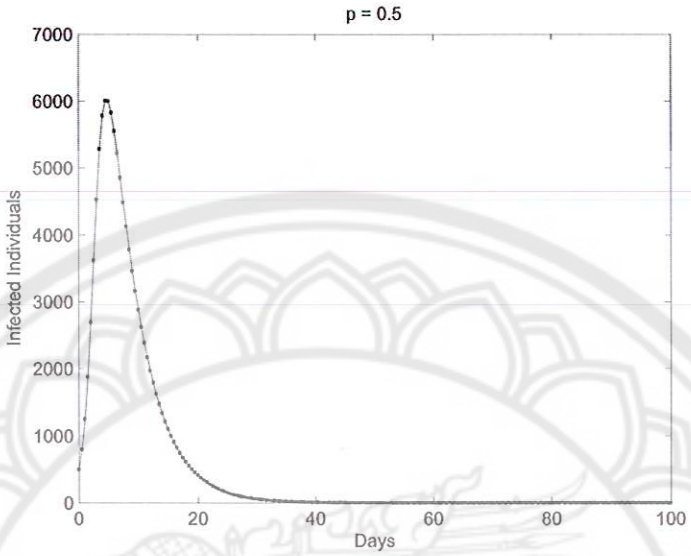

Figure 2.15: Infected Individuals

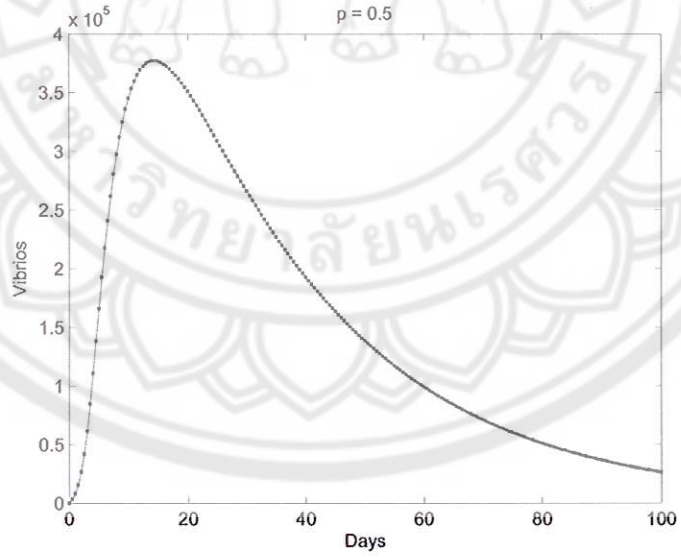

Figure 2.16: Vibrios

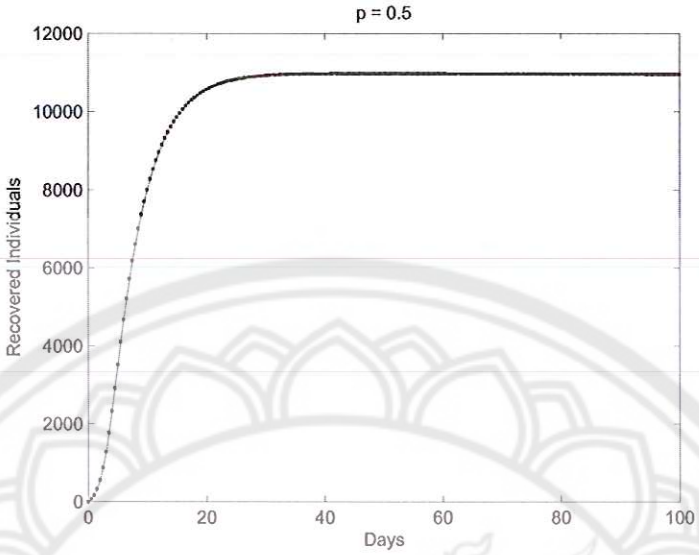

Figure 2.17: Recovered Individuals

Since p represents a partial of immigration rate, clearly when $p = 0.5$, the new population is divided into two classes equally. Next we will show that when all new populations are infected, the number of infections is higher than that of $p = 0.5$.

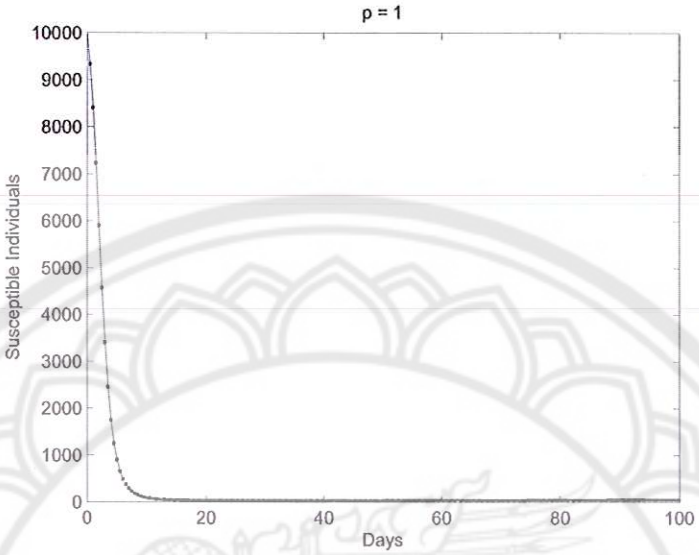

Figure 2.18: Susceptible Individuals

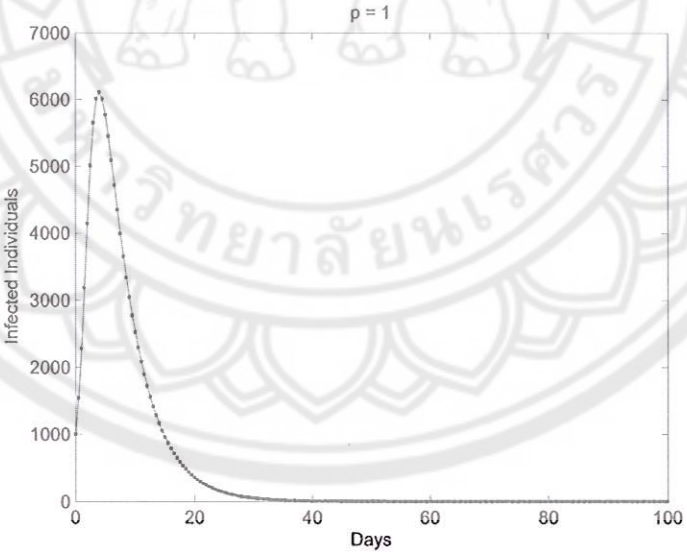

Figure 2.19: Infected Individuals

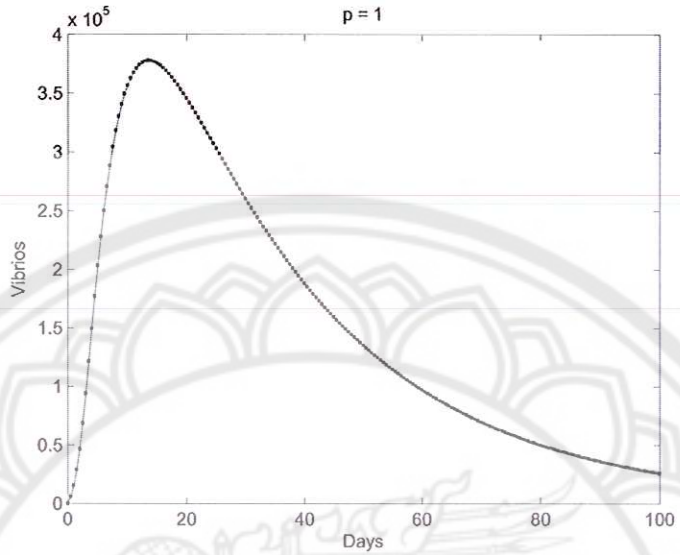

Figure 2.20: Vibrios

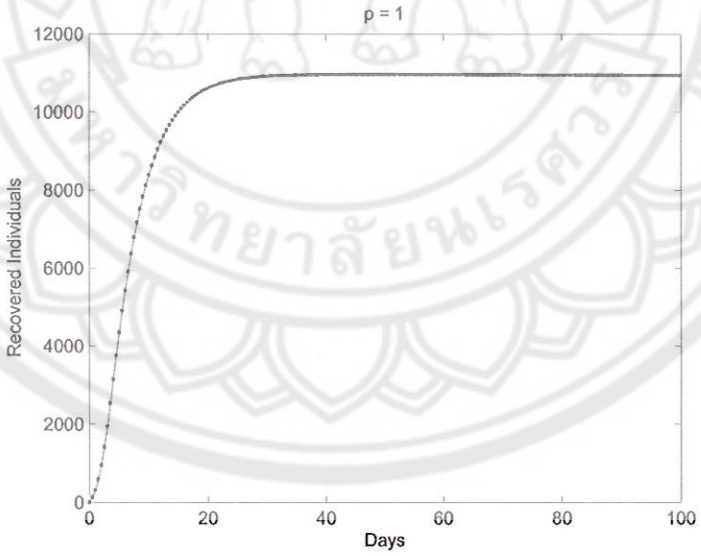

Figure 2.21: Recovered Individuals

2.2 Optimal control study.

2.2.1 The Basic Problem and Necessary Conditions

In our basic optimal control problem for ordinary differential equations, we use u(t) for the control and x(t) for the state. The state variable satisfies a differential equation which depends on the control variable:

$$x'(t) = g(t, x(t), u(t)).$$

As the control function is changed, the solution to the differential equation will change. Thus we can view the control-to-state relationship as a map $u(t) \mapsto x = x(u)$ (of course, x is really a function of the independent variable t; we write x(u) simply to remind us of the dependence on u). Our basic optimal control problem consists of finding a piecewise continuous control $u(t)$ and the associated state variable $x(t)$ to maximize the given objective functional, i.e.,

$$\max_u \int_{t_0}^{t_1} f(t, x(t), u(t))dt.$$

subject to $x'(t) = g(t, x(t), u(t)), \quad x(t_0) = x_0 \, and \, x(t_1)$ free.

Such a maximizing control is called an optimal control. By $x(t_1)$ free, it is meant that the value of $x(t_1)$ is unrestricted. For our purposes, f and g will always be continuously differentiable functions in all three arguments. Thus, as the control(s) will always be piecewise continuous, the associated states will always be piecewise differentiable.

The principle technique for such an optimal control problem is to solve a set of "necessary conditions" that an optimal control and corresponding state must satisfy. It is important to understand the logical difference between necessary conditions and sufficient conditions of solution sets.

Necessary Conditions : If $u^*(t), x^*(t)$ are optimal, then the following conditions hold ...

Sufficient Conditions : If $u^*(t), x^*(t)$ satisfy the following conditions ..., then $u^*(t), x^*(t)$ are optimal.

We will discuss sufficient conditions in the next chapter. For now, let us derive the necessary conditions. Express our objective functional in terms of the control:

$$J(u) = \int_{t_0}^{t_1} f(t, x(t), u(t))dt,$$

where $x = x(u)$ is the corresponding state.

The necessary conditions that we derive were developed by Pontryagin and his co-workers in Moscow in the 1950's. Pontryagin introduced the idea of "adjoint" functions to append the differential equation to the objective functional. Adjoint function have a similar purpose as Lagrange multipliers in multivariate calculus, which append constraints to the function of several variable to be maximized or minimized. Thus, we begin by finding appropriate conditions that the adjoint function should satisfy. Then, by differentiating the map from the control to the objective functional, we will derive a characterization of the optimal control in terms of the optimal state and corresponding adjoint. So do not feel as if we are "pulling a rabbit out of the hat" when we define the adjoint equation.

2.2.2 Pontryagin's Maximum Principle

These conclusions can be extended to a version of Pontryagin's Maximum Principle.

Theorem 2.1. *If $u^*(t)$ and $x^*(t)$ are optimal for problem (2.2.1), then there exists a piecewise differentiable adjoint variable $\lambda(t)$ such that*

$$H(t, x^*(t), u(t), \lambda(t)) \leq H(t, x^*(t), u^*(t), \lambda(t))$$

for all control u at each time t, where the Hamiltonian H is

$$H = f(t, x(t), u(t)) + \lambda(t)g(t, x(t), u(t)),$$

and

$$\lambda'(t) = -\frac{\partial H(t, x^*(t), u^*(t), \lambda(t))}{\partial x} \lambda(t_1) = 0$$

Theorem 2.2. *Suppose that $f(t, x, u)$ and $g(t, x, u)$ are both continuously differentiable functions in thier three arguments and concave in u. Suppose u^* is an optimal control for problem (2.2.1), with associated state x^*, and λ a piecewise differentiable function with $\lambda \geq 0$ for all t. Suppose for all $t_0 \leq t \leq t_1$*

$$0 = H_u(t, x^*(t), u^*(t), \lambda(t)).$$

Then for all controls u and each $t_0 \leq t \leq t_1$, we have

$$H(t, x^*(t), u(t), \lambda(t)) \leq H(t, x^*(t), u^*(t), \lambda(t))$$

Now we turn to the more general model with time-dependent control v(t). We consider the system on a time interval [0,T]. The function v(t) is assumed to be at least Lebesgue measurable on [0,T]. The control set is defined as

$$\Omega = \{v(t)|0 \leq v(t) \leq v_{max}\}$$

where v_{max} denotes the upper bounds for the effort of vaccination. The bound reflects practical limitation on the maximum rate of control in given time period.

The presence of time-dependent controls makes the analysis of our system difficult. In fact, the disease dynamics now depend on the evolution of control. In what follows we perform an optimal control study on this problem. We aim to minimize the total number of infections and the costs of control over the time interval $[0, T]$; i.e.,

$$\min_{(v,a)\in\Omega} \int_0^T [I(t) + c_{21}v(t)S(t) + c_{22}v(t)^2]dt \tag{2.1}$$

Here, the parameters c_{21} and c_{22} with appropriate units, define the appropriate costs associated with these controls. Quadratic terms are introduced to indicate nonlinear costs potentially arising at high intervention level. The minimization process is subject to the differential equation of our system, which are now referred to as the state equations. Correspondingly, the unknows S,I and B are now called the state variable, in contrast to the control variable v. Our goal is to determine the optimal control $v^*(t)$, so as to minimize the objective functional in (2.1).

We first establish the following theorem on the existence of optimal control.

Theorem 2.3. *There exists $v^*(t) \in \Omega$ such that the objective functional in (2.1) is minimized.*

Proof. Note that the control set Ω is closed and convex, and the integrand of the objective functional in (2.1) is convex. Hence, based on the standard optimal control theorems in [6] the conditions for the existence of the optimal control are satisfied, as our model is linear in the control variables. Indeed, the optimal control is also unique for small T due to the Lipschitz structure of the state equations and the boundedness of the state variables[6, 7].

We will follow the method described in [4],[8] to seek the optimal control solution. This method is based on Pontryagin's Maximum Principle [10] which introduces the adjoint functions and represents an optimal control in terms of the state and adjoint functions. Essentially, this approach transfers the problem of minimizing the objective functional (under the constraint of the state equations) into minimizing the Hamiltonian with respect

ว RA 644 .C3 ธ4245 2558
i 6986444
สำนักหอสมุด
15 มี.ย. 2559

to the controls.

$$\frac{dS}{dt} = \mu(1-p)A + \mu N - \frac{\beta_e SB}{k+B} - \beta_h SI - \mu S - v(t)S$$
$$\frac{dI}{dt} = \mu(pA) + \frac{\beta_e SB}{k+B} + \beta_h SI - (\gamma+\mu)I$$
$$\frac{dB}{dt} = \varepsilon I - \delta B$$
$$\frac{dR}{dt} = \gamma I - \mu R$$

Let us first define the adjoint functions λ_S, λ_I and λ_B associated with the state equations for S,I amd B, respectively. We then form the Hamiltonian, H, by corresponding state equation, and adding each of these products to the integrand of the objective functional. As a result, we obtain

$$\begin{aligned} H = I(t) &+ c_{21}v(t)S(t) + c_{22}v(t)^2 \\ &+ \lambda_S\left[\mu(1-p)A + \mu N - \frac{\beta_e SB}{k+B} - \beta_h SI - \mu S - v(t)\right] \\ &+ \lambda_I\left[\mu(pA) + \frac{\beta_e SB}{k+B} + \beta_h SI - (\gamma+\mu)I\right] \\ &+ \lambda_B\left[\varepsilon I - \delta B\right] \end{aligned}$$

To achieve the optimal control, the adjoint functions must satisfy

$$\begin{aligned} \frac{d\lambda_S}{dt} = -\frac{\partial H}{\partial S} &= -c_{21}v(t) + \lambda_S\left[\frac{\beta_e B}{k+B} + \beta_h I + \mu + v(t)\right] \\ &\quad - \lambda_I\left[\frac{\beta_e B}{k+B} + \beta_h I\right] \\ \frac{d\lambda_I}{dt} = -\frac{\partial H}{\partial I} &= -1 + \lambda_S\beta_h S - \lambda_I[\beta_h S - (\gamma+\mu)] - \lambda_B\varepsilon \\ \frac{d\lambda_B}{dt} = -\frac{\partial H}{\partial B} &= -\lambda_I\frac{\beta_e kS}{(k+B)^2} + \lambda_S\frac{\beta_e kS}{(k+B)^2} + \lambda_B\delta \end{aligned}$$

with transversality conditions (or final time conditions):

$$\lambda_S(T) = 0, \qquad \lambda_I(T) = 0, \qquad \lambda_B(T) = 0$$

The characterization of the optimal control $v^*(t)$ based on the condition

$$\frac{\partial H}{\partial v} = 0$$

respectively, subject to the constraint $0 \le v \le v_{max}$.Specifically, we have

$$v^*(t) = max[0, min(\tilde{v}(t), v_{max})]$$

where

$$\tilde{v}(t) = [(\lambda_S - c_{21})S(t)]/(2c_{22})$$

The following graphs show that with vaccination in the model, the number of infections are reduced to about 1000 from 6000. This study shows

that in order to control an outbreak, vaccination plan should be deployed in the early of outbreak.

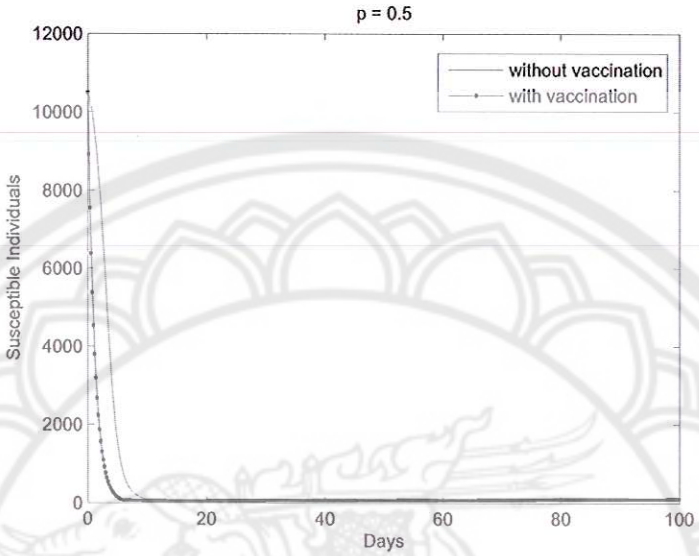

Figure 2.22: Susceptible individuals

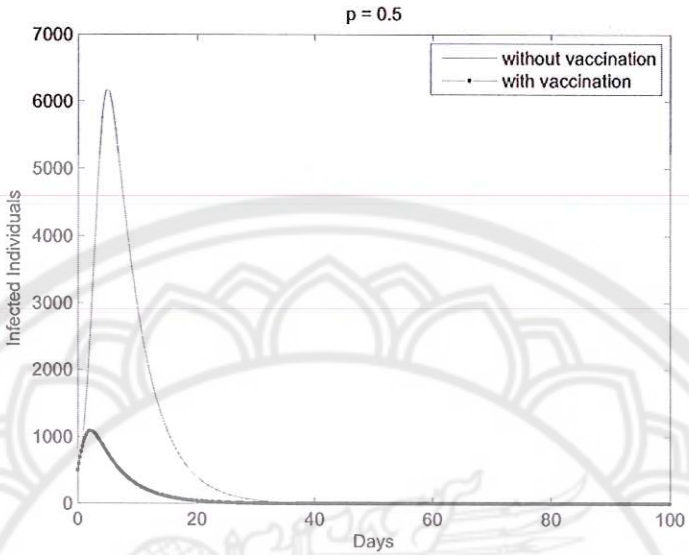

Figure 2.23: Infected individuals

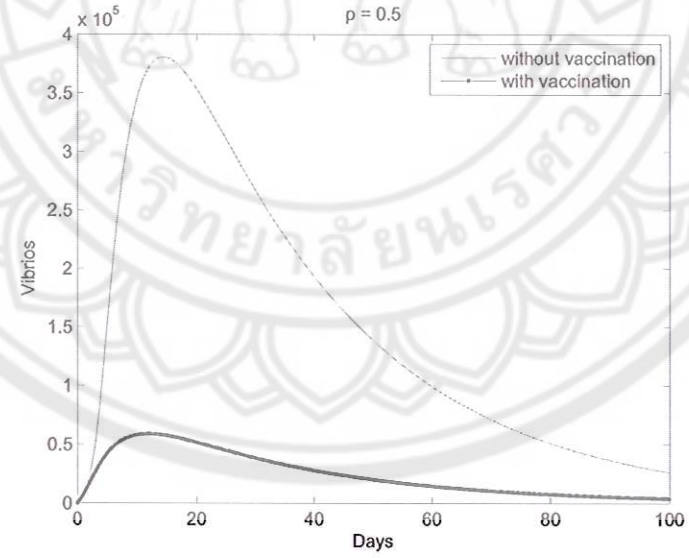

Figure 2.24: Vibrios

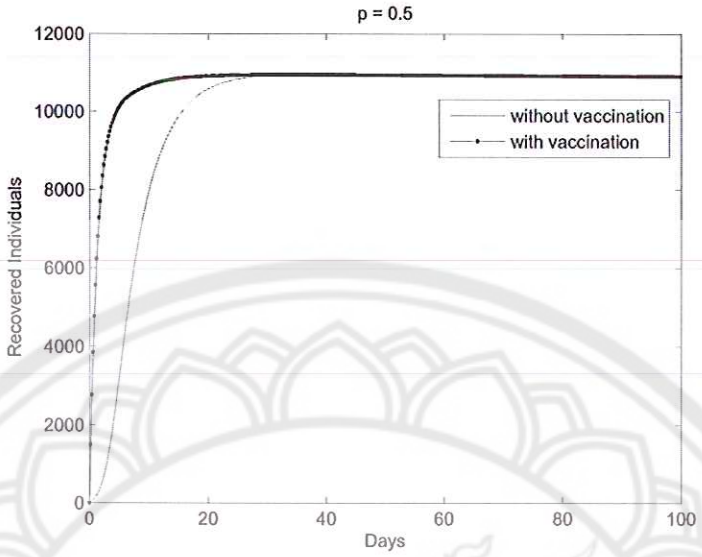

Figure 2.25: Recovered individuals

Chapter 3

Methodology and Results

We modify the model of Mukandavire et al. [34] by adding three disease control measures: vaccination, treatment, and water sanitation, and by introducing a new class of vaccinated people. Thus, our model classifies the human population, denoted by *N*, into the susceptibles (*S*), the vaccinated (*V*), the infected or infectives (*I*), and the recovered (*R*).

We assume that individuals are born and die at an average rate μ. The concentration of vibrios in contaminated water is denoted by *B*. Susceptible individuals acquire cholera infection either by ingesting environmental vibrios from contaminated aquatic reservoirs or through human-to-human transmission, at rates $\lambda_e = (1-\rho)\frac{\beta_e B}{\kappa + B}$ and $\lambda_h = (1-\rho)\beta_h I$ respectively, with the subscripts *e* and *h* denoting environment-to-human and human-to-human transmissions. Here, κ is the pathogen concentration that yields 50% chance of infection cholera, $\rho = \varepsilon p$ is the sanitation-induced preventability to cholera infection which is a product of the sanitation efficacy ε and compliance *p*. We further assume that susceptible individuals are vaccinated at a rate $\phi(t)$, where *t* is the time variable, with a vaccine that has a degree of protection $\sigma = (1-\varepsilon)$, where ε is the vaccine efficacy. Infected individuals are treated at a rate $\tau(t)$, and some recover naturally at a rate γ into the recovered class. Infected individuals contribute to *V. cholerae* in the aquatic environment at a rate ξ, and vibrios have a net death rate δ in the environment. In addition, water sanitation leads to the death of vibrios at a rate $\nu(t)$. As mentioned before, the case fatality rates for cholera generally are pretty low (at or below 1%) even just the simple oral hydration is administered [53]; hence we assume cholera-induced mortality can be neglected in this study.

We thus have the following system of differential equations describing the cholera dynamics with controls:

$$\begin{cases} \dfrac{dS}{dt} = \mu N - (1-\rho)\left[\beta_e \dfrac{B}{\kappa + B} + \beta_h I\right] S - (\phi(t) + \mu) S, \\ \dfrac{dV}{dt} = \phi(t) S - \sigma(1-\rho)\left[\beta_e \dfrac{B}{\kappa + B} + \beta_h I\right] V - \mu V, \\ \dfrac{dI}{dt} = (1-\rho)\left[\beta_e \dfrac{B}{\kappa + B} + \beta_h I\right](S + \sigma V) - (\tau(t) + \gamma + \mu) I, \\ \dfrac{dB}{dt} = \xi I - (\delta + \nu(t)) B, \end{cases} \tag{1}$$

together with

$$\frac{dR}{dt} = (\tau(t) + \gamma)\mathrm{I} - \mu R \tag{2}$$

Since N, the total population, is fixed such that $N = S + V + I + R$, we will not need Eq. (2) in our model analysis. In general, $\phi(t)$, $\tau(t)$, and $\nu(t)$ are functions of t, representing non-uniform and time-dependent controls. For the special case when the rates of all the three controls are positive constants, i.e.

$$\varphi(t) = \phi > 0, \tau(\mathrm{t}) = \tau > 0, \text{ and } \nu(t) = \nu > 0 \tag{3}$$

the model (1) is reduced to an autonomous system. This allows us to conduct a careful equilibrium analysis, in Sections 3 and 4, on both the disease-free and endemic equilibria. It is clear to see that in this case, the feasible region of the system (1) is

$$\Omega = \left\{ (S, V, I, B) \,\middle|\, S \geq 0,\ V \geq 0,\ I \geq 0,\ 0 \leq S + V + I \leq N,\ 0 \leq B \leq \frac{\xi N}{\delta + \nu} \right\} \tag{4}$$

which is positively invariant for the flow of the system (1).

Disease-free equilibrium

With constant controls, the disease-free equilibrium (DFE) of the system (1) is given by

$$x_0 = \left(\frac{\mu N}{\phi + \mu}, \frac{\phi N}{\phi + \mu}, 0, 0 \right)$$

For convenience, let us denote

$$E = (1-\rho)\beta_e, H = (1-\rho)\beta_h, T = \tau + \gamma + \mu \tag{6}$$

The Jacobian matrix of the system (1) is

$$J = \begin{bmatrix} -\frac{EB}{\kappa+B} - HI - (\phi+\mu) & 0 & -HS & -\frac{E\kappa S}{(\kappa+B)^2} \\ \phi & -\frac{\sigma EB}{\kappa+B} - \sigma HI - \mu & -\sigma HV & -\frac{\sigma E\kappa V}{(\kappa+B)^2} \\ \frac{EB}{\kappa+B} + HI & \frac{\sigma EB}{\kappa+B} + \sigma HI & H(S+\sigma V) - T & \frac{E\kappa(S+\sigma V)}{(\kappa+B)^2} \\ 0 & 0 & \xi & -(\delta+\nu) \end{bmatrix}. \tag{7}$$

We obtain the characteristic polynomial by evaluating the Jacobian (7) at the DFE (5),

$$\Delta = (\lambda + \phi + \mu)(\lambda + \mu) \times \left[\left(\lambda - \frac{H(\mu + \sigma\phi)N}{\phi + \mu} + T \right)(\lambda + \delta + \nu) - \frac{\xi E(\mu + \sigma\phi)N}{\kappa(\phi + \mu)} \right]. \tag{8}$$

It is clear that (8) has two negative roots $\lambda = -(\phi+\mu)$ and $\lambda = -\mu$. Note that we may expand the last factor of (8) such that it has the form

$$a_0\lambda^2 + a_1\lambda + a_2 = 0,$$

where

$$a_0 = 1, \quad a_1 = \delta + \nu + T - \frac{H(\mu + \sigma\phi)N}{\phi + \mu},$$
$$a_2 = (\delta + \nu)\left(T - \frac{H(\mu + \sigma\phi)N}{\phi + \mu} \right) - \frac{\xi E(\mu + \sigma\phi)N}{\kappa(\phi + \mu)}.$$

From the well-known Routh–Hurwitz stability criterion, the necessary and sufficient conditions for a stable quadratic are $a_0 > 0$, $a_1 > 0$, $a_2 > 0$. Clearly, $a_0 > 0$ is satisfied and if $a_2 > 0$, then it must be true that $a_1 > 0$. Therefore, we obtain a threshold value on$N$:

$$N < \frac{T\kappa(\delta+\nu)(\phi+\mu)}{(\kappa(\delta+\nu)H+\xi E)(\mu+\sigma\phi)} \tag{10}$$

such that $a_2 > 0$. Hence, the DFE (5) is locally stable under the condition (10). Eq. (10) implies that the basic reproduction number for the model with constant controls is given by

$$\mathcal{R}_0(\phi,\nu,\tau) = \frac{(\kappa(\delta+\nu)H+\xi E)(\mu+\sigma\phi)}{T\kappa(\delta+\nu)(\phi+\mu)} Nw. \tag{11}$$

This result can also be obtained through the standard next-generation matrix approach[48], by noting that

$$\begin{bmatrix} \frac{dI}{dt} \\ \frac{dB}{dt} \end{bmatrix} = \mathcal{F} - \mathcal{V} = \begin{bmatrix} (1-\rho)\left(\beta_e \frac{B}{\kappa+B} + \beta_h I\right)(S+\sigma V) \\ 0 \end{bmatrix} - \begin{bmatrix} (\tau+\gamma+\mu)I \\ (\delta+\nu)B - \xi I \end{bmatrix}, \tag{12}$$

with the next-generation matrices

$$\widehat{F} = \begin{bmatrix} \frac{H(\mu+\sigma\phi)N}{\phi+\mu} & \frac{E(\mu+\sigma\phi)N}{\kappa(\phi+\mu)} \\ 0 & 0 \end{bmatrix} \quad \text{and} \quad \widehat{V} = \begin{bmatrix} \tau+\gamma+\mu & 0 \\ -\xi & \delta+\nu \end{bmatrix}. \tag{13}$$

Then R_0 is determined by the spectral radius of the matrix FV^{-1}.Biologically speaking, $R_0=1$ provides a threshold for disease epidemics: if $R_0<1$, the disease will die out; if $R_0>1$, the disease will typically spread. Mathematically, based on the result in [48], we have the following theorem.

Theorem 1.

With constant controls, the DFE (5) is locally asymptotically stable when $R_0<1$, *and unstable when* $R_0>1$.

We mention that the basic reproduction number for the original model in [34] is given by

$$\tilde{\mathcal{R}}_0 = \frac{N}{\delta\kappa(\gamma+\mu)}[\xi\beta_e + \delta\kappa\beta_h]. \tag{14}$$

Comparing the expressions in (11) and (14), we note that

$$R_0 < \tilde{R}_0 \tag{15}$$

for all $\phi > 0, \tau > 0, \text{and}\, \nu > 0,$ due to the effects of disease controls.

Theorem 1 states that if the strengths of the (constant) controls are strong enough to reduce the basic reproduction number below 1, then cholera will be eradicated. Otherwise, a cholera epidemic would occur, though with a lower infection level than that without controls owing to the reduced value of the reproduction number. Indeed, the DFE is also globally asymptotically stable when $R_0<1$. We prove this by using the global stability result established in [8]. For completeness, we have included the result in Appendix A, Theorem 8.

Applying Theorem 8 to the model (1), we have that

$$F(X_1, 0) = \begin{bmatrix} \frac{dS}{dt} \\ \frac{dV}{dt} \end{bmatrix}_{(X_1,0)} = \begin{bmatrix} \mu N - (\phi+\mu)S \\ \phi S - \mu V \end{bmatrix}. \tag{16}$$

It follows from solving these differential equations that

$$S(t) = \frac{\mu N}{\phi+\mu} + C_1 e^{-(\phi+\mu)t}$$

and

$$V(t) = \frac{\phi N}{\phi+\mu} + C_2 e^{-\mu t} + C_3 e^{-(\phi+\mu)t}$$

for some constants C_1 , C_2 and C_3 . Hence,

$S(t) = \frac{\mu N}{\phi + \mu}$ and $V(t) = \frac{\phi N}{\phi + \mu} + C_2 e^{-\mu t} + C_3 e^{-(\phi+\mu)t}$ as $t \longrightarrow \infty$, showing that X_1^E is globally asymptotically stable and condition 1 holds.

Now, consider

$$G(X_1, X_2) = AX_2 - \hat{G}(X_1, X_2) \tag{17}$$

Where

$$A = \frac{\partial G}{\partial X_2}(X_1^E, 0)$$

Specifically,

$$A = \begin{bmatrix} H(S+\sigma V) - T & \frac{E\kappa(S+\sigma V)}{(\kappa+B)^2} \\ \xi & -(\delta+\nu) \end{bmatrix}_{(X_1^E,0)} \tag{18}$$

$$= \begin{bmatrix} \frac{H(\mu+\sigma\phi)N}{\phi+\mu} - T & \frac{E(\mu+\sigma\phi)N}{\kappa(\phi+\mu)} \\ \xi & -(\delta+\nu) \end{bmatrix},$$

where the off-diagonal elements are obviously non negative. Substituting into (17)gives,

$$\hat{G}(X_1, X_2) = \begin{bmatrix} \frac{(\mu+\sigma\phi)EB^2N}{\kappa(\kappa+B)(\phi+\mu)} \\ 0 \end{bmatrix} \geq 0. \tag{19}$$

Thus, condition 2 holds as well.

Summarizing these results, we obtain the theorem below.

Theorem 2.

When $R_0 < 1$, *the DFE of the system (1) with constant controls is globally asymptotically stable.*

In addition, the following result now can be easily derived.

Theorem 3.

When $R_0 > 1$, *the system (1) with constant controls is uniformly persistent; i.e., there exists a constant d > 0 such that*

$$\liminf_{t\to\infty}\{S(t),\ I(t),\ B(t)\} > d.$$

Proof.

The uniform persistence follows directly from Theorem 2.2 in [44]. Here we briefly verify the conditions in that theorem. From Eq. (13), it is clear that $F \geq 0, V^{-1} \geq 0$ and $V^{-1}F$ is irreducible. Meanwhile, consider the function

$$f(X_1, X_2) = (\widehat{F} - \widehat{V})X_2 - \mathcal{F}(X_1, X_2) + \mathcal{V}(X_1, X_2),$$

where F and V are defined in Eq. (12). It is straightforward to obtain that $f(X_1, X_2) \geq 0$ and $f(X_1^E, X_2) = 0$ where X_1^E has been shown as globally asymptotically stable in the disease-free subsystem following Eq. (16). Hence, the instability of the DFE when $R_0 > 1$ implies the uniform persistence of the system (1). □

We comment that the uniform persistence result can also be obtained from Theorem 4.3 in [18], by observing that the DFE is unique and located on the boundary of the domain Ω, and establishing that the DFE is a repeller when $R_0 > 1$ (e.g., using a suitable Lyapunov function; see [27] and [44]).

Numerical evidence of the global stability of the DFE when $R_0 > 1$ is provided in Fig. 1. We set the total population as N = 1, 000 and the model parameters in such a way that $R_0 \approx 0.8$. We then choose different initial conditions $I(0)$ = 1, 50, 100, 150, 200, and 250, conduct a numerical simulation for each, and plot the solution curves for the phase plane portrait of I vs. S in Fig. 1. We observe that all these curves converge to the DFE. We also observe the same pattern for various other initial conditions (though not shown here).

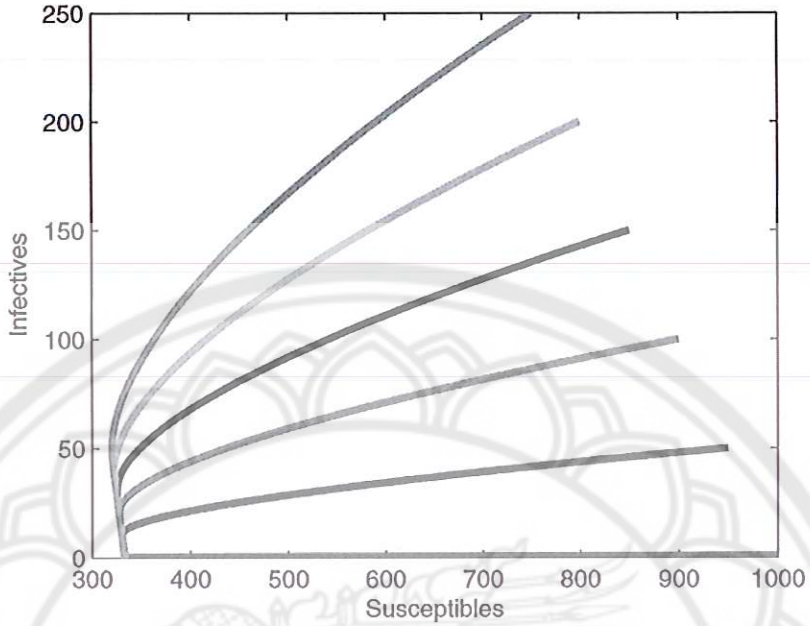

Fig. 1.

The phase portrait of I vs. S for the system (1) with parameters set such that $R_0 \approx 0.8$. The curves correspond to six different initial conditions with $I(0)$ = 1, 50, 100, 150, 200, and 250. All the curves converge to the DFE where $S_0 = \mu N/(\phi+\mu) \approx 333.3$ and $I_0 = 0$.

Endemic equilibrium

Now that we have completely described the dynamics at the DFE, by Theorems 1–3, we turn to the analysis of the endemic equilibrium. As discussed before, when the effects of the controls are not strong enough to reduce R_0 below 1, the DFE becomes unstable and the disease will persist. Below we will study the endemic equilibrium when $R_0 > 1$, which is related to the long-term behavior of cholera dynamics.

Existence and uniqueness

Let us denote the endemic equilibrium of the system (1) by $X^* = (S^*, V^*, I^*, B^*)$, where

$$S^* = \frac{\mu N}{E\frac{\xi I^*}{\kappa(\delta+\nu)+\xi I^*} + HI^* + (\phi+\mu)}, \tag{20}$$

$$V^* = \frac{\mu\phi N}{\left[\sigma E\frac{\xi I^*}{\kappa(\delta+\nu)+\xi I^*} + \sigma HI^* + \mu\right]\left[E\frac{\xi I^*}{\kappa(\delta+\nu)+\xi I^*} + HI^* + (\phi+\mu)\right]}, \tag{21}$$

$$I^* = \frac{\frac{E\xi I^*}{\kappa(\delta+\nu)+\xi I^*}(S^* + \sigma V^*)}{T - H(S^* + \sigma V^*)}, \tag{22}$$

$$B^* = \frac{\xi I^*}{\delta+\nu}. \tag{23}$$

To proceed, we treat S and V as (implicit) functions of I, as suggested by Eqs. (20) and(21). Also, let

$g(I) = S(I) + \sigma V(I)$, $g_1(I) = \frac{E\xi I}{\kappa(\delta+\nu)+\xi I} + HI + (\phi+\mu)$, and $g_2(I) = \sigma\left[\frac{E\xi I}{\kappa(\delta+\nu)+\xi I} + HI\right] + \mu$.

Therefore, from Eqs. (20)–(23), we have that at an equilibrium,

$$S(I) = \frac{\mu N}{g_1(I)}, \quad V(I) = \frac{\mu\phi N}{g_1(I)g_2(I)}, \quad I = \frac{\frac{E\xi I}{\kappa(\delta+\nu)+\xi I}g(I)}{T - Hg(I)}, \quad B(I) = \frac{\xi I}{\delta+\nu}. \tag{24}$$

(24)

From (24) and $I \neq 0$, it follows that for an endemic equilibrium to exist we must have,

$$\frac{T - Hg(I)}{g(I)} = \frac{E\xi}{\kappa(\delta+\nu)+\xi I} \tag{25}$$

for some $I = I^* > 0$.

Now, let us denote

$$f_1(I) = \frac{T - Hg(I)}{g(I)} = \frac{T}{g(I)} - H \text{ and } f_2(I) = \frac{E\xi}{\kappa(\delta+\nu)+\xi I}.$$

Clearly both f_1 and f_2 are differentiable functions for $I \geq 0$. It is easy to see that

$$f_2'(I) = -\frac{E\xi^2}{\left[\kappa(\delta+\nu)+\xi I\right]^2} < 0$$

whereas

$$f_1'(I) = \frac{-Tg'(I)}{\left[g'(I)\right]^2}$$

Since

$$g(I) = \frac{\mu N}{g_1(I)} + \frac{\sigma\mu\phi N}{g_1(I)g_2(I)}$$

the sign of $f_1'(I)$ is determined by the sign of $g_1'(I)$ and $g_2'(I)$. For $I \geq 0$, it is obvious that $g_1(I) > 0$ and $g_2(I) > 0$. Also, we see that

$$g_1'(I) = \frac{\kappa(\delta+\nu)E\xi}{[\kappa(\delta+\nu)+\xi I]^2} + H > 0, \text{ and } g_2'(I) = \sigma g_1'(I) > 0.$$

Thus,

$$g'(I) = -\frac{\mu N g_1'(I)}{[g_1(I)]^2} - \frac{\sigma\mu\phi N[g_1'(I)g_2(I) + g_1(I)g_2'(I)]}{[g_1(I)g_2(I)]^2} < 0,$$

which yields $f_1'(I) > 0$.

Hence, on $[0, \infty]$, $f_1(I)$ is an increasing curve and $f_2(I)$ is a decreasing one. We can compare their vertical intercepts to determine if the two curves intersect and thus, if a positive endemic equilibrium exists. We have that

$$f_2(0) = \frac{E\xi}{\kappa(\delta+\nu)},$$

and

$$f_1(0) = \frac{T}{S(0)+\sigma V(0)} - H = \frac{T(\mu+\phi)}{N(\mu+\sigma\phi)} - H \ .$$

Using Eq. (11), we can easily observe that if $R_0 > 1$, then $f_1(0) < f_2(0)$, and there is a unique endemic equilibrium $I = I^*$; if $R_0 \leq 1$, then $f_1(0) \geq f_2(0)$, and there is no endemic equilibrium. Therefore, we can establish the following theorem.

Theorem 4.

When $R_0 > 1$, there exists a unique endemic equilibrium of the system (1) with constant controls.

Bifurcation

Let us now investigate the bifurcation of the system (1) at the bifurcation point $R_0 = 1$. We pick β_h as the bifurcation parameter. Our analysis makes uses of the bifurcation theorem based on the center manifold theory, originally stated in [9]. We have also included the result in Appendix A, Theorem 9.
Let us consider R_0 as a function of β_h such that

$$R_0(\beta_h) = \frac{(\kappa(\delta+\nu)(1-\rho)\beta_h + \xi(1-\rho)\beta_e)(\mu+\sigma\phi)}{T\kappa(\delta+\nu)(\phi+\mu)} N$$

Setting R_0 equal to 1 and solving for $\beta_h = \beta_h^*$ gives

$$\beta_h^* = \frac{1}{\kappa(\delta+\nu)(1-\rho)} \left[\frac{T\kappa(\delta+\nu)(\phi+\mu)}{(\mu+\sigma\phi)N} - \xi(1-\rho)\beta_e \right].$$

We consider the DFE (5) and $R_0 = 1$ in terms of the parameter β_h^* and we have the following Jacobian,

$$J(X_0, \beta_h^*) = \begin{bmatrix} -(\phi+\mu) & 0 & -\frac{\mu(1-\rho)\beta_h^* N}{\phi+\mu} & -\frac{\mu(1-\rho)\beta_e N}{\kappa(\phi+\mu)} \\ \phi & -\mu & -\frac{\sigma\phi(1-\rho)\beta_h^* N}{\phi+\mu} & -\frac{\sigma\phi(1-\rho)\beta_e N}{\kappa(\phi+\mu)} \\ 0 & 0 & \frac{(1-\rho)\beta_h^*(\mu+\sigma\phi)N}{\phi+\mu} - T & \frac{(1-\rho)\beta_e(\mu+\sigma\phi)N}{\kappa(\phi+\mu)} \\ 0 & 0 & \xi & -(\delta+\nu) \end{bmatrix}.$$

Denote $w = (w_1, w_2, w_3, w_4)^T$, a right eigenvector such that

$$\begin{cases} -(\phi+\mu)w_1 - \frac{\mu(1-\rho)\beta_h^* N}{\phi+\mu} w_3 - \frac{\mu(1-\rho)\beta_e N}{\kappa(\phi+\mu)} w_4 = 0, \\ \phi w_1 - \mu w_2 - \frac{\sigma\phi(1-\rho)\beta_h^* N}{\phi+\mu} w_3 - \frac{\sigma\phi(1-\rho)\beta_e N}{\kappa(\phi+\mu)} w_4 = 0, \\ \left(\frac{(1-\rho)\beta_h^*(\mu+\sigma\phi)N}{\phi+\mu} - T\right) w_3 + \frac{(1-\rho)\beta_e(\mu+\sigma\phi)N}{\kappa(\phi+\mu)} w_4 = 0, \\ \xi w_3 - (\delta+\nu) w_4 = 0. \end{cases}$$

Solving this system of equations gives

$$w = \left(-\frac{\mu T}{(\phi+\mu)(\mu+\sigma\phi)}, -\frac{\phi T}{\mu+\sigma\phi}\left(\frac{1}{\phi+\mu} + \frac{\sigma}{\mu}\right), 1, \frac{\xi}{\delta+\nu} \right)^T. \tag{26}$$

Now, denote $v = (v_1, v_2, v_3, v_4)$, a left eigenvector such that

$$\begin{cases} -(\phi+\mu)v_1 + \phi v_2 = 0, \\ -\mu v_2 = 0, \\ -\frac{\mu(1-\rho)\beta_h^* N}{\phi+\mu} v_1 - \frac{\sigma\phi(1-\rho)\beta_h^* N}{\phi+\mu} v_2 + \left(\frac{(1-\rho)\beta_h^*(\mu+\sigma\phi)N}{\phi+\mu} - T\right) v_3 + \xi v_4 = 0, \\ -\frac{\mu(1-\rho)\beta_e N}{\kappa(\phi+\mu)} v_1 - \frac{\sigma\phi(1-\rho)\beta_e N}{\kappa(\phi+\mu)} v_2 + \frac{(1-\rho)\beta_e(\mu+\sigma\phi)N}{\kappa(\phi+\mu)} v_3 - (\delta+\nu) v_4 = 0, \end{cases}$$

and

$$v_4 \left(\frac{\kappa(\delta+\nu)(\phi+\mu)}{(1-\rho)\beta_e(\mu+\sigma\phi)N} + \frac{\xi}{\delta+\nu} \right) = 1.$$

Solving this system of equations gives

$$v = \left(0,\ 0,\ \frac{\kappa(\delta+\nu)^2(\phi+\mu)}{\kappa(\delta+\nu)^2(\phi+\mu) + \xi(1-\rho)\beta_e(\mu+\sigma\phi)N},\ \frac{(1-\rho)\beta_e(\mu+\sigma\phi)N(\delta+\nu)}{\kappa(\delta+\nu)^2(\phi+\mu) + \xi(1-\rho)\beta_e(\mu+\sigma\phi)N} \right). \tag{27}$$

Note that we have $v \cdot w = 1, J \cdot w = 0$ and $v \cdot J = 0$.

From Eqs. (A.2)–(A.3), and considering only the nonzero derivatives for the terms

$$\frac{\partial^2 f_k}{\partial x_i \partial x_j}(X_0, \beta_h^*)$$

And

$$\frac{\partial^2 f_k}{\partial x_i \partial \beta_h}(X_0, \beta_h^*)$$

it follows that

$$\begin{aligned} a = {} & 2v_1 w_1 w_3 \frac{\partial^2 f_1}{\partial S \partial I}(X_0, \beta_h^*) + 2v_1 w_1 w_4 \frac{\partial^2 f_1}{\partial S \partial B}(X_0, \beta_h^*) \\ & + 2v_2 w_2 w_3 \frac{\partial^2 f_2}{\partial V \partial I}(X_0, \beta_h^*) + 2v_2 w_2 w_4 \frac{\partial^2 f_2}{\partial V \partial B}(X_0, \beta_h^*) \\ & + 2v_3 w_1 w_3 \frac{\partial^2 f_3}{\partial S \partial I}(X_0, \beta_h^*) + 2v_3 w_1 w_4 \frac{\partial^2 f_3}{\partial S \partial B}(X_0, \beta_h^*) \\ & + 2v_3 w_2 w_3 \frac{\partial^2 f_3}{\partial V \partial I}(X_0, \beta_h^*) + 2v_3 w_2 w_4 \frac{\partial^2 f_3}{\partial V \partial B}(X_0, \beta_h^*) \end{aligned}$$

and

$$\begin{aligned} b = {} & 2v_1 w_3 \frac{\partial^2 f_1}{\partial I \partial \beta_h}(X_0, \beta_h^*) + 2v_2 w_3 \frac{\partial^2 f_2}{\partial I \partial \beta_h}(X_0, \beta_h^*) \\ & + 2v_3 w_3 \frac{\partial^2 f_3}{\partial I \partial \beta_h}(X_0, \beta_h^*). \end{aligned}$$

With our definitions of v and w and some algebra, we obtain

$$\begin{aligned} a = {} & \frac{-2\kappa(\delta+\nu)^2(\phi+\mu)}{\kappa(\delta+\nu)^2(\phi+\mu) + \xi(1-\rho)\beta_e(\mu+\sigma\phi)N} \\ & \left[\frac{T^2}{(\mu+\sigma\phi)^2 N}\left(\mu+\sigma\phi+\frac{\sigma^2\phi(\phi+\mu)}{\mu}\right)\right], \\ b = {} & \frac{2\kappa(\delta+\nu)^2(\mu+\sigma\phi)(1-\rho)N}{\kappa(\delta+nu)^2(\phi+\mu) + \xi(1-\rho)\beta_e(\mu+\sigma\phi)N}. \end{aligned}$$

Clearly, $a < 0$ and $b > 0$. Hence, based on Theorem 9, the following result holds:

Theorem 5.

The system (1) with constant controls exhibits a forward bifurcation at $R_0 = 1$.

A typical bifurcation diagram of I^* vs. R_0 near the bifurcation point $R_0=1$ is presented inFig. 2, which is generated numerically by varying the bifurcation parameter β_h. The diagram clearly shows a forward transcritical bifurcation at $R_0=1$.

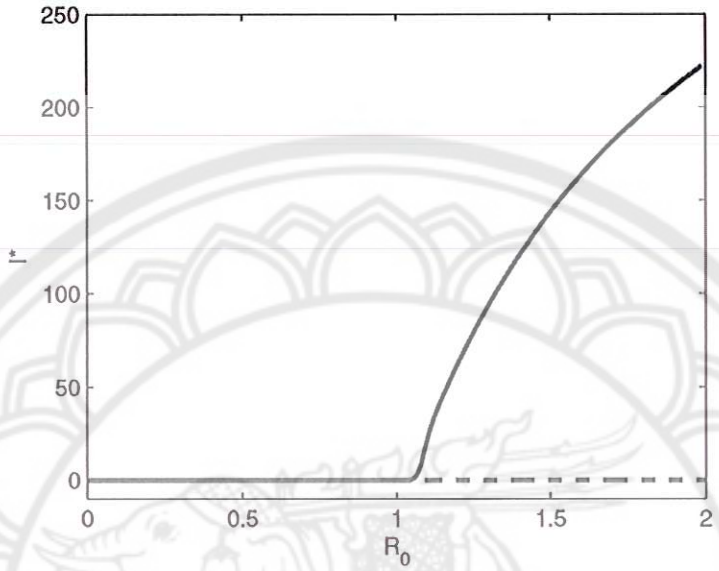

Fig. 2.
A bifurcation diagram of I^* vs. R_0 which shows a forward transcritical bifurcation at $R_0=1$. Red solid line represents the stable DFE (when $0<R_0<1$) and red dashed line represents the unstable DFE (when$R_0>1$); blue solid line represents the positive stable endemic equilibrium (when $R_0>1$). The negative unstable endemic equilibrium (when $0<R_0<1$) is biologically non-feasible and not shown here. (For interpretation of the references to colour in this figure legend, the reader is referred to the web version of this article.)

Theorem 5 precludes the possibility of backward bifurcation for the cholera model (1). This reinforces our observation from the DFE analysis that reducing the basic reproductive number below one by using control measures would be sufficient to eradicate the disease.

Endemic stability

We have presented Theorem 5 that describes the local dynamics of the system (1) near the bifurcation point $R_0=1$. Furthermore, we can establish the following theorem regarding the stability of the endemic equilibrium.

Theorem 6.

When $R_0>1$, the unique endemic equilibrium of the system (1) with constant controls is both locally and globally asymptotically stable.

The proof of the local asymptotic stability follows direct algebraic calculation. For simplicity, set

$$P=\frac{EB^*}{\kappa+B^*}+HI^* \quad \text{and} \quad Q=\frac{E\kappa}{(\kappa+B^*)^2}. \tag{28}$$

The Jacobian evaluated at the endemic equilibrium is,

$$J(X^*)=\begin{bmatrix} -P-(\phi+\mu) & 0 & -HS^* & -QS^* \\ \phi & -\sigma P-\mu & -\sigma HV^* & -\sigma QV^* \\ P & \sigma P & H(S^*+\sigma V^*)-T & Q(S^*+\sigma V^*) \\ 0 & 0 & \xi & -(\delta+\nu) \end{bmatrix}, \tag{29}$$

giving the following characteristic polynomial,

$$det(\lambda I-J(X^*))=a_0\lambda^4+a_1\lambda^3+a_2\lambda^2+a_3\lambda+a_4 \tag{30}$$

where

$$\begin{cases} a_0=1, \\ a_1=P+\phi+\mu+\sigma P+\mu+\delta+\nu+T-H(S^*+\sigma V^*), \\ a_2=(P+\phi+\mu)(\sigma P+\mu+\delta+\nu+T-H(S^*+\sigma V^*)) \\ \quad +(\delta+\nu)(T-H(S^*+\sigma V^*))-\xi Q(S^*+\sigma V^*) \\ \quad +(\sigma P+\mu)(\delta+\nu+T-H(S^*+\sigma V^*))+\sigma^2PHV^*+PHS^*, \\ a_3=(P+\phi+\mu)[(\sigma P+\mu)(\delta+\nu+T-H(S^*+\sigma V^*)) \\ \quad +(\delta+\nu)(T-H(S^*+\sigma V^*))-\xi Q(S^*+\sigma V^*)+\sigma^2PHV^*] \\ \quad +(\sigma P+\mu)[(\delta+\nu)(T-H(S^*+\sigma V^*))-\xi Q(S^*+\sigma V^*)] \\ \quad +\sigma P((\delta+\nu)\sigma HV^*+\sigma\xi QV^*)+\sigma\phi PHS^*+P((\sigma P+\mu)HS^* \\ \quad +HS^*(\delta+\nu)+\xi QS^*), \\ a_4=(P+\phi+\mu)[(\sigma P+\mu)[(\delta+\nu)(T-H(S^*+\sigma V^*)) \\ \quad -\xi Q(S^*+\sigma V^*)]+\sigma P((\delta+\nu)\sigma HV^*+\sigma\xi QV^*)] \\ \quad +\sigma\phi P(HS^*(\delta+\nu)+\xi QS^*) \\ \quad +P[(\sigma P+\mu)(HS^*(\delta+\nu)+\xi QS^*)]. \end{cases}$$

Based on the Routh–Hurwitz stability criterion, the necessary and sufficient conditions for the stability of a quartic polynomial are

$$a_i > 0 \quad (0 \le i \le 4); \quad a_1a_2 - a_0a_3 > 0, \quad a_3(a_1a_2 - a_0a_3) > a_1^2a_4. \tag{31}$$

Clearly, $a_0 > 0$ is satisfied. From (22) and the fact that $S^*, V^*, I^* > 0$, it follows that

$$T - H(S^* + \sigma V^*) = \frac{\xi E(\kappa(\delta+\nu) + \xi I^*)}{(\kappa(\delta+\nu) + \xi I^*)^2}(S^* + \sigma V^*) > 0. \tag{32}$$

Note that

$$\xi Q = \frac{\xi E\kappa(\delta+\nu)^2}{(\kappa(\delta+\nu)+\xi I^*)^2}$$

and thus

$$(\delta+\nu)(T - H(S^* + \sigma V^*)) > \xi Q(S^* + \sigma V^*). \tag{33}$$

The inequalities (32) and (33) are both necessary and sufficient to show that $a_i > 0$ for $1 \le i \le 4$. Next we show $a_1a_2 - a_0a_3 > 0$. Consider the following,

$$\begin{cases}
(P+\phi+\mu+\sigma P+\mu+\delta+\nu)a_2 - a_3 \\
=(1-\sigma)PHS^* + (P+\phi+\mu)^2(\sigma P+\mu+\delta+\nu+T-H(S^*+\sigma V^*)) \\
+(P+\phi+\mu)(\sigma P+\mu)(\delta+\nu+T-H(S^*+\sigma V^*)) + (P+\mu)PHS^* \\
+(\sigma P+\mu)^2(P+\phi+\mu) + (\sigma P+\mu)^2(\delta+\nu+T-H(S^*+\sigma V^*)) \\
+(\sigma P+\mu)\sigma^2 PHV^* + (\delta+\nu)P(\sigma P+\mu+\delta+\nu) \\
+(\delta+\nu)(\phi+\mu)(\sigma P+\mu+\delta+\nu+T-H(S^*+\sigma V^*)) \\
+[(\delta+\nu)^2(T-H(S^*+\sigma V^*)) - (\delta+\nu)\xi Q(S^*+\sigma V^*)] \\
+(\delta+\nu)^2\sigma P + (\delta+\nu)\mu(\delta+\nu+T-H(S^*+\sigma V^*)) \\
+[(\delta+\nu)P(T-H(S^*+\sigma V^*)) - P\xi QS^*] \\
+[(\delta+\nu)\sigma P(T-H(S^*+\sigma V^*)) - \sigma^2 P\xi QV^*].
\end{cases}$$

Using condition (33), we have that

$$\begin{cases} (\delta+\nu)^2(T-H(S^*+\sigma V^*)) & >(\delta+\nu)\xi Q(S^*+\sigma V^*), \\ (\delta+\nu)P(T-H(S^*+\sigma V^*)) & >P\xi QS^*, \\ (\delta+\nu)\sigma P(T-H(S^*+\sigma V^*)) & >\sigma^2 P\xi QV^*. \end{cases}$$

Thus, $(P+\phi+\mu+\sigma P+\mu+\delta+\nu)a_2>a_3$ holds. From condition (32), we see that $a_1>P+\phi+\mu+\sigma P+\mu+\delta+\nu$. Hence, $a_1a_2 > a_3$. The last inequality in (31) can be proved with similar algebraic manipulation.

The global asymptotic stability of the endemic equilibrium, however, is more challenging and requires significantly more work. The main reason for this difficulty is that the model(1) is a four-dimensional dynamical system, for which very few analytical theories and techniques can be applied. We establish the global endemic stability of our model by using the geometric approach originally proposed by Li and Muldowney [28] and [29]. The proof is provided in the Appendix B.

The existence of a stable the endemic equilibrium when $R_0>1$ is demonstrated in Fig. 3. We set the total population as N = 1,000 and the model parameters in such a way that $R_0 \approx 2.0$. We again pick different initial conditions $I(0)$ = 1, 50, 100, 150, 200, *and* 250 , conduct a numerical simulation for each, and plot the phase plane portrait of *I* vs. *S* for each case in Fig. 3. We observe that all these curves converge to the endemic equilibrium over time, a pattern that also takes place for various other initial conditions.

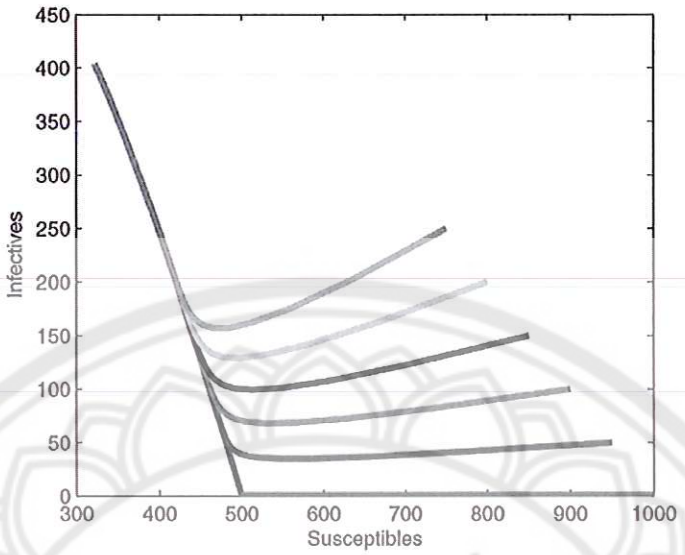

Fig. 3.

The phase portrait of I vs. S for the system (1) with parameters set such that $R_0 \approx 2$. The curves correspond to six different initial conditions with $I(0) = 1, 50, 100, 150, 200,$ and 250. All these curves converge to the endemic equilibrium where $S^* \approx 322.5$ and $I^* \approx 403.1$.

Sensitivity analysis

There are various parameters present in our model (1) and the values of these parameters will directly affect the dynamics of cholera infection and transmission. In order to identify which parameters are more influential than others in determining disease dynamics, we carry out a sensitivity analysis using the Latin Hypercube Sampling (LHS) method [4] and [35]. The LHS method, which is one of the most efficient ways to analyze sensitivity and uncertainty, calculates the Partial Rank Correlation Coefficients (PRCC) in the range of $[-1, 1]$ for the model parameters with respect to outcome measurements. A small PRCC value (close to 0) indicates that changes in the input parameter have little impact on the outcome, whereas a bigger PRCC value suggests that the outcome is significantly influenced by, thus sensitive to, the changes of the input parameter. In this study we pick the

maximum daily infected population and the cumulative total infected population as the two outcome measurements, and present the results in Table 1 with a sample size n = 500 ; similar patterns are observed for differing sample sizes. We also mention that similar outcome measurements were used in the sensitivity analysis in [37].

Table 1.

LHS sensitivity analysis for model parameters. The sample size is n = 500 . Asterisks indicate the corresponding p-values are below 0.01 ; i.e., the nonzero PRCC are significant.

Parameters	Parameter ranges Min	Max	Maximum daily infection PRCC values	t-values	Total infection PRCC values	t-values
ϕ	0.001	1	− 0.24	− 4.8*	− 0.085	− 1.82
ρ	0.01	0.5	− 0.39	− 7.32*	− 0.059	− 1.28
β_e	0.01	0.2	0.14	3.24*	0.092	2.15*
β_h	0.00001	0.002	0.8	39.8*	0.33	8.97*
σ	0.2	1	0.086	2.0	0.029	0.66
τ	0.001	1	− 0.67	− 11.5*	− 0.82	− 13.6*
γ	0.05	0.4	− 0.64	− 11.2*	− 0.77	− 12.9*
ξ	1	20	0.035	0.8	− 0.043	− 0.93
δ	0.0001	0.3	− 0.087	− 1.85	− 0.088	− 1.87
ν	0.01	1	− 0.014	− 0.31	0.0052	0.12

Results in Table 1 show that the control terms ϕ (vaccination rate) and τ (treatment rate) are both sensitive in affecting the maximum daily infection; the treatment rate is also sensitive to the total infection. Meanwhile, the parameter ρ (sanitation-induced preventability) is also sensitive to the maximum daily infection. In addition, the recovery rate γ and the contact rates β_e and β_h are sensitive to both daily and total infections. We note that the sensitivity of β_e and β_h was also observed in [34] for the cholera model without controls.

In terms of disease control, the sensitivity analysis results indicate that both the environment-to-human and human-to-human transmission pathways are sensitive, and important, in determining the cholera infections, and that all three types of control measures (vaccination, treatment, and sanitation) are important in

containing the cholera epidemics. Clearly, the multiple transmission routes and intervention strategies will closely interplay with each other. To better understand these relations and to predict how the control strategies can be effectively designed, we will conduct an optimal control study in next section.

Optimal control

Now we study the general model (1) with time-dependent controls $\phi(t)$,$\tau(t)$, and $\nu(t)$. The presence of time-dependent controls makes equilibrium analysis of the system (1)difficult, as the system becomes non-autonomous and the disease dynamics now depend on the evolution of each control profile. We will, instead, perform an optimal control study on this problem, to explore how the intervention effects and costs can be best balanced and how the control strategy can be best designed to account for the complex and multiple transmission pathways of cholera.

We consider the system on a time interval $[0, T_1]$ for some $T_1 > 0$. The control set is defined as

$$\begin{aligned}\Gamma = \{(\phi(t),\, \tau(t),\, \nu(t)) \mid 0 \le \phi(t) \le \phi_{\max},\\ 0 \le \tau(t) \le \tau_{\max},\ 0 \le \nu(t) \le \nu_{\max}\},\end{aligned} \tag{34}$$

where ϕ_{max}, $\tau_{\max}$ and ν_{max} denote the upper bounds for the effort of vaccination, treatment, and sanitation, respectively. These bounds reflect practical limitations on the maximum rates of controls that can be implemented in a given time period.

We aim to minimize the total number of infections and the costs of controls over the time interval $[0, T_1]$; i.e.,

$$\begin{aligned}\min_{(\phi,\tau,\nu)\in\Gamma} \int_0^{T_1} [I(t) + c_{21}\phi(t)S(t) + c_{22}\phi(t)^2 + c_{31}\tau(t)I(t)\\ + c_{32}\tau(t)^2 + c_{41}\nu(t)B(t) + c_{42}\nu(t)^2]\, dt.\end{aligned} \tag{35}$$

Here the parameters c_{ij} $(i=2,3,4; j=1,2)$, define the appropriate costs associated with these controls. Quadratic terms are introduced to account for nonlinear costs potentially arising at high intervention levels [2], [5] and [37]. The minimization process is subject to the differential equations in (1), which we now refer to as the state equations. Correspondingly, the unknowns *S*, I, and *B* are now called the *state variables*, in contrast to the *control variables* $\phi, \tau, \text{and } \nu$. Our goal is then to determine the optimal control, $\phi^*(t), \tau^*(t), \text{and } \nu^*(t)$, so as to minimize the objective functional in (35).

We first note that the control set Γ is closed and convex, and the integrand of the objective functional in (35) is also convex. Meanwhile, our model is linear in the control variables. Hence, based on the standard optimal control theorems in [17], we obtain the following theorem.

Theorem 7.

There exists $(\phi^*(t), \tau^*(t), \nu^*(t)) \in \Omega$ *such that the objective functional in (35) is minimized.*

To proceed, we will use the Pontryagin's Maximum/Minimum Principle [39] to seek the optimal control solution. This approach introduces the adjoint functions and represents an optimal control in terms of the state and adjoint functions, thus transferring the problem of minimizing the objective functional into minimizing the Hamiltonian with respect to the controls.

We define the adjoint functions $\lambda_S, \lambda_V, \lambda_I, \text{and } \lambda_B$ associated with the state equations for *S, V*, I, and *B*, respectively. We then form the Hamiltonian, H, by multiplying each adjoint function with the right-hand side of its corresponding state equation, and adding each of these products to the integrand of the objective functional. As a result, we obtain

$$\begin{aligned}\mathcal{H} = {} & I(t) + c_{21}\phi(t)S(t) + c_{22}\phi(t)^2 + c_{31}\tau(t)I(t) + c_{32}\tau(t)^2 \\ & + c_{41}\nu(t)B(t) + c_{42}\nu(t)^2 \\ & + \lambda_S\left[\mu N - (1-\rho)\left[\beta_e\frac{B}{\kappa+B} + \beta_h I\right]S - (\phi(t)+\mu)S\right] \\ & + \lambda_V\left[\phi(t)S - \sigma(1-\rho)\left[\beta_e\frac{B}{\kappa+B} + \beta_h I\right]V - \mu V\right] \\ & + \lambda_I\left[(1-\rho)\left[\beta_e\frac{B}{\kappa+B} + \beta_h I\right](S+\sigma V) - (\tau(t)+\gamma+\mu)I\right] \\ & + \lambda_B[\xi I - (\delta+\nu(t))B].\end{aligned}$$

To achieve the optimal control, the adjoint functions must satisfy

$\frac{d\lambda_S}{dt} = -\frac{\partial\mathcal{H}}{\partial S}$, $\frac{d\lambda_V}{dt} = -\frac{\partial\mathcal{H}}{\partial V}$, etc. These yield

$$\begin{aligned}\frac{d\lambda_S}{dt} = {} & -c_{21}\phi + \lambda_S\left[(1-\rho)\left[\beta_e\frac{B}{\kappa+B} + \beta_h I\right] + (\phi+\mu)\right] \\ & - \lambda_V\phi - \lambda_I\left[(1-\rho)\left[\beta_e\frac{B}{\kappa+B} + \beta_h I\right]\right],\end{aligned} \tag{36}$$

$$\begin{aligned}\frac{d\lambda_V}{dt} = {} & \lambda_V\left[\sigma(1-\rho)\left[\beta_e\frac{B}{\kappa+B} + \beta_h I\right] + \mu\right] \\ & - \lambda_I\left[\sigma(1-\rho)\left[\beta_e\frac{B}{\kappa+B} + \beta_h I\right]\right],\end{aligned} \tag{37}$$

$$\begin{aligned}\frac{d\lambda_I}{dt} = {} & -1 - c_{31}\tau + \lambda_S(1-\rho)\beta_h S + \lambda_V\sigma(1-\rho)\beta_h V \\ & - \lambda_I[(1-\rho)\beta_h(S+\sigma V) - (\tau+\gamma+\mu)] - \lambda_B\xi,\end{aligned} \tag{38}$$

$$\begin{aligned}\frac{d\lambda_B}{dt} = {} & -c_{41}\nu + \lambda_S(1-\rho)\beta_e\frac{\kappa S}{(\kappa+B)^2} + \lambda_V\sigma(1-\rho)\beta_e\frac{\kappa V}{(\kappa+B)^2} \\ & - \lambda_I(1-\rho)\beta_e\frac{\kappa(S+\sigma V)}{(\kappa+B)^2} + \lambda_B(\delta+\nu),\end{aligned} \tag{39}$$

with transversality conditions (i.e., final time conditions):

$$\lambda_S(T_1) = 0, \quad \lambda_V(T_1) = 0, \quad \lambda_I(T_1) = 0, \quad \lambda_B(T_1) = 0. \tag{40}$$

The characterizations of the optimal controls, $\phi^*(t)$, $\tau^*(t)$, and $\nu^*(t)$, are based on the conditions

$$\frac{\partial \mathcal{H}}{\partial \phi} = 0, \quad \frac{\partial \mathcal{H}}{\partial \tau} = 0, \quad \frac{\partial \mathcal{H}}{\partial \nu} = 0, \tag{41}$$

respectively, subject to the constraints given in (34). Thus we have

$$\phi^*(t) = \max[0,\ \min(\tilde{\phi}(t),\ \phi_{\max})], \tag{42}$$

$$\tau^*(t) = \max[0,\ \min(\tilde{\tau}(t),\ \tau_{\max})], \tag{43}$$

$$\nu^*(t) = \max[0,\ \min(\tilde{\nu}(t),\ \nu_{\max})], \tag{44}$$

where $\tilde{\phi}(t) = [(\lambda_S - \lambda_V - c_{21})S(t)] / (2c_{22})$, $\tilde{\tau}(t) = [(\lambda_I - c_{31})I(t)] / (2c_{32})$, $\tilde{\nu}(t) = [(\lambda_B - c_{41})B(t)] / (2c_{42})$.

To summarize, our optimal control problem consists of the state system (1) with initial conditions, the adjoint Eqs. (36)–(39) with the transversality conditions, and Eqs. (42)–(44) to characterize the optimal controls. Such a problem has to be solved numerically. We apply the forward-backward sweep method [26] to solve it in an iterative manner. This algorithm is briefly described as follows. First, the state equations are solved forward in time by a fourth-order Runge–Kutta method, with an initial guess for the control variables. Next, the adjoint equations are solved backward in time using the solutions of the state equations. The control is then updated with the new values of the state and adjoint solutions, and the process is repeated until the solutions converge.

Table 2.

Cholera model parameters and values.

Parameter	Symbol	Value	Source
Total population	N	10,000	-
Natural human birth and death rate	μ	$(43.5 \text{ years})^{-1}$	[52]
Concentration of *V. cholerae* in environment	κ	10^6 cells/ml	[12]
Rate of recovery from cholera	γ	$(5 \text{ day})^{-1}$	[20]
Rate of human contribution to *V. cholerae*	ξ	10 cells/ml-day	[20]
Death rate of vibrios in the environment	δ	$(30 \text{ days})^{-1}$	[20]
Ingestion rate from the environment	β_e	0.075/day	[34]
Ingestion rate through human-human interaction	β_h	0.00011/day	[34]

To carry out the numerical simulation, we list the values for the various transmission rates in the state Eq. (1) in Table 2. Meanwhile, we assume that the unit costs for vaccination and treatment are about the same, whereas the cost for per percent reduction of vibrio concentration through sanitation is doubled. We further assume that for each control, the per capita cost at the quadratic level is about 20% of that at the linear level. Thus, we assign the following set of values (with appropriate units) to the cost parameters in (35):

$$c_{21} = 50, \quad c_{22} = 10, \quad c_{31} = 50, \quad c_{32} = 10, \quad c_{41} = 100, \quad c_{42} = 20. \tag{45}$$

Based on practical observations and empirical values [51] and [52], we set the upper bounds of the rates for the three controls as $\phi_{max} = 0.7, \tau_{max} = 0.5, \text{ and } \nu_{max} = 0.1$. We also set the initial infection

number $I(0) = 1000$ and the entire period of time T = 100 days. Fig. 4 (a) shows the infection curves for the model without controls (dashed line), i.e., $\phi(t) = \tau(t) = \nu(t) = 0$, and that with the optimal controls implemented (solid line). We clearly see that the number of infections has been significantly reduced due to the incorporation of the three types of controls. Here we also present the case with vaccination being the only control measure; in this case the optimal control problem is reformulated to determine the optimal strategy for vaccination, by setting $\tau(t) = \nu(t) = 0$ and using the same cost parameters for vaccination. The infection curve with this vaccination-only strategy is shown in Fig. 4(a) with the dash-dot line. We observe that with vaccination only, the infections still reach a high level, though the peak value is lower than that without controls. This is an evidence that multiple intervention methods, which target both the direct and indirect transmission routes of cholera, would achieve better results than a single control such as vaccination only. This result is consistent with the observation from our sensitivity analysis in Section 5. Fig. 4(b)–(d) further show the profile of each of the three controls in their optimal balance. We observe that both the vaccination rate and the treatment rate start with their maximum values and remain at that level for a number of days (about 7 days for vaccination, and 35 days treatment), before decreasing to lower levels of strength. The pattern is similar for sanitation, except that the start of maximum sanitation rate lags for 1–2 days.

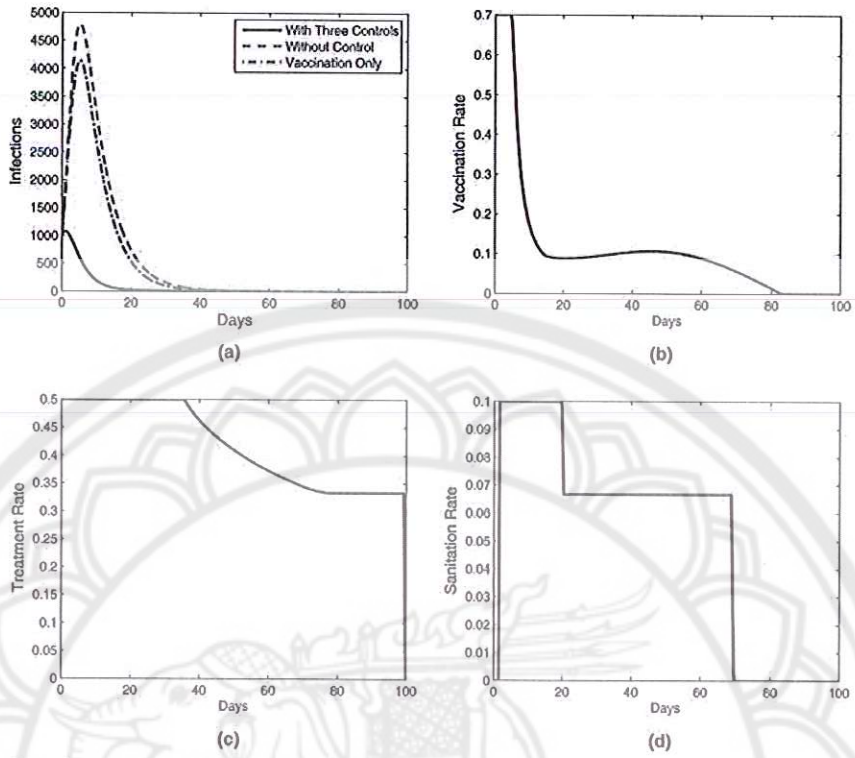

Fig. 4.

Optimal control simulation results based on the cost parameters in (45): (a) Infection curves for the cholera model without control, with three controls in optimal balance, and with vaccination only; (b) the optimal vaccination rate; (c) the optimal treatment rate; (d) the optimal sanitation rate.

As can be naturally expected, the costs of these controls directly affect the strength and duration of the controls in their optimal balance. For demonstration, we now assume that the linear per capita costs for vaccination and treatment (i.e., c_{21} and c_{31}) can be significantly reduced compared to those in (45), and consider the following cost parameters:

$$c_{21} = 2, \quad c_{22} = 10, \quad c_{31} = 2, \quad c_{32} = 10, \quad c_{41} = 100, \quad c_{42} = 20. \tag{46}$$

This set of cost parameters lead to improved control results. The reason is that with lower costs for vaccination and treatment, these two controls can be

implemented with higher average strength and longer duration, thus further reducing the infections. Indeed, Fig. 5 show the profiles for the optimal vaccination and treatment rates in this case, where we see that the vaccination and treatment rates remain at their maximum levels for about 12 days and 60 days, respectively; both are significantly longer than those in Fig. 4. In addition, the vaccination rate now stays at the level of 0.3 from day 20 until near the end of the time interval.

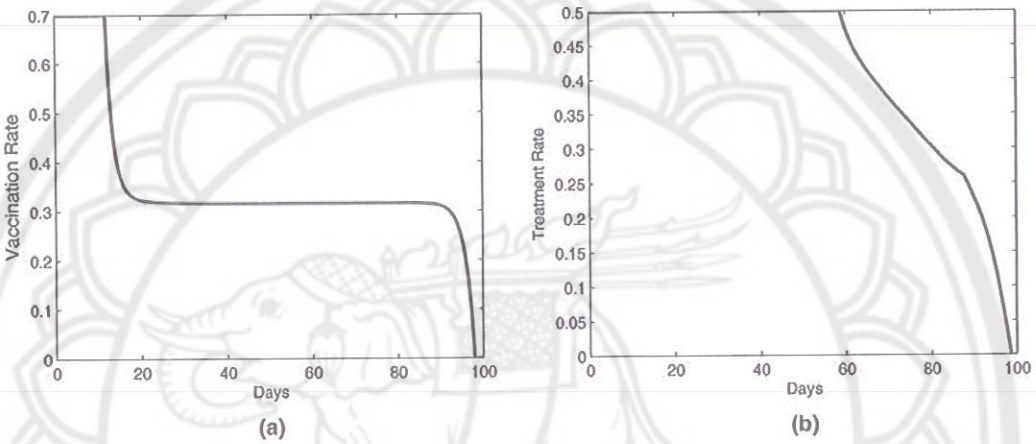

Fig. 5.

Optimal control profiles based on the cost parameters in (46): (a) the optimal vaccination rate; (b) the optimal treatment rate.

Chapter 4

Conclusion

Cholera is currently in its seventh pandemic and remains a growing public health problem in different parts of the world, with outbreaks showing complex patterns, partly explained with changes in the organisms [36] and [40]. Despite the available knowledge on its prevention and treatment, the disease is emerging as one of the leading cause of mortality in developing countries. Successful control and/or eradication of the disease requires good understanding of the biological, epidemiological and environmental factors shaping these outbreaks. Infectious disease modeling helps understand the mechanisms influencing disease transmission dynamics. With the continued and increasing burden of cholera there is need to prioritize the implementation and use of different public health control measures. Effective control of cholera requires investment in long-term provision of public-sector clean water and adequate sanitation, but achieving these in epidemic and emergence setting is impossible. The proposed use of cholera vaccines in these settings to complement disease control has suffered a lot of debates on the effectiveness [11] and associated logistic, financial and human resources challenges during outbreaks [15]. These challenges call for the need to assess the optimal requirement of each intervention measure when considered as a package.

The focus of this study is to better understand the effects of different control strategies coupled with multiple transmission pathways of cholera, using a mathematical model that fully captures the epidemiology and pathogenesis of the disease in order to comprehensively explore the usefulness of public health control measures towards effective response to cholera epidemics in resource constrained settings. The model consists of three types of public health controls: vaccination, treatment, and sanitation. Comprehensive mathematical analysis of the model using both analytical and numerical approaches is carried out and

presented. The mathematical results demonstrate that despite including vaccination in a framework that has previously shown backward bifurcation [21], our model does not exhibit such a phenomenon and retains R_0 as an epidemic threshold governing the dynamics of the model system. This model shows that the unity of R_0 as quantitative statistic to quantify the amount of control effort required to contain epidemic cholera is not compromised. Thus even with public health interventions, cholera epidemics and endemism could still occur and the disease could persist, if the controls are not strong enough to reduce R_0 to values below unity.

In order to assess the effectiveness of implementing the proposed package of public health controls, we have also performed a preliminary study based on optimal control theory to seek cost-effective solutions by assuming these interventions are time-dependent. Optimal control techniques have vastly been used to determine effectiveness of control strategies of infectious disease dynamics [16], [23], [24],[25] and [26]. Our results suggest that different controls (such as vaccination and treatment) closely interplay with each other, and the costs of controls directly affect the length and strength of each control in an optimal strategy. We have found that due to the multiple transmission routes of cholera, a combination of multiple intervention methods achieves better results than a single-strategy approach.

Effective control and/or eradication of cholera in the developing world remains a public health challenge because of the complex biological, epidemiological, and environmental factors that contribute to the dynamics of the disease. The recognition of cholera burden combined with efforts to implement efficient control measures have become critical with the growing trends in cholera incidence in developing countries, and require a comprehensive and integrated strategy to implement public health control measures. The present paper, through careful mathematical modeling and analysis, contributes to the basic knowledge of cholera transmission dynamics and helps improve our understanding of the effects

and limitations of these public health interventions. In addition, the current study can be extended by a number of ways. Our model assumes that the vaccine efficacy σ and sanitation-induced preventability ρ are constants, whereas in reality both decrease after several months, thus time-dependent. It would be worthwhile to incorporate this aspect into model analysis and optimal control study to address the long-term dynamics of cholera with interventions. Meanwhile, we have assumed that all the control measures, including vaccination, can be implemented from the very beginning of disease outbreak. Practically, an important question is to assess the value of cholera vaccination in controlling ongoing outbreaks [15], and guidelines for vaccine use in cholera outbreaks in post-disaster settings are still to be established. A careful mathematical analysis and optimal control study for delayed deployment of cholera vaccine would shed light on this question.

References

[1] J.R. Andrews, S. Basu, Transmission dynamics and control of cholera in haiti: an epidemic model, Lancet 377 (2011) 1248–1255.

[2] E. Asano, L.J. Gross, S. Lenhart, L.A. Real, Optimal control of vaccine distribution in a rabies metapopulation model, Math. Biosci. Eng. 5 (2008) 219–238.

[3] E. Bertuzzo, et al., Prediction of the spatial evolution and effects of control measures for the unfolding haiti cholera outbreak, Geophys. Res. Lett. 38 (2011) L06403.

[4] S.M. Blower, H. Dowlatabadi, Sensitivity and uncertainty analysis of complex models of disease transmission: an hiv model, as an example, Int. Stat. Rev. 62 (1994) 229–243.

[5] B. Buonomo, A simple analysis of vaccination strategies for rubella, Math. Biosci. Eng. 8 (2011) 677–687.

[6] G.J. Butler, P. Waltman, Persistence in dynamical systems, Proc. Am. Math. Soc. 96 (1986) 425–430.

[7] V. Capasso, S.L. Paveri-Fontana, A mathematical model for the 1973 cholera epidemic in the european mediterranean region, Rev. Dépidémol. Publ. 27 (1979) 121–132.

[8] C. Castillo-Chavez, Z. Feng, W. Huang, On the computation of $\mathcal{R}_0$ and its role on global stability, Mathematical Approaches for Emerging and\ Reemerging Infectious Diseases: An Introduction, IMA vol. 125, Springer-Verlag, 2002.

[9] C. Castillo-Chavez, B. Song, Dynamical models of tuberculosis and their applications, Math. Biosci. Eng. 1 (2004) 361–404.

[10] D.L. Chao, M.E. Halloran, I.M. Longini, Vaccination strategies for epidemic cholera in haiti with implications for the developing world, Proc. Natl. Acad. Sci. U.S.A. 108 (2011) 7081–7085.

[11] Cholera vaccines: who position paper, WKly Epidemiol. Rec. 85 (117–128) (2010).

[12] C.T. Codeço, Endemic and epidemic dynamics of cholera: the role of the aquatic reservoir, BMC Infect. Dis. 1 (2001) 1.

[13] W.A. Coppel, Stability and Asymptotic Behavior of Differential Equations, Heath Mathematical Monographs, DC Heath, Boston, 1965.

[14] S. Cumberland, An old enemy returns, Bull. World Health Organ. 87 (2009) 85–86.

[15] K.A. Date, et al., Consideration for oral cholera vaccine use during outbreak after earthquake in haiti, 2010–2011, Emerg. Infect. Dis. 17 (11) (2011).
[16] K.R. Fister, S. Lenhart, J.S. McNally, Optimizing chemothearpy in an hiv model, Electron. J. Differ. Equ. 32 (1998) 1–12.
[17] W.H. Fleming, R.W. Rishel, Deterministic and Stochastic Optimal Control, Springer, New York, 1975.
[18] H.I. Freedman, S. Ruan, M. Tang, Uniform persistence and flows near a closed positively invariant set, J. Dyn. Differ. Eq. 6 (1994) 583–600.
[19] A.B. Gumel, C.C. McCluskey, J. Watmough, An SVEIR model assessing potential impact of an imperfect anti-SARS vaccine, Math. Biosci. Eng. 3 (2006) 485–512.
[20] D.M. Hartley, J.G. Morris, D.L. Smith, Hyperinfectivity: a critical element in the ability of v. cholerae to cause epidemics? PLoS Med. 3 (2006) 0063–0069.
[21] C.M. Kribs-Zaleta, J.X. Velasco-Hernandez, A simple vaccination model with multiple endemic states, Math. Biosci. 164 (2000) 183–201.
[22] R.I. Joh, H. Wang, H. Weiss, J.S. Weitz, Dynamics of indirectly transmitted infectious diseases with immunological threshold, Bull. Math. Biol. 71 (2009) 845–862.
[23] H.R. Joshi, Optimal control of an hiv immunology model, Optim. Control Appl. Methods 23 (2002) 199–213.
[24] E. Jung, S. Lenhart, Z. Feng, Optimal control of treatments in a two-strain tuberculosis model, Discrete Contin. Dyn. Syst., Ser. B 2 (4) (2002) 473–482.
[25] D. Kirschner, G.F. Webb, A model for treatment strategy in the chemotherapy of aids, Bull. Math. Biol. 58 (2) (1996) 367–390.
[26] S. S. Lenhart, J. Workman, Optimal control applied to biological models, Chapman Hall/CRC, 2007.
[27] M.Y. Li, J.R. Graef, L. Wang, J. Karsai, Global dynamics of a seir model with varying total population size, Math. Biosci. 160 (1999) 191–213.
[28] M.Y. Li, J.S. Muldowney, A geometirc approach to global-stability problems, SIAM J. Mathe. Anal. 27 (1996) 1070–1083.
[29] M.Y. Li, H.L. Smith, L. Wang, Global dynamics of an seir epidemic model with vertical transmission, SIAM J. Math. Anal. 62 (2001) 58–69.
[30] S. Liao, J. Wang, Stability analysis and application of a mathematical cholera model, Math. Biosci. Eng. 8 (2011) 733–752.
[31] P.R. Mason, Zimbabwe experiences the worst epidemic of cholera in africa, J. Infect. Dev. Ctries. 3 (2009) 148–151.

[32] D.S. Merrell, et al., Host-induced epidemic spread of the cholera bacterium, Nature 417 (2002) 642–645.
[33] J.G. Morris Jr., Cholera: modern pandemic disease of ancient lineage, Emerg. Infect. Dis. 17 (11) (2011).
[34] Z. Mukandavire, S. Liao, J. Wang, H. Gaff, D.L. Smith, J.G. Morris, Estimating the reproductive numbers for the 2008-2009 cholera outbreaks in zimbabwe, Proc. Nat. Acad. Sci. U.S.A. 108 (2011) 8767–8772.
[35] S. Marino, I. Hogue, C.J. Ray, D.E. Kirschner, A methodology for performing global uncertainty and sensitivity analysis in system biology, J. Theor. Biol. 254 (2008) 178–196.
[36] G.B. Nair, et al., New variants of Vibrio cholerae O1 biotype El Tor with attributes of the classical biotype from hospitalized patients with acute diarrhea in bangladesh, J. Clin. Microbiol. 40 (2002) 3296–3299.
[37] R.L.M. Neilan, E. Schaefer, H. Gaff, K.R. Fister, S. Lenhart, Modeling optimal intervention strategies for cholera, Bull. Math. Biol. 72 (2010) 2004–2018.
[38] E.J. Nelson, J.B. Harris, J.G. Morris, S.B. Calderwood, A. Camilli, Cholera transmission: the host, pathogen and bacteriophage dynamics, Nat. Rev.: Microbiol. 7 (2009) 693–702.
[39] L.S. Pontryagin, V.G. Boltyanski, R.V. Gamkrelize, E.F. Mishchenko, The Mathematical Theory of Optimal Processes, Wiley, New York, 1967.
[40] A. Safa, G.B. Nair, R.Y.C. Kong, Evolution of new variants of Vibrio cholerae O1, Trends Microbiol. 18 (2010) 46–54.
[41] S. Shin, S.N. Desai, B.K. Sah, J.D. Clemence, Oral vaccines against cholera, Clin. Infect. Dis. 52 (11) (2011) 1343–1349.
[42] Z. Shuai, J.H. Tien, P. van den Driessche, Cholera models with hyperinfectivity and temporary immunity, Bull. Math. Biol 74 (2012) 2423–2445.

[43] Z. Shuai, P. van den Driessche, Global dynamics of cholera models with differential infectivity, Math. Biosci. 234 (2011) 118–126.
[44] Z. Shuai, P. van den Driessche, Global stability of infectious disease models using lyapunov functions, SIAM J. Appl. Math. 73 (2013) 1513–1532.
[45] J.P. Tian, J. Wang, Global stability for cholera epidemic models, Math. Biosci. 232 (2011) 31–41.
[46] J.H. Tien, D.J.D. Earn, Multiple transmission pathways and disease dynamics in a waterborne pathogen model, Bull. Math. Biol. 72 (2010) 1502–1533.
[47] A.L. Tuite, et al., Cholera epidemic in haiti, 2010: Using a transmission model to explain spatial spread of disease and identify optimal control interventions, Ann. Intern. Med. 154 (2011) 293–302.
[48] P. van den Driessche, J. Watmough, Reproduction numbers and sub-threshold endemic equilibria for compartmental models of disease transmission, Math. Biosci. 180 (2002) 29–48.
[49] J. Wang, S. Liao, A generalized cholera model and epidemic-endemic analysis, J. Biol. Dyn. 6 (2) (2012) 568–589.
[50] X. Zhou, J. Cui, Z. Zhang, Global results for a cholera model with imperfect vaccination, J. Franklin Int. 349 (2012) 770–791.
[51] Center for Disease Control and Prevention, web page: www.cdc.gov.
[52] World Health Organization (WHO), web page: www.who.org.
[53] WHO Cholera-fact sheet number 107: February 2014. http://www.who.int/mediacentre/factsheets/fs107/en/.
[54] WHO report on global surveillance of epidemic-prone infectious diseases, 2000, pp. 39–54. http://www.who.int/csr/resources/publications/surveillance/WHO_Report_Infectious_Diseases.pdf.

Output ที่ได้จากโครงการ

1. ได้ผลงานตีพิมพ์ในวารสารวิชาการนานาชาติ

Drew Posny, Jin Wang, Zindoga Mukandavire, Chairat Modnak, "Analyzing transmission dynamics of cholera with public health interventions," Mathematical Biosciences, vol. 264, Article ID 0025-5564, 16 pages, 2015. doi:10.1016/j.mbs.2015.03.006 (Impact Factor 1.303 (2014))

ภาคผนวก

ประกอบด้วย

1. ผลงานตีพิมพ์ในวารสารวิชาการนานาชาติ เรื่อง

. Analyzing transmission dynamics of cholera with public health interventions

Mathematical Biosciences 264 (2015) 38–53

Contents lists available at ScienceDirect

Mathematical Biosciences

journal homepage: www.elsevier.com/locate/mbs

Analyzing transmission dynamics of cholera with public health interventions

Drew Posny[a], Jin Wang[a,*], Zindoga Mukandavire[b], Chairat Modnak[c]

[a] Department of Mathematics and Statistics, Old Dominion University, Norfolk, VA 23529, USA
[b] Social and Mathematical Epidemiology Group, London School of Hygiene and Tropical Medicine, London, UK
[c] Department of Mathematics, Naresuan University, Phitsanulok 65000, Thailand

ARTICLE INFO

Article history:
Received 13 July 2014
Revised 20 March 2015
Accepted 23 March 2015
Available online 28 March 2015

Keywords:
Cholera model
Disease control
Stability
Optimal control

ABSTRACT

Cholera continues to be a serious public health concern in developing countries and the global increase in the number of reported outbreaks suggests that activities to control the diseases and surveillance programs to identify or predict the occurrence of the next outbreaks are not adequate. These outbreaks have increased in frequency, severity, duration and endemicity in recent years. Mathematical models for infectious diseases play a critical role in predicting and understanding disease mechanisms, and have long provided basic insights in the possible ways to control infectious diseases. In this paper, we present a new deterministic cholera epidemiological model with three types of control measures incorporated into a cholera epidemic setting: treatment, vaccination and sanitation. Essential dynamical properties of the model with constant intervention controls which include local and global stabilities for the equilibria are carefully analyzed. Further, using optimal control techniques, we perform a study to investigate cost-effective solutions for time-dependent public health interventions in order to curb disease transmission in epidemic settings. Our results show that the basic reproductive number ($\mathcal{R}_0$) remains the model's epidemic threshold despite the inclusion of a package of cholera interventions. For time-dependent controls, the results suggest that these interventions closely interplay with each other, and the costs of controls directly affect the length and strength of each control in an optimal strategy.

© 2015 Elsevier Inc. All rights reserved.

1. Introduction

Cholera, a severe intestinal infectious disease caused by the bacterium *Vibrio cholerae*, remains a serious public health threat in developing countries. The persistence of cholera epidemics has been evidenced by recent outbreaks in Haiti (2010–2011), Nigeria (2010), Vietnam (2009), Zimbabwe (2008–2009), among others. It is estimated that there are 3–5 million cases of cholera infection each year [51,52]. The growing burden of cholera has revived research interests on the disease and attempts to establish realistic goals to control the disease in the developing world.

The transmission of cholera involves both direct (human-to-human) and indirect (environment-to-human) routes, due to the multiple interactions between the human host, the pathogen, and the environment [38]. In order to better understand the complex transmission dynamics of cholera, a number of mathematical models have been proposed and analyzed in recent years [1,3,10,12,20,22,30,34,42,43,45–47,49]; among these several models have been driven by the cholera outbreaks in Haiti [1,3,10,47]. In particular, Codeço [12] published a model that incorporated the environmental component into a regular SIR epidemiological model, building on the previous work in [7]. In [12], a saturation incidence given by $a\frac{B}{\kappa+B}$ was used to model the infection from the environment, where B is the concentration of cholera vibrios, a is the rate of exposure to contaminated environment and κ is the half saturation concentration of environmental vibrios.

Recently, Mukandavire et al. [34] proposed a new model framework to study the 2008–2009 cholera outbreaks in Zimbabwe. The model explicitly considered environment-to-human and human-to-human transmission routes with human-to-human transmission being defined in the context of infection by hyperinfectious vibrios [20,32,33,38]. The incidence term was modeled as $\beta_e\frac{B}{\kappa+B}+\beta_h I$ where I is the number of infected individuals, β_e and β_h are rates of exposure to environmental and hyperinfectious vibrios respectively. The results in [34] elucidates the importance of human-to-human transmission in shaping cholera epidemics in non-riverine/estuarine environments such as Zimbabwe.

* Corresponding author at: Department of Mathematics, University of Tennessee at Chattanooga, Chattanooga, TN 37403, USA.
E-mail address: J3Wang@odu.edu (J. Wang).

http://dx.doi.org/10.1016/j.mbs.2015.03.006
0025-5564/© 2015 Elsevier Inc. All rights reserved.

Cholera can be successfully controlled by provision of clean water with adequate sanitation and appropriate treatment of patients. However, water and sanitation investments which are the key for long-term cholera prevention and control are usually not possible in most cholera epidemic and emergency settings. The availability of effective oral cholera vaccines have renewed interests in the use of vaccines for cholera control [41] with overwhelming evidence supporting their effectiveness in endemic settings. In 2010, WHO recommended the use of vaccines in cholera endemic settings and preemptively during outbreaks and emergency settings [11]. However, guidelines on the use of vaccines in cholera epidemic and emergency settings are urgently needed [15]. Cholera is usually an easily treatable disease and many cases can be successfully treated using oral rehydration salts. Basic oral rehydration salts (salt, sugar, and clean water) are credited for preventing 40 million deaths since they were formally endorsed by WHO with the ability of reducing case fatality rates below 1% if properly administered [53,54]. However such a basic therapy may not even be available in some cholera epidemic and emergency settings [14,31]. Antibiotics are recommended for use in very severe cases and their effects in mass administration are unclear, as they contribute to increasing antimicrobial resistance [53]. In the present paper, we extend our model in [34] to theoretically assess the utility of a holistic approach to intervention strategies in responding to cholera outbreaks and explore optimal strategy for disease control. This study includes testing the robustness of the proposed model as a simple and effective tool for understanding cholera transmission dynamics and control. A package of public health cholera control measures consisting of vaccination, treatment (including oral rehydration, antibiotics, etc.), and water sanitation is considered. We begin by analyzing an autonomous version of the model system with constant controls and carry out rigorous mathematical analysis of the system. Further, we consider a model system with time-dependent controls to examine the optimal implementation of the intervention measures by assessing their effects and costs.

In the remainder of this paper, we will first present the cholera model with control measures incorporated. We will then conduct an equilibrium analysis for the epidemic and endemic dynamics of the system when the controls are constant. Following a sensitivity analysis of the model parameters, we will turn to the time-dependent control system and perform an optimal control study for the cholera model. Finally we round up the paper by conclusion and discussion.

2. Cholera model

We modify the model of Mukandavire et al. [34] by adding three disease control measures: vaccination, treatment, and water sanitation, and by introducing a new class of vaccinated people. Thus, our model classifies the human population, denoted by N, into the susceptibles (S), the vaccinated (V), the infected or infectives (I), and the recovered (R).

We assume that individuals are born and die at an average rate μ. The concentration of vibrios in contaminated water is denoted by B. Susceptible individuals acquire cholera infection either by ingesting environmental vibrios from contaminated aquatic reservoirs or through human-to-human transmission, at rates $\lambda_e = (1-\rho)\frac{\beta_e B}{\kappa+B}$ and $\lambda_h = (1-\rho)\beta_h I$ respectively, with the subscripts e and h denoting environment-to-human and human-to-human transmissions. Here, κ is the pathogen concentration that yields 50% chance of infection cholera, $\rho = \varepsilon p$ is the sanitation-induced preventability to cholera infection which is a product of the sanitation efficacy ε and compliance p. We further assume that susceptible individuals are vaccinated at a rate $\phi(t)$, where t is the time variable, with a vaccine that has a degree of protection $\sigma = (1-\varepsilon)$, where ε is the vaccine efficacy. Infected individuals are treated at a rate $\tau(t)$, and some recover naturally at a rate γ into the recovered class. Infected individuals contribute to *V. cholerae* in the aquatic environment at a rate ξ, and vibrios have a net death rate δ in the environment. In addition, water sanitation leads to the death of vibrios at a rate $\nu(t)$. As mentioned before, the case fatality rates for cholera generally are pretty low (at or below 1%) even just the simple oral hydration is administered [53]; hence we assume cholera-induced mortality can be neglected in this study.

We thus have the following system of differential equations describing the cholera dynamics with controls:

$$\begin{cases} \dfrac{dS}{dt} = \mu N - (1-\rho)\left[\beta_e \dfrac{B}{\kappa+B} + \beta_h I\right] S - (\phi(t)+\mu)S, \\ \dfrac{dV}{dt} = \phi(t)S - \sigma(1-\rho)\left[\beta_e \dfrac{B}{\kappa+B} + \beta_h I\right] V - \mu V, \\ \dfrac{dI}{dt} = (1-\rho)\left[\beta_e \dfrac{B}{\kappa+B} + \beta_h I\right](S+\sigma V) - (\tau(t)+\gamma+\mu)I, \\ \dfrac{dB}{dt} = \xi I - (\delta+\nu(t))B, \end{cases} \tag{1}$$

together with

$$\frac{dR}{dt} = (\tau(t)+\gamma)I - \mu R. \tag{2}$$

Since N, the total population, is fixed such that $N = S + V + I + R$, we will not need Eq. (2) in our model analysis.

In general, $\phi(t)$, $\tau(t)$, and $\nu(t)$ are functions of t, representing non-uniform and time-dependent controls. For the special case when the rates of all the three controls are positive constants, i.e.,

$$\phi(t) = \phi > 0, \quad \tau(t) = \tau > 0, \quad \text{and} \quad \nu(t) = \nu > 0, \tag{3}$$

the model (1) is reduced to an autonomous system. This allows us to conduct a careful equilibrium analysis, in Sections 3 and 4, on both the disease-free and endemic equilibria. It is clear to see that in this case, the feasible region of the system (1) is

$$\Omega = \left\{ (S,V,I,B) \,\middle|\, S \geq 0,\ V \geq 0,\ I \geq 0,\ 0 \leq S+V+I \leq N,\ 0 \leq B \leq \frac{\xi N}{\delta+\nu} \right\} \tag{4}$$

which is positively invariant for the flow of the system (1).

3. Disease-free equilibrium

With constant controls, the disease-free equilibrium (DFE) of the system (1) is given by

$$X_0 = \left(\frac{\mu N}{\phi+\mu}, \frac{\phi N}{\phi+\mu}, 0, 0\right). \tag{5}$$

For convenience, let us denote

$$E = (1-\rho)\beta_e, \quad H = (1-\rho)\beta_h, \quad T = \tau+\gamma+\mu. \tag{6}$$

The Jacobian matrix of the system (1) is

$$J = \begin{bmatrix} -\frac{EB}{\kappa+B} - HI - (\phi+\mu) & 0 & -HS & -\frac{E\kappa S}{(\kappa+B)^2} \\ \phi & -\frac{\sigma EB}{\kappa+B} - \sigma HI - \mu & -\sigma HV & -\frac{\sigma E\kappa V}{(\kappa+B)^2} \\ \frac{EB}{\kappa+B} + HI & \frac{\sigma EB}{\kappa+B} + \sigma HI & H(S+\sigma V) - T & \frac{E\kappa(S+\sigma V)}{(\kappa+B)^2} \\ 0 & 0 & \xi & -(\delta+\nu) \end{bmatrix}. \tag{7}$$

We obtain the characteristic polynomial by evaluating the Jacobian (7) at the DFE (5),

$$\Delta = (\lambda+\phi+\mu)(\lambda+\mu) \times \left[\left(\lambda - \frac{H(\mu+\sigma\phi)N}{\phi+\mu} + T\right)(\lambda+\delta+\nu) - \frac{\xi E(\mu+\sigma\phi)N}{\kappa(\phi+\mu)}\right]. \tag{8}$$

It is clear that (8) has two negative roots $\lambda = -(\phi+\mu)$ and $\lambda = -\mu$. Note that we may expand the last factor of (8) such that it has the form

$$a_0\lambda^2 + a_1\lambda + a_2 = 0, \tag{9}$$

where

$$a_0 = 1, \quad a_1 = \delta + \nu + T - \frac{H(\mu + \sigma\phi)N}{\phi + \mu},$$

$$a_2 = (\delta + \nu)\left(T - \frac{H(\mu + \sigma\phi)N}{\phi + \mu}\right) - \frac{\xi E(\mu + \sigma\phi)N}{\kappa(\phi + \mu)}.$$

From the well-known Routh–Hurwitz stability criterion, the necessary and sufficient conditions for a stable quadratic are $a_0 > 0, a_1 > 0, a_2 > 0$. Clearly, $a_0 > 0$ is satisfied and if $a_2 > 0$, then it must be true that $a_1 > 0$. Therefore, we obtain a threshold value on N:

$$N < \frac{T\kappa(\delta + \nu)(\phi + \mu)}{(\kappa(\delta + \nu)H + \xi E)(\mu + \sigma\phi)} \tag{10}$$

such that $a_2 > 0$. Hence, the DFE (5) is locally stable under the condition (10).

Eq. (10) implies that the basic reproduction number for the model with constant controls is given by

$$\mathcal{R}_0(\phi, \nu, \tau) = \frac{(\kappa(\delta + \nu)H + \xi E)(\mu + \sigma\phi)}{T\kappa(\delta + \nu)(\phi + \mu)} Nw. \tag{11}$$

This result can also be obtained through the standard next-generation matrix approach [48], by noting that

$$\begin{bmatrix} \frac{dI}{dt} \\ \frac{dB}{dt} \end{bmatrix} = \mathcal{F} - \mathcal{V} = \begin{bmatrix} (1-\rho)\left(\beta_e \frac{B}{\kappa + B} + \beta_h I\right)(S + \sigma V) \\ 0 \end{bmatrix} - \begin{bmatrix} (\tau + \gamma + \mu)I \\ (\delta + \nu)B - \xi I \end{bmatrix}, \tag{12}$$

with the next-generation matrices

$$\widehat{F} = \begin{bmatrix} \frac{H(\mu+\sigma\phi)N}{\phi+\mu} & \frac{E(\mu+\sigma\phi)N}{\kappa(\phi+\mu)} \\ 0 & 0 \end{bmatrix} \quad \text{and} \quad \widehat{V} = \begin{bmatrix} \tau + \gamma + \mu & 0 \\ -\xi & \delta + \nu \end{bmatrix}. \tag{13}$$

Then $\mathcal{R}_0$ is determined by the spectral radius of the matrix $\widehat{F}\widehat{V}^{-1}$.

Biologically speaking, $\mathcal{R}_0 = 1$ provides a threshold for disease epidemics: if $\mathcal{R}_0 < 1$, the disease will die out; if $\mathcal{R}_0 > 1$, the disease will typically spread. Mathematically, based on the result in [48], we have the following theorem.

Theorem 1. *With constant controls, the DFE (5) is locally asymptotically stable when $\mathcal{R}_0 < 1$, and unstable when $\mathcal{R}_0 > 1$.*

We mention that the basic reproduction number for the original model in [34] is given by

$$\widetilde{\mathcal{R}}_0 = \frac{N}{\delta\kappa(\gamma + \mu)}[\xi\beta_e + \delta\kappa\beta_h]. \tag{14}$$

Comparing the expressions in (11) and (14), we note that

$$\mathcal{R}_0 < \widetilde{\mathcal{R}}_0 \tag{15}$$

for all $\phi > 0$, $\tau > 0$, and $\nu > 0$, due to the effects of disease controls.

Theorem 1 states that if the strengths of the (constant) controls are strong enough to reduce the basic reproduction number below 1, then cholera will be eradicated. Otherwise, a cholera epidemic would occur, though with a lower infection level than that without controls owing to the reduced value of the reproduction number.

Indeed, the DFE is also globally asymptotically stable when $\mathcal{R}_0 < 1$. We prove this by using the global stability result established in [8]. For completeness, we have included the result in Appendix A, Theorem 8.

Applying Theorem 8 to the model (1), we have that

$$F(X_1, 0) = \begin{bmatrix} \frac{dS}{dt} \\ \frac{dV}{dt} \end{bmatrix}_{(X_1,0)} = \begin{bmatrix} \mu N - (\phi + \mu)S \\ \phi S - \mu V \end{bmatrix}. \tag{16}$$

It follows from solving these differential equations that $S(t) = \frac{\mu N}{\phi+\mu} + C_1 e^{-(\phi+\mu)t}$ and $V(t) = \frac{\phi N}{\phi+\mu} + C_2 e^{-\mu t} + C_3 e^{-(\phi+\mu)t}$ for some constants C_1, C_2 and C_3. Hence, $S(t) \to \frac{\mu N}{\phi+\mu}$ and $V(t) \to \frac{\phi N}{\phi+\mu}$ as $t \to \infty$, showing that X_1^E is globally asymptotically stable and condition 1 holds.

Now, consider

$$G(X_1, X_2) = AX_2 - \hat{G}(X_1, X_2) \tag{17}$$

where $A = \frac{\partial G}{\partial X_2}(X_1^E, 0)$. Specifically,

$$A = \begin{bmatrix} H(S + \sigma V) - T & \frac{E\kappa(S+\sigma V)}{(\kappa+B)^2} \\ \xi & -(\delta + \nu) \end{bmatrix}_{(X_1^E,0)} = \begin{bmatrix} \frac{H(\mu+\sigma\phi)N}{\phi+\mu} - T & \frac{E(\mu+\sigma\phi)N}{\kappa(\phi+\mu)} \\ \xi & -(\delta + \nu) \end{bmatrix}, \tag{18}$$

where the off-diagonal elements are obviously non negative. Substituting into (17) gives,

$$\hat{G}(X_1, X_2) = \begin{bmatrix} \frac{(\mu+\sigma\phi)EB^2N}{\kappa(\kappa+B)(\phi+\mu)} \\ 0 \end{bmatrix} \geq 0. \tag{19}$$

Thus, condition 2 holds as well.

Summarizing these results, we obtain the theorem below.

Theorem 2. *When $\mathcal{R}_0 < 1$, the DFE of the system (1) with constant controls is globally asymptotically stable.*

In addition, the following result now can be easily derived.

Theorem 3. *When $\mathcal{R}_0 > 1$, the system (1) with constant controls is uniformly persistent; i.e., there exists a constant $d > 0$ such that*

$$\liminf_{t\to\infty} \{S(t), I(t), B(t)\} > d.$$

Proof. The uniform persistence follows directly from Theorem 2.2 in [44]. Here we briefly verify the conditions in that theorem. From Eq. (13), it is clear that $\widehat{F} \geq 0$, $\widehat{V}^{-1} \geq 0$, and $\widehat{V}^{-1}F$ is irreducible. Meanwhile, consider the function

$$f(X_1, X_2) = (\widehat{F} - \widehat{V})X_2 - \mathcal{F}(X_1, X_2) + \mathcal{V}(X_1, X_2),$$

where $\mathcal{F}$ and $\mathcal{V}$ are defined in Eq. (12). It is straightforward to obtain that $f(X_1, X_2) \geq 0$ and $f(X_1^E, X_2) = 0$, where X_1^E has been shown as globally asymptotically stable in the disease-free subsystem following Eq. (16). Hence, the instability of the DFE when $\mathcal{R}_0 > 1$ implies the uniform persistence of the system (1). □

We comment that the uniform persistence result can also be obtained from Theorem 4.3 in [18], by observing that the DFE is unique and located on the boundary of the domain Ω, and establishing that the DFE is a repeller when $\mathcal{R}_0 > 1$ (e.g., using a suitable Lyapunov function; see [27,44]).

Numerical evidence of the global stability of the DFE when $\mathcal{R}_0 < 1$ is provided in Fig. 1. We set the total population as $N = 1,000$ and the model parameters in such a way that $\mathcal{R}_0 \approx 0.8$. We then choose different initial conditions $I(0) = 1, 50, 100, 150, 200$, and 250, conduct a numerical simulation for each, and plot the solution curves for the phase plane portrait of I vs. S in Fig. 1. We observe that all these curves converge to the DFE. We also observe the same pattern for various other initial conditions (though not shown here).

4. Endemic equilibrium

Now that we have completely described the dynamics at the DFE, by Theorems 1–3, we turn to the analysis of the endemic equilibrium. As discussed before, when the effects of the controls are not strong enough to reduce $\mathcal{R}_0$ below 1, the DFE becomes unstable and the disease will persist. Below we will study the endemic equilibrium when $\mathcal{R}_0 > 1$, which is related to the long-term behavior of cholera dynamics.

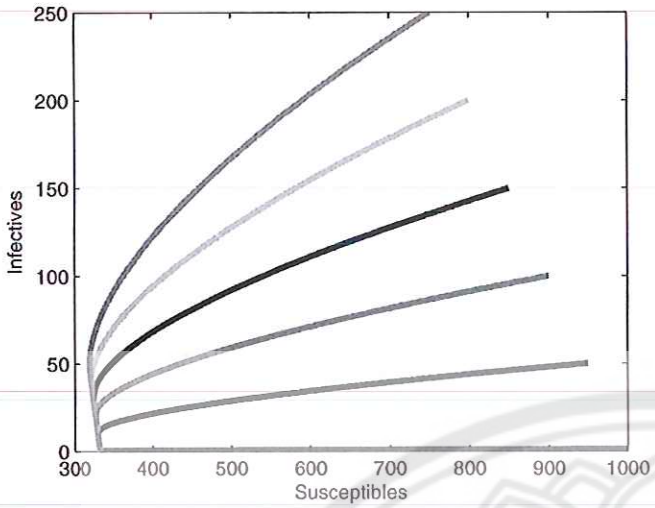

Fig. 1. The phase portrait of I vs. S for the system (1) with parameters set such that $\mathcal{R}_0 \approx 0.8$. The curves correspond to six different initial conditions with $I(0) = 1$, 50, 100, 150, 200, and 250. All the curves converge to the DFE where $S_0 = \mu N/(\phi + \mu) \approx 333.3$ and $I_0 = 0$.

4.1. Existence and uniqueness

Let us denote the endemic equilibrium of the system (1) by $X^* = (S^*, V^*, I^*, B^*)$, where

$$S^* = \frac{\mu N}{E\frac{\xi I^*}{\kappa(\delta+\nu)+\xi I^*} + HI^* + (\phi+\mu)}, \tag{20}$$

$$V^* = \frac{\mu\phi N}{\left[\sigma E\frac{\xi I^*}{\kappa(\delta+\nu)+\xi I^*} + \sigma HI^* + \mu\right]\left[E\frac{\xi I^*}{\kappa(\delta+\nu)+\xi I^*} + HI^* + (\phi+\mu)\right]}, \tag{21}$$

$$I^* = \frac{\frac{E\xi I^*}{\kappa(\delta+\nu)+\xi I^*}(S^* + \sigma V^*)}{T - H(S^* + \sigma V^*)}, \tag{22}$$

$$B^* = \frac{\xi I^*}{\delta+\nu}. \tag{23}$$

To proceed, we treat S and V as (implicit) functions of I, as suggested by Eqs. (20) and (21). Also, let

$g(I) = S(I) + \sigma V(I)$, $g_1(I) = \frac{E\xi I}{\kappa(\delta+\nu)+\xi I} + HI + (\phi+\mu)$, and $g_2(I) = \sigma\left[\frac{E\xi I}{\kappa(\delta+\nu)+\xi I} + HI\right] + \mu$.

Therefore, from Eqs. (20)–(23), we have that at an equilibrium,

$$S(I) = \frac{\mu N}{g_1(I)}, \quad V(I) = \frac{\mu\phi N}{g_1(I)g_2(I)}, \quad I = \frac{\frac{E\xi I}{\kappa(\delta+\nu)+\xi I}g(I)}{T - Hg(I)}, \quad B(I) = \frac{\xi I}{\delta+\nu}. \tag{24}$$

From (24) and $I \neq 0$, it follows that for an endemic equilibrium to exist we must have,

$$\frac{T - Hg(I)}{g(I)} = \frac{E\xi}{\kappa(\delta+\nu)+\xi I} \tag{25}$$

for some $I = I^* > 0$.

Now, let us denote $f_1(I) = \frac{T-Hg(I)}{g(I)} = \frac{T}{g(I)} - H$ and $f_2(I) = \frac{E\xi}{\kappa(\delta+\nu)+\xi I}$. Clearly both f_1 and f_2 are differentiable functions for $I \geq 0$. It is easy to see that $f_2'(I) = -\frac{E\xi^2}{[\kappa(\delta+\nu)+\xi I]^2} < 0$, whereas $f_1'(I) = \frac{-Tg'(I)}{[g'(I)]^2}$. Since $g(I) = \frac{\mu N}{g_1(I)} + \frac{\sigma\mu\phi N}{g_1(I)g_2(I)}$, the sign of $f_1'(I)$ is determined by the sign of $g_1'(I)$ and $g_2'(I)$. For $I \geq 0$, it is obvious that $g_1(I) > 0$ and $g_2(I) > 0$. Also, we see that $g_1'(I) = \frac{\kappa(\delta+\nu)E\xi}{[\kappa(\delta+\nu)+\xi I]^2} + H > 0$, and $g_2'(I) = \sigma g_1'(I) > 0$. Thus,

$$g'(I) = -\frac{\mu N g_1'(I)}{[g_1(I)]^2} - \frac{\sigma\mu\phi N[g_1'(I)g_2(I) + g_1(I)g_2'(I)]}{[g_1(I)g_2(I)]^2} < 0,$$

which yields $f_1'(I) > 0$.

Hence, on $[0, \infty]$, $f_1(I)$ is an increasing curve and $f_2(I)$ is a decreasing one. We can compare their vertical intercepts to determine if the two curves intersect and thus, if a positive endemic equilibrium exists. We have that $f_2(0) = \frac{E\xi}{\kappa(\delta+\nu)}$, and $f_1(0) = \frac{T}{S(0)+\sigma V(0)} - H = \frac{T(\mu+\phi)}{N(\mu+\sigma\phi)} - H$. Using Eq. (11), we can easily observe that if $\mathcal{R}_0 > 1$, then $f_1(0) < f_2(0)$, and there is a unique endemic equilibrium $I = I^*$; if $\mathcal{R}_0 \leq 1$, then $f_1(0) \geq f_2(0)$, and there is no endemic equilibrium. Therefore, we can establish the following theorem.

Theorem 4. *When $\mathcal{R}_0 > 1$, there exists a unique endemic equilibrium of the system (1) with constant controls.*

4.2. Bifurcation

Let us now investigate the bifurcation of the system (1) at the bifurcation point $\mathcal{R}_0 = 1$. We pick β_h as the bifurcation parameter. Our analysis makes uses of the bifurcation theorem based on the center manifold theory, originally stated in [9]. We have also included the result in Appendix A, Theorem 9.

Let us consider $\mathcal{R}_0$ as a function of β_h such that $\mathcal{R}_0(\beta_h) = \frac{(\kappa(\delta+\nu)(1-\rho)\beta_h + \xi(1-\rho)\beta_\epsilon)(\mu+\sigma\phi)}{T\kappa(\delta+\nu)(\phi+\mu)}N$. Setting $\mathcal{R}_0$ equal to 1 and solving for $\beta_h = \beta_h^*$ gives

$$\beta_h^* = \frac{1}{\kappa(\delta+\nu)(1-\rho)}\left[\frac{T\kappa(\delta+\nu)(\phi+\mu)}{(\mu+\sigma\phi)N} - \xi(1-\rho)\beta_\epsilon\right].$$

We consider the DFE (5) and $\mathcal{R}_0 = 1$ in terms of the parameter β_h^*, and we have the following Jacobian,

$$J(X_0, \beta_h^*) = \begin{bmatrix} -(\phi+\mu) & 0 & -\frac{\mu(1-\rho)\beta_h^* N}{\phi+\mu} & -\frac{\mu(1-\rho)\beta_\epsilon N}{\kappa(\phi+\mu)} \\ \phi & -\mu & -\frac{\sigma\phi(1-\rho)\beta_h^* N}{\phi+\mu} & -\frac{\sigma\phi(1-\rho)\beta_\epsilon N}{\kappa(\phi+\mu)} \\ 0 & 0 & \frac{(1-\rho)\beta_h^*(\mu+\sigma\phi)N}{\phi+\mu} - T & \frac{(1-\rho)\beta_\epsilon(\mu+\sigma\phi)N}{\kappa(\phi+\mu)} \\ 0 & 0 & \xi & -(\delta+\nu) \end{bmatrix}.$$

Denote $w = (w_1, w_2, w_3, w_4)^T$, a right eigenvector such that

$$\begin{cases} -(\phi+\mu)w_1 - \frac{\mu(1-\rho)\beta_h^* N}{\phi+\mu}w_3 - \frac{\mu(1-\rho)\beta_\epsilon N}{\kappa(\phi+\mu)}w_4 = 0, \\ \phi w_1 - \mu w_2 - \frac{\sigma\phi(1-\rho)\beta_h^* N}{\phi+\mu}w_3 - \frac{\sigma\phi(1-\rho)\beta_\epsilon N}{\kappa(\phi+\mu)}w_4 = 0, \\ \left(\frac{(1-\rho)\beta_h^*(\mu+\sigma\phi)N}{\phi+\mu} - T\right)w_3 + \frac{(1-\rho)\beta_\epsilon(\mu+\sigma\phi)N}{\kappa(\phi+\mu)}w_4 = 0, \\ \xi w_3 - (\delta+\nu)w_4 = 0. \end{cases}$$

Solving this system of equations gives

$$w = \left(-\frac{\mu T}{(\phi+\mu)(\mu+\sigma\phi)}, -\frac{\phi T}{\mu+\sigma\phi}\left(\frac{1}{\phi+\mu} + \frac{\sigma}{\mu}\right), 1, \frac{\xi}{\delta+\nu}\right)^T. \tag{26}$$

Now, denote $v = (v_1, v_2, v_3, v_4)$, a left eigenvector such that

$$\begin{cases} -(\phi+\mu)v_1 + \phi v_2 = 0, \\ -\mu v_2 = 0, \\ -\frac{\mu(1-\rho)\beta_h^* N}{\phi+\mu}v_1 - \frac{\sigma\phi(1-\rho)\beta_h^* N}{\phi+\mu}v_2 + \left(\frac{(1-\rho)\beta_h^*(\mu+\sigma\phi)N}{\phi+\mu} - T\right)v_3 + \xi v_4 = 0, \\ -\frac{\mu(1-\rho)\beta_\epsilon N}{\kappa(\phi+\mu)}v_1 - \frac{\sigma\phi(1-\rho)\beta_\epsilon N}{\kappa(\phi+\mu)}v_2 + \frac{(1-\rho)\beta_\epsilon(\mu+\sigma\phi)N}{\kappa(\phi+\mu)}v_3 - (\delta+\nu)v_4 = 0, \end{cases}$$

and

$$v_4\left(\frac{\kappa(\delta+\nu)(\phi+\mu)}{(1-\rho)\beta_\epsilon(\mu+\sigma\phi)N} + \frac{\xi}{\delta+\nu}\right) = 1.$$

Solving this system of equations gives

$$v = \left(0,\ 0,\ \frac{\kappa(\delta+\nu)^2(\phi+\mu)}{\kappa(\delta+\nu)^2(\phi+\mu)+\xi(1-\rho)\beta_e(\mu+\sigma\phi)N},\right.$$
$$\left.\frac{(1-\rho)\beta_e(\mu+\sigma\phi)N(\delta+\nu)}{\kappa(\delta+\nu)^2(\phi+\mu)+\xi(1-\rho)\beta_e(\mu+\sigma\phi)N}\right). \quad (27)$$

Note that we have $v \cdot w = 1$, $J \cdot w = 0$ and $v \cdot J = 0$.

From Eqs. (A.2)–(A.3), and considering only the nonzero derivatives for the terms $\frac{\partial^2 f_k}{\partial x_i \partial x_j}(X_0, \beta_h^*)$ and $\frac{\partial^2 f_k}{\partial x_i \partial \beta_h}(X_0, \beta_h^*)$, it follows that

$$a = 2v_1w_1w_3\frac{\partial^2 f_1}{\partial S\partial I}(X_0,\beta_h^*) + 2v_1w_1w_4\frac{\partial^2 f_1}{\partial S\partial B}(X_0,\beta_h^*)$$
$$+2v_2w_2w_3\frac{\partial^2 f_2}{\partial V\partial I}(X_0,\beta_h^*) + 2v_2w_2w_4\frac{\partial^2 f_2}{\partial V\partial B}(X_0,\beta_h^*)$$
$$+2v_3w_1w_3\frac{\partial^2 f_3}{\partial S\partial I}(X_0,\beta_h^*) + 2v_3w_1w_4\frac{\partial^2 f_3}{\partial S\partial B}(X_0,\beta_h^*)$$
$$+2v_3w_2w_3\frac{\partial^2 f_3}{\partial V\partial I}(X_0,\beta_h^*) + 2v_3w_2w_4\frac{\partial^2 f_3}{\partial V\partial B}(X_0,\beta_h^*)$$

and

$$b = 2v_1w_3\frac{\partial^2 f_1}{\partial I\partial\beta_h}(X_0,\beta_h^*) + 2v_2w_3\frac{\partial^2 f_2}{\partial I\partial\beta_h}(X_0,\beta_h^*)$$
$$+2v_3w_3\frac{\partial^2 f_3}{\partial I\partial\beta_h}(X_0,\beta_h^*).$$

With our definitions of v and w and some algebra, we obtain

$$a = \frac{-2\kappa(\delta+\nu)^2(\phi+\mu)}{\kappa(\delta+\nu)^2(\phi+\mu)+\xi(1-\rho)\beta_e(\mu+\sigma\phi)N}$$
$$\left[\frac{T^2}{(\mu+\sigma\phi)^2N}\left(\mu+\sigma\phi+\frac{\sigma^2\phi(\phi+\mu)}{\mu}\right)\right],$$

$$b = \frac{2\kappa(\delta+\nu)^2(\mu+\sigma\phi)(1-\rho)N}{\kappa(\delta+nu)^2(\phi+\mu)+\xi(1-\rho)\beta_e(\mu+\sigma\phi)N}.$$

Clearly, $a < 0$ and $b > 0$. Hence, based on Theorem 9, the following result holds:

Theorem 5. *The system (1) with constant controls exhibits a forward bifurcation at* $\mathcal{R}_0 = 1$.

A typical bifurcation diagram of I^* vs. $\mathcal{R}_0$ near the bifurcation point $\mathcal{R}_0 = 1$ is presented in Fig. 2, which is generated numerically by varying the bifurcation parameter β_h. The diagram clearly shows a forward transcritical bifurcation at $\mathcal{R}_0 = 1$.

Theorem 5 precludes the possibility of backward bifurcation for the cholera model (1). This reinforces our observation from the DFE analysis that reducing the basic reproductive number below one by using control measures would be sufficient to eradicate the disease.

4.3. Endemic stability

We have presented Theorem 5 that describes the local dynamics of the system (1) near the bifurcation point $\mathcal{R}_0 = 1$. Furthermore, we can establish the following theorem regarding the stability of the endemic equilibrium.

Theorem 6. *When* $\mathcal{R}_0 > 1$, *the unique endemic equilibrium of the system (1) with constant controls is both locally and globally asymptotically stable.*

The proof of the local asymptotic stability follows direct algebraic calculation. For simplicity, set

$$P = \frac{EB^*}{\kappa + B^*} + HI^* \quad \text{and} \quad Q = \frac{E\kappa}{(\kappa + B^*)^2}. \quad (28)$$

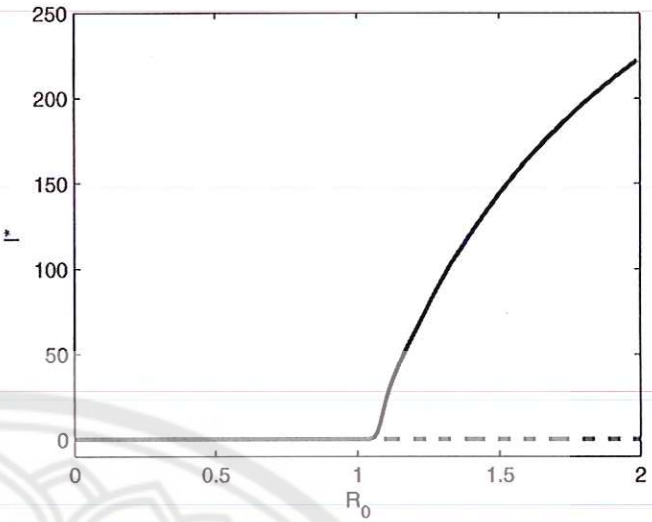

Fig. 2. A bifurcation diagram of I^* vs. $\mathcal{R}_0$ which shows a forward transcritical bifurcation at $\mathcal{R}_0 = 1$. Red solid line represents the stable DFE (when $0 < \mathcal{R}_0 < 1$) and red dashed line represents the unstable DFE (when $\mathcal{R}_0 > 1$); blue solid line represents the positive stable endemic equilibrium (when $\mathcal{R}_0 > 1$). The negative unstable endemic equilibrium (when $0 < \mathcal{R}_0 < 1$) is biologically non-feasible and not shown here. (For interpretation of the references to colour in this figure legend, the reader is referred to the web version of this article.)

The Jacobian evaluated at the endemic equilibrium is,

$$J(X^*) = \begin{bmatrix} -P-(\phi+\mu) & 0 & -HS^* & -QS^* \\ \phi & -\sigma P-\mu & -\sigma HV^* & -\sigma QV^* \\ P & \sigma P & H(S^*+\sigma V^*)-T & Q(S^*+\sigma V^*) \\ 0 & 0 & \xi & -(\delta+\nu) \end{bmatrix}, \quad (29)$$

giving the following characteristic polynomial,

$$\det(\lambda I - J(X^*)) = a_0\lambda^4 + a_1\lambda^3 + a_2\lambda^2 + a_3\lambda + a_4 \quad (30)$$

where

$$\begin{cases} a_0 = 1, \\ a_1 = P+\phi+\mu+\sigma P+\mu+\delta+\nu+T-H(S^*+\sigma V^*), \\ a_2 = (P+\phi+\mu)(\sigma P+\mu+\delta+\nu+T-H(S^*+\sigma V^*)) \\ \quad +(\delta+\nu)(T-H(S^*+\sigma V^*))-\xi Q(S^*+\sigma V^*) \\ \quad +(\sigma P+\mu)(\delta+\nu+T-H(S^*+\sigma V^*))+\sigma^2 PHV^*+PHS^*, \\ a_3 = (P+\phi+\mu)[(\sigma P+\mu)(\delta+\nu+T-H(S^*+\sigma V^*)) \\ \quad +(\delta+\nu)(T-H(S^*+\sigma V^*))-\xi Q(S^*+\sigma V^*)+\sigma^2 PHV^*] \\ \quad +(\sigma P+\mu)[(\delta+\nu)(T-H(S^*+\sigma V^*))-\xi Q(S^*+\sigma V^*)] \\ \quad +\sigma P((\delta+\nu)\sigma HV^*+\sigma\xi QV^*)+\sigma\phi PHS^*+P((\sigma P+\mu)HS^* \\ \quad +HS^*(\delta+\nu)+\xi QS^*), \\ a_4 = (P+\phi+\mu)[(\sigma P+\mu)[(\delta+\nu)(T-H(S^*+\sigma V^*)) \\ \quad -\xi Q(S^*+\sigma V^*)]+\sigma P((\delta+\nu)\sigma HV^*+\sigma\xi QV^*)] \\ \quad +\sigma\phi P(HS^*(\delta+\nu)+\xi QS^*) \\ \quad +P[(\sigma P+\mu)(HS^*(\delta+\nu)+\xi QS^*)]. \end{cases}$$

Based on the Routh–Hurwitz stability criterion, the necessary and sufficient conditions for the stability of a quartic polynomial are

$$a_i > 0 \quad (0 \le i \le 4); \quad a_1a_2 - a_0a_3 > 0, \quad a_3(a_1a_2 - a_0a_3) > a_1^2a_4. \quad (31)$$

Clearly, $a_0 > 0$ is satisfied. From (22) and the fact that $S^*, V^*, I^* > 0$, it follows that

$$T - H(S^* + \sigma V^*) = \frac{\xi E(\kappa(\delta+\nu) + \xi I^*)}{(\kappa(\delta+\nu)+\xi I^*)^2}(S^* + \sigma V^*) > 0. \tag{32}$$

Note that $\xi Q = \frac{\xi E \kappa (\delta+\nu)^2}{(\kappa(\delta+\nu)+\xi I^*)^2}$, and thus

$$(\delta+\nu)(T - H(S^* + \sigma V^*)) > \xi Q(S^* + \sigma V^*). \tag{33}$$

The inequalities (32) and (33) are both necessary and sufficient to show that $a_i > 0$ for $1 \le i \le 4$. Next we show $a_1 a_2 - a_0 a_3 > 0$. Consider the following,

$$\begin{cases} (P+\phi+\mu+\sigma P+\mu+\delta+\nu)a_2 - a_3 \\ = (1-\sigma)PHS^* + (P+\phi+\mu)^2(\sigma P+\mu+\delta+\nu+T-H(S^*+\sigma V^*)) \\ +(P+\phi+\mu)(\sigma P+\mu)(\delta+\nu+T-H(S^*+\sigma V^*)) + (P+\mu)PHS^* \\ +(\sigma P+\mu)^2(P+\phi+\mu) + (\sigma P+\mu)^2(\delta+\nu+T-H(S^*+\sigma V^*)) \\ +(\sigma P+\mu)\sigma^2 PHV^* + (\delta+\nu)P(\sigma P+\mu+\delta+\nu) \\ +(\delta+\nu)(\phi+\mu)(\sigma P+\mu+\delta+\nu+T-H(S^*+\sigma V^*)) \\ +[(\delta+\nu)^2(T-H(S^*+\sigma V^*)) - (\delta+\nu)\xi Q(S^*+\sigma V^*)] \\ +(\delta+\nu)^2\sigma P + (\delta+\nu)\mu(\delta+\nu+T-H(S^*+\sigma V^*)) \\ +[(\delta+\nu)P(T-H(S^*+\sigma V^*)) - P\xi QS^*] \\ +[(\delta+\nu)\sigma P(T-H(S^*+\sigma V^*)) - \sigma^2 P\xi QV^*]. \end{cases}$$

Using condition (33), we have that

$$\begin{cases} (\delta+\nu)^2(T-H(S^*+\sigma V^*)) & > (\delta+\nu)\xi Q(S^*+\sigma V^*), \\ (\delta+\nu)P(T-H(S^*+\sigma V^*)) & > P\xi QS^*, \\ (\delta+\nu)\sigma P(T-H(S^*+\sigma V^*)) & > \sigma^2 P\xi QV^*. \end{cases}$$

Thus, $(P+\phi+\mu+\sigma P+\mu+\delta+\nu)a_2 > a_3$ holds. From condition (32), we see that $a_1 > P+\phi+\mu+\sigma P+\mu+\delta+\nu$. Hence, $a_1 a_2 > a_3$. The last inequality in (31) can be proved with similar algebraic manipulation.

The global asymptotic stability of the endemic equilibrium, however, is more challenging and requires significantly more work. The main reason for this difficulty is that the model (1) is a four-dimensional dynamical system, for which very few analytical theories and techniques can be applied. We establish the global endemic stability of our model by using the geometric approach originally proposed by Li and Muldowney [28,29]. The proof is provided in the Appendix B.

The existence of a stable the endemic equilibrium when $\mathcal{R}_0 > 1$ is demonstrated in Fig. 3. We set the total population as $N = 1{,}000$ and the model parameters in such a way that $\mathcal{R}_0 \approx 2.0$. We again pick different initial conditions $I(0) = 1, 50, 100, 150, 200$, and 250, conduct a numerical simulation for each, and plot the phase plane portrait of I vs. S for each case in Fig. 3. We observe that all these curves converge to the endemic equilibrium over time, a pattern that also takes place for various other initial conditions.

5. Sensitivity analysis

There are various parameters present in our model (1) and the values of these parameters will directly affect the dynamics of cholera infection and transmission. In order to identify which parameters are more influential than others in determining disease dynamics, we carry out a sensitivity analysis using the Latin Hypercube Sampling (LHS) method [4,35]. The LHS method, which is one of the most efficient ways to analyze sensitivity and uncertainty, calculates the Partial Rank Correlation Coefficients (PRCC) in the range of $[-1, 1]$ for the model parameters with respect to outcome measurements. A small PRCC value (close to 0) indicates that changes in the input parameter have little impact on the outcome, whereas a bigger PRCC value suggests that the outcome is significantly influenced by, thus sensitive to, the changes of the input parameter. In this study we pick

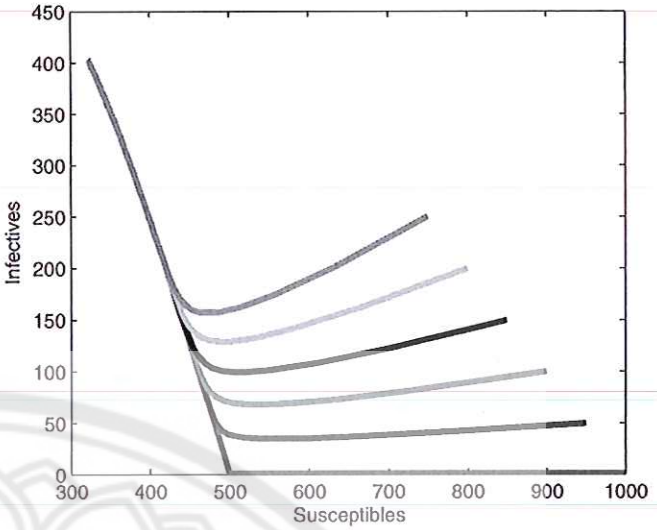

Fig. 3. The phase portrait of I vs. S for the system (1) with parameters set such that $\mathcal{R}_0 \approx 2$. The curves correspond to six different initial conditions with $I(0) = 1, 50, 100, 150, 200$, and 250. All these curves converge to the endemic equilibrium where $S^* \approx 322.5$ and $I^* \approx 403.1$.

the maximum daily infected population and the cumulative total infected population as the two outcome measurements, and present the results in Table 1 with a sample size $n = 500$; similar patterns are observed for differing sample sizes. We also mention that similar outcome measurements were used in the sensitivity analysis in [37].

Results in Table 1 show that the control terms ϕ (vaccination rate) and τ (treatment rate) are both sensitive in affecting the maximum daily infection; the treatment rate is also sensitive to the total infection. Meanwhile, the parameter ρ (sanitation-induced preventability) is also sensitive to the maximum daily infection. In addition, the recovery rate γ and the contact rates β_e and β_h are sensitive to both daily and total infections. We note that the sensitivity of β_e and β_h was also observed in [34] for the cholera model without controls.

In terms of disease control, the sensitivity analysis results indicate that both the environment-to-human and human-to-human transmission pathways are sensitive, and important, in determining the cholera infections, and that all three types of control measures (vaccination, treatment, and sanitation) are important in containing the cholera epidemics. Clearly, the multiple transmission routes and intervention strategies will closely interplay with each other. To better understand these relations and to predict how the control strategies can be effectively designed, we will conduct an optimal control study in next section.

6. Optimal control

Now we study the general model (1) with time-dependent controls $\phi(t)$, $\tau(t)$, and $\nu(t)$. The presence of time-dependent controls makes equilibrium analysis of the system (1) difficult, as the system becomes non-autonomous and the disease dynamics now depend on the evolution of each control profile. We will, instead, perform an optimal control study on this problem, to explore how the intervention effects and costs can be best balanced and how the control strategy can be best designed to account for the complex and multiple transmission pathways of cholera.

We consider the system on a time interval $[0, T_1]$ for some $T_1 > 0$. The control set is defined as

$$\Gamma = \{(\phi(t), \tau(t), \nu(t)) \mid 0 \le \phi(t) \le \phi_{\max}, \\ 0 \le \tau(t) \le \tau_{\max}, \ 0 \le \nu(t) \le \nu_{\max}\}, \tag{34}$$

Table 1
LHS sensitivity analysis for model parameters. The sample size is $n = 500$. Asterisks indicate the corresponding p-values are below 0.01 ; i.e., the nonzero PRCC are significant.

Parameters	Parameter ranges Min	Max	Maximum daily infection PRCC values	t-values	Total infection PRCC values	t-values
ϕ	0.001	1	− 0.24	− 4.8*	− 0.085	− 1.82
ρ	0.01	0.5	− 0.39	− 7.32*	− 0.059	− 1.28
β_e	0.01	0.2	0.14	3.24*	0.092	2.15*
β_h	0.00001	0.002	0.8	39.8*	0.33	8.97*
σ	0.2	1	0.086	2.0	0.029	0.66
τ	0.001	1	− 0.67	− 11.5*	− 0.82	− 13.6*
γ	0.05	0.4	− 0.64	− 11.2*	− 0.77	− 12.9*
ξ	1	20	0.035	0.8	− 0.043	− 0.93
δ	0.0001	0.3	− 0.087	− 1.85	− 0.088	− 1.87
ν	0.01	1	− 0.014	− 0.31	0.0052	0.12

where $\phi_{\max}$, $\tau_{\max}$, and $\nu_{\max}$ denote the upper bounds for the effort of vaccination, treatment, and sanitation, respectively. These bounds reflect practical limitations on the maximum rates of controls that can be implemented in a given time period.

We aim to minimize the total number of infections and the costs of controls over the time interval $[0, T_1]$; i.e.,

$$\min_{(\phi,\tau,\nu)\in\Gamma} \int_0^{T_1} [I(t) + c_{21}\phi(t)S(t) + c_{22}\phi(t)^2 + c_{31}\tau(t)I(t) + c_{32}\tau(t)^2 + c_{41}\nu(t)B(t) + c_{42}\nu(t)^2]\,dt. \tag{35}$$

Here the parameters c_{ij} $(i = 2,3,4;\ j = 1,2)$, define the appropriate costs associated with these controls. Quadratic terms are introduced to account for nonlinear costs potentially arising at high intervention levels [2,5,37]. The minimization process is subject to the differential equations in (1), which we now refer to as the state equations. Correspondingly, the unknowns S, I, and B are now called the *state variables*, in contrast to the *control variables* ϕ, τ, and ν. Our goal is then to determine the optimal control, $\phi^*(t)$, $\tau^*(t)$, and $\nu^*(t)$, so as to minimize the objective functional in (35).

We first note that the control set Γ is closed and convex, and the integrand of the objective functional in (35) is also convex. Meanwhile, our model is linear in the control variables. Hence, based on the standard optimal control theorems in [17], we obtain the following theorem.

Theorem 7. *There exists $(\phi^*(t), \tau^*(t), \nu^*(t)) \in \Omega$ such that the objective functional in (35) is minimized.*

To proceed, we will use the Pontryagin's Maximum/Minimum Principle [39] to seek the optimal control solution. This approach introduces the adjoint functions and represents an optimal control in terms of the state and adjoint functions, thus transferring the problem of minimizing the objective functional into minimizing the Hamiltonian with respect to the controls.

We define the adjoint functions λ_S, λ_V, λ_I, and λ_B associated with the state equations for S, V, I, and B, respectively. We then form the Hamiltonian, $\mathcal{H}$, by multiplying each adjoint function with the right-hand side of its corresponding state equation, and adding each of these products to the integrand of the objective functional. As a result, we obtain

$$\begin{aligned}\mathcal{H} = {} & I(t) + c_{21}\phi(t)S(t) + c_{22}\phi(t)^2 + c_{31}\tau(t)I(t) + c_{32}\tau(t)^2 \\ & + c_{41}\nu(t)B(t) + c_{42}\nu(t)^2 \\ & + \lambda_S\left[\mu N - (1-\rho)\left[\beta_e\frac{B}{\kappa+B} + \beta_h I\right]S - (\phi(t)+\mu)S\right] \\ & + \lambda_V\left[\phi(t)S - \sigma(1-\rho)\left[\beta_e\frac{B}{\kappa+B} + \beta_h I\right]V - \mu V\right] \\ & + \lambda_I\left[(1-\rho)\left[\beta_e\frac{B}{\kappa+B} + \beta_h I\right](S+\sigma V) - (\tau(t)+\gamma+\mu)I\right] \\ & + \lambda_B[\xi I - (\delta+\nu(t))B].\end{aligned}$$

To achieve the optimal control, the adjoint functions must satisfy $\frac{d\lambda_S}{dt} = -\frac{\partial\mathcal{H}}{\partial S}$, $\frac{d\lambda_V}{dt} = -\frac{\partial\mathcal{H}}{\partial V}$, etc. These yield

$$\begin{aligned}\frac{d\lambda_S}{dt} = {} & -c_{21}\phi + \lambda_S\left[(1-\rho)\left[\beta_e\frac{B}{\kappa+B} + \beta_h I\right] + (\phi+\mu)\right] \\ & - \lambda_V\phi - \lambda_I\left[(1-\rho)\left[\beta_e\frac{B}{\kappa+B} + \beta_h I\right]\right],\end{aligned} \tag{36}$$

$$\begin{aligned}\frac{d\lambda_V}{dt} = {} & \lambda_V\left[\sigma(1-\rho)\left[\beta_e\frac{B}{\kappa+B} + \beta_h I\right] + \mu\right] \\ & - \lambda_I\left[\sigma(1-\rho)\left[\beta_e\frac{B}{\kappa+B} + \beta_h I\right]\right],\end{aligned} \tag{37}$$

$$\begin{aligned}\frac{d\lambda_I}{dt} = {} & -1 - c_{31}\tau + \lambda_S(1-\rho)\beta_h S + \lambda_V\sigma(1-\rho)\beta_h V \\ & - \lambda_I[(1-\rho)\beta_h(S+\sigma V) - (\tau+\gamma+\mu)] - \lambda_B\xi,\end{aligned} \tag{38}$$

$$\begin{aligned}\frac{d\lambda_B}{dt} = {} & -c_{41}\nu + \lambda_S(1-\rho)\beta_e\frac{\kappa S}{(\kappa+B)^2} + \lambda_V\sigma(1-\rho)\beta_e\frac{\kappa V}{(\kappa+B)^2} \\ & - \lambda_I(1-\rho)\beta_e\frac{\kappa(S+\sigma V)}{(\kappa+B)^2} + \lambda_B(\delta+\nu),\end{aligned} \tag{39}$$

with transversality conditions (i.e., final time conditions):

$$\lambda_S(T_1) = 0, \quad \lambda_V(T_1) = 0, \quad \lambda_I(T_1) = 0, \quad \lambda_B(T_1) = 0. \tag{40}$$

The characterizations of the optimal controls, $\phi^*(t)$, $\tau^*(t)$, and $\nu^*(t)$, are based on the conditions

$$\frac{\partial\mathcal{H}}{\partial\phi} = 0, \quad \frac{\partial\mathcal{H}}{\partial\tau} = 0, \quad \frac{\partial\mathcal{H}}{\partial\nu} = 0, \tag{41}$$

respectively, subject to the constraints given in (34). Thus we have

$$\phi^*(t) = \max[0,\ \min(\tilde{\phi}(t),\ \phi_{\max})], \tag{42}$$

$$\tau^*(t) = \max[0,\ \min(\tilde{\tau}(t),\ \tau_{\max})], \tag{43}$$

$$\nu^*(t) = \max[0,\ \min(\tilde{\nu}(t),\ \nu_{\max})], \tag{44}$$

where $\tilde{\phi}(t) = [(\lambda_S - \lambda_V - c_{21})S(t)]\,/\,(2c_{22})$, $\tilde{\tau}(t) = [(\lambda_I - c_{31})I(t)]/(2c_{32})$, $\tilde{\nu}(t) = [(\lambda_B - c_{41})B(t)]\,/\,(2c_{42})$.

To summarize, our optimal control problem consists of the state system (1) with initial conditions, the adjoint Eqs. (36)–(39) with the transversality conditions, and Eqs. (42)–(44) to characterize the optimal controls. Such a problem has to be solved numerically. We apply the forward-backward sweep method [26] to solve it in an iterative manner. This algorithm is briefly described as follows. First, the state

Table 2
Cholera model parameters and values.

Parameter	Symbol	Value	Source
Total population	N	10,000	-
Natural human birth and death rate	μ	$(43.5\,\text{years})^{-1}$	[52]
Concentration of *V. cholerae* in environment	κ	10^6 cells/ml	[12]
Rate of recovery from cholera	γ	$(5\,\text{day})^{-1}$	[20]
Rate of human contribution to *V. cholerae*	ξ	10 cells/ml-day	[20]
Death rate of vibrios in the environment	δ	$(30\,\text{days})^{-1}$	[20]
Ingestion rate from the environment	β_e	0.075/day	[34]
Ingestion rate through human-human interaction	β_h	0.00011/day	[34]

equations are solved forward in time by a fourth-order Runge–Kutta method, with an initial guess for the control variables. Next, the adjoint equations are solved backward in time using the solutions of the state equations. The control is then updated with the new values of the state and adjoint solutions, and the process is repeated until the solutions converge.

To carry out the numerical simulation, we list the values for the various transmission rates in the state Eq. (1) in Table 2. Meanwhile, we assume that the unit costs for vaccination and treatment are about the same, whereas the cost for per percent reduction of vibrio concentration through sanitation is doubled. We further assume that for each control, the per capita cost at the quadratic level is about 20% of that at the linear level. Thus, we assign the following set of values (with appropriate units) to the cost parameters in (35):

$$c_{21} = 50, \quad c_{22} = 10, \quad c_{31} = 50, \quad c_{32} = 10, \quad c_{41} = 100, \quad c_{42} = 20. \tag{45}$$

Based on practical observations and empirical values [51,52], we set the upper bounds of the rates for the three controls as $\phi_{\max} = 0.7$, $\tau_{\max} = 0.5$, and $\nu_{\max} = 0.1$. We also set the initial infection number $I(0) = 1000$ and the entire period of time $T = 100$ days.

Fig. 4 (a) shows the infection curves for the model without controls (dashed line), i.e., $\phi(t) = \tau(t) = \nu(t) = 0$, and that with the optimal controls implemented (solid line). We clearly see that the number of infections has been significantly reduced due to the incorporation of the three types of controls. Here we also present the case with vaccination being the only control measure; in this case the optimal control problem is reformulated to determine the optimal strategy for vaccination, by setting $\tau(t) = \nu(t) = 0$ and using the same cost parameters for vaccination. The infection curve with this vaccination-only strategy is shown in Fig. 4(a) with the dash-dot line. We observe that with vaccination only, the infections still reach a high level, though the peak value is lower than that without controls. This is an evidence that multiple intervention methods, which target both the direct and indirect transmission routes of cholera, would achieve better results than a single control such as vaccination only. This result is consistent with the observation from our sensitivity analysis in Section 5. Fig. 4(b)–(d) further show the profile of each of the three controls in their optimal balance. We observe that both the vaccination rate and the treatment rate start with their maximum values and remain at that level for a number of days (about 7 days for vaccination, and 35 days treatment), before decreasing to lower levels of strength. The pattern is similar for sanitation, except that the start of maximum sanitation rate lags for 1–2 days.

As can be naturally expected, the costs of these controls directly affect the strength and duration of the controls in their optimal balance. For demonstration, we now assume that the linear per capita costs for vaccination and treatment (i.e., c_{21} and c_{31}) can be significantly reduced compared to those in (45), and consider the following cost parameters:

$$c_{21} = 2, \quad c_{22} = 10, \quad c_{31} = 2, \quad c_{32} = 10, \quad c_{41} = 100, \quad c_{42} = 20. \tag{46}$$

This set of cost parameters lead to improved control results. The reason is that with lower costs for vaccination and treatment, these two controls can be implemented with higher average strength and longer duration, thus further reducing the infections. Indeed, Fig. 5 show the profiles for the optimal vaccination and treatment rates in this case, where we see that the vaccination and treatment rates remain at their maximum levels for about 12 days and 60 days, respectively; both are significantly longer than those in Fig. 4. In addition, the vaccination rate now stays at the level of 0.3 from day 20 until near the end of the time interval.

7. Discussion

Cholera is currently in its seventh pandemic and remains a growing public health problem in different parts of the world, with outbreaks showing complex patterns, partly explained with changes in the organisms [36,40]. Despite the available knowledge on its prevention and treatment, the disease is emerging as one of the leading cause of mortality in developing countries. Successful control and/or eradication of the disease requires good understanding of the biological, epidemiological and environmental factors shaping these outbreaks. Infectious disease modeling helps understand the mechanisms influencing disease transmission dynamics. With the continued and increasing burden of cholera there is need to prioritize the implementation and use of different public health control measures. Effective control of cholera requires investment in long-term provision of public-sector clean water and adequate sanitation, but achieving these in epidemic and emergence setting is impossible. The proposed use of cholera vaccines in these settings to complement disease control has suffered a lot of debates on the effectiveness [11] and associated logistic, financial and human resources challenges during outbreaks [15]. These challenges call for the need to assess the optimal requirement of each intervention measure when considered as a package.

The focus of this study is to better understand the effects of different control strategies coupled with multiple transmission pathways of cholera, using a mathematical model that fully captures the epidemiology and pathogenesis of the disease in order to comprehensively explore the usefulness of public health control measures towards effective response to cholera epidemics in resource constrained settings. The model consists of three types of public health controls: vaccination, treatment, and sanitation. Comprehensive mathematical analysis of the model using both analytical and numerical approaches is carried out and presented. The mathematical results demonstrate that despite including vaccination in a framework that has previously shown backward bifurcation [21], our model does not exhibit such a phenomenon and retains $\mathcal{R}_0$ as an epidemic threshold governing the dynamics of the model system. This model shows that the unity of $\mathcal{R}_0$ as quantitative statistic to quantify the amount of control effort required to contain epidemic cholera is not compromised. Thus even with public health interventions, cholera epidemics and endemism could still occur and the disease could persist, if the controls are not strong enough to reduce $\mathcal{R}_0$ to values below unity.

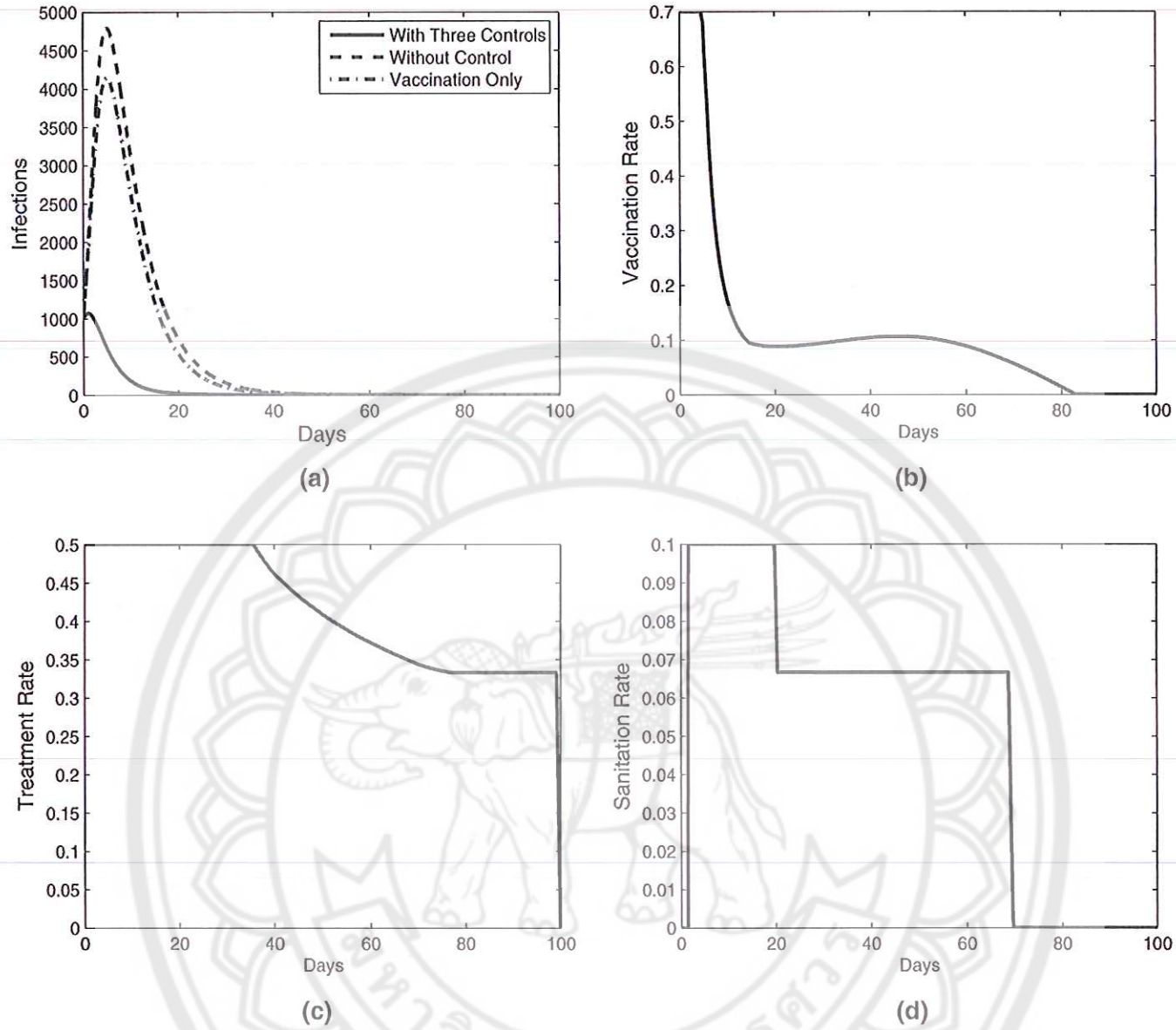

Fig. 4. Optimal control simulation results based on the cost parameters in (45): (a) Infection curves for the cholera model without control, with three controls in optimal balance, and with vaccination only; (b) the optimal vaccination rate; (c) the optimal treatment rate; (d) the optimal sanitation rate.

In order to assess the effectiveness of implementing the proposed package of public health controls, we have also performed a preliminary study based on optimal control theory to seek cost-effective solutions by assuming these interventions are time-dependent. Optimal control techniques have vastly been used to determine effectiveness of control strategies of infectious disease dynamics [16,23–26]. Our results suggest that different controls (such as vaccination and treatment) closely interplay with each other, and the costs of controls directly affect the length and strength of each control in an optimal strategy. We have found that due to the multiple transmission routes of cholera, a combination of multiple intervention methods achieves better results than a single-strategy approach.

Effective control and/or eradication of cholera in the developing world remains a public health challenge because of the complex biological, epidemiological, and environmental factors that contribute to the dynamics of the disease. The recognition of cholera burden combined with efforts to implement efficient control measures have become critical with the growing trends in cholera incidence in developing countries, and require a comprehensive and integrated strategy to implement public health control measures. The present paper, through careful mathematical modeling and analysis, contributes to the basic knowledge of cholera transmission dynamics and helps improve our understanding of the effects and limitations of these public health interventions. In addition, the current study can be extended by a number of ways. Our model assumes that the vaccine efficacy σ and sanitation-induced preventability ρ are constants, whereas in reality both decrease after several months, thus time-dependent. It would be worthwhile to incorporate this aspect into model analysis and optimal control study to address the long-term dynamics of cholera with interventions. Meanwhile, we have assumed that all the control measures, including vaccination, can be implemented from the very beginning of disease outbreak. Practically, an important question is to assess the value of cholera vaccination in controlling ongoing outbreaks [15], and guidelines for vaccine use in cholera outbreaks in post-disaster settings are still to be established. A careful mathematical analysis and optimal control study

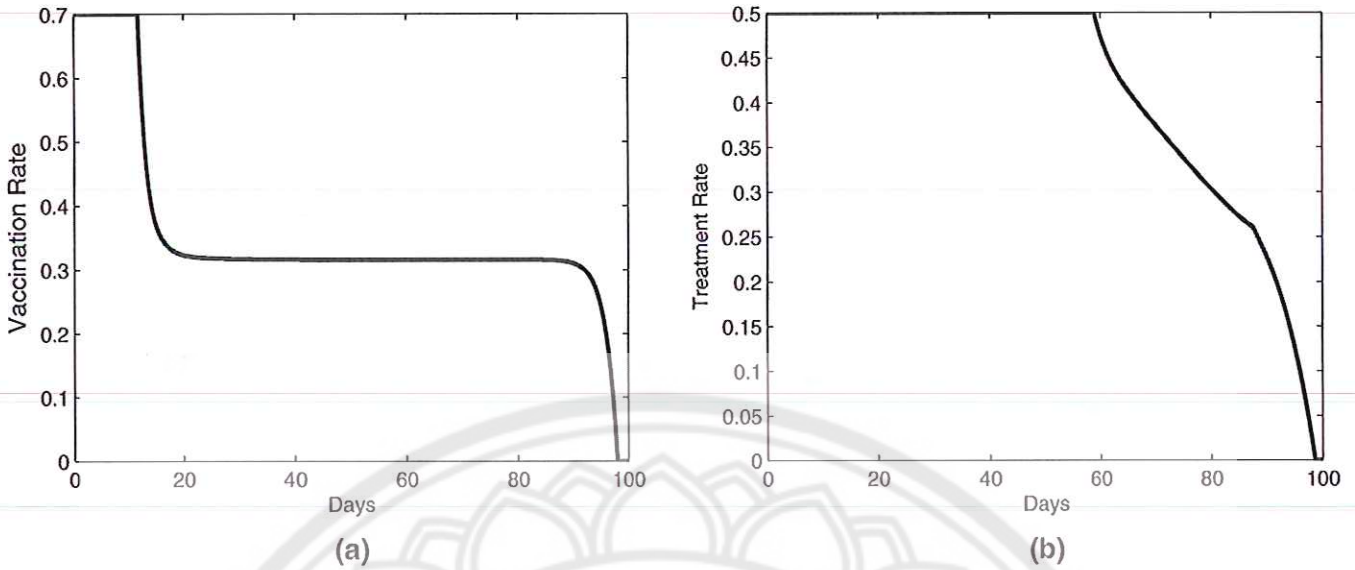

Fig. 5. Optimal control profiles based on the cost parameters in (46): (a) the optimal vaccination rate; (b) the optimal treatment rate.

for delayed deployment of cholera vaccine would shed light on this question.

Acknowledgments

J. Wang acknowledges partial support from the National Science Foundation under grant numbers 1216936 and 1412826. The authors are grateful to the reviewer's comments that have improved this paper.

Appendix A

The following global stability theorem for a disease-free equilibrium (DFE) was established in [8]:

Theorem 8. *Consider a model system written in the form*

$$\frac{dX_1}{dt} = F(X_1, X_2) \quad \text{and} \quad \frac{dX_2}{dt} = G(X_1, X_2)$$

with $G(X_1, 0) = 0$, where $X_1 \in \mathbb{R}^m$ denotes (its components) the number of uninfected individuals and $X_2 \in \mathbb{R}^n$ denotes (its components) the number of infectious individuals; $X_0 = (X_1^E, 0)$ denotes the DFE of the system. And assume,

1. *For $\frac{dX_1}{dt} = F(X_1, 0)$, X_1^E is globally asymptotically stable;*
2. *$G(X_1, X_2) = AX_2 - \hat{G}(X_1, X_2)$, $\hat{G}(X_1, X_2) \geq 0$ for $(X_1 X_2) \in \Omega$, where the Jacobian $A = \frac{\partial G}{\partial X_2}(X_1^E, 0)$ is an M-matrix (the off-diagonal elements of A are nonnegative) and Ω is the region where the model makes biological sense.*

Then the DFE $X_0 = (X_1^E, 0)$ is globally asymptotically stable provided that $\mathcal{R}_0 < 1$.

The following bifurcation theorem based on the center manifold theory was established in [9]:

Theorem 9. *Consider a general system of ODEs with a real parameter β:*

$$\frac{dx}{dt} = f(x, \beta); \quad f : \mathbb{R}^n \times \mathbb{R} \to \mathbb{R}^n, \quad \text{and} \quad f \in C^2(\mathbb{R}^n \times \mathbb{R}). \tag{47}$$

Assume $x = X_0$ is an equilibrium of system (47) for all β. Also Assume

(A1) *$A = D_x f(X_0, \beta^*) = \left(\frac{\partial f_i}{\partial x_j}(X_0, \beta^*)\right)$ is the linearization matrix of system (47) at the equilibrium $x = X_0$ with β evaluated at β^*. Zero is a simple eigenvalue of A and all other eigenvalues of A have negative real parts.*

(A2) *Matrix A has a right eigenvector w and a left eigenvector v corresponding to the zero eigenvalue.*

Let f_k be the kth component of f and,

$$a = \sum_{k,i,j=1}^{4} v_k w_i w_j \frac{\partial^2 f_k}{\partial x_i \partial x_j}(X_0, \beta^*), \tag{48}$$

$$b = \sum_{k,i=1}^{3} v_k w_i \frac{\partial^2 f_k}{\partial x_i \partial \beta}(X_0, \beta^*). \tag{49}$$

The local dynamics of the system (47) around $x = X_0$ are totally determined by a and b.

(i) *$a > 0$, $b > 0$. When $\beta - \beta^* < 0$ with $|\beta - \beta^*| \ll 1$, $x = X_0$ is locally asymptotically stable, and there exists a positive unstable equilibrium; when $0 < \beta - \beta^* \ll 1$, $x = X_0$ is unstable and there exists a negative and locally asymptotically stable equilibrium;*

(ii) *$a < 0$, $b < 0$. When $\beta - \beta^* < 0$ with $|\beta - \beta^*| \ll 1$, $x = X_0$ is unstable; when $0 < \beta - \beta^* \ll 1$, $x = X_0$ is locally asymptotically stable, and there exists a positive unstable equilibrium;*

(iii) *$a > 0$, $b < 0$. When $\beta - \beta^* < 0$ with $|\beta - \beta^*| \ll 1$, $x = X_0$ is unstable, and there exists a locally asymptotically stable negative equilibrium; when $0 < \beta - \beta^* \ll 1$, $x = X_0$ is stable, and a positive unstable equilibrium appears;*

(iv) *$a < 0$, $b > 0$. When $\beta - \beta^*$ changes from negative to positive, $x = X_0$ changes its stability from stable to unstable. Correspondingly a negative unstable equilibrium becomes positive and locally asymptotically stable.*

Appendix B

We prove the global asymptotic stability of the endemic equilibrium for the system (1) with constant controls, when $\mathcal{R}_0 > 1$. Our analysis below is based on the geometric approach originally proposed by Li and Muldowney (see [28,29]), and extended in [19,50].

First let us present the main result of the geometric approach based on the second additive compound matrix. For a 4×4 matrix

$A = [a_{ij}]$, the second additive compound matrix is defined as

$$A^{[2]} = \begin{pmatrix} a_{11}+a_{22} & a_{23} & a_{24} & -a_{13} & -a_{14} & 0 \\ a_{32} & a_{11}+a_{33} & a_{34} & a_{12} & 0 & -a_{14} \\ a_{42} & a_{43} & a_{11}+a_{44} & 0 & a_{12} & a_{13} \\ -a_{31} & a_{21} & 0 & a_{22}+a_{33} & a_{34} & -a_{24} \\ -a_{41} & 0 & a_{21} & a_{43} & a_{22}+a_{44} & a_{23} \\ 0 & -a_{41} & a_{31} & -a_{42} & a_{32} & a_{33}+a_{44} \end{pmatrix}.$$

Now consider the dynamical system

$$\frac{dX}{dt} = F(X) \tag{50}$$

where $F : \Omega \mapsto \mathbb{R}^n$ is a C^1 function and where $\Omega \subset \mathbb{R}^n$ is a simply connected open set. Let $X(t, X_0)$ denote the solution of Eq. (50) with the initial condition $X(0) = X_0$. We assume:

(H1) There exists a compact absorbing set $K \subset \Omega$;
(H2) The system (50) has a unique equilibrium point X^* in Ω.

Moreover, let $X \mapsto W(X)$ be a $\binom{n}{2} \times \binom{n}{2}$ matrix-valued C^1 function in Ω. Set

$$P = W_F W^{-1} + W J^{[2]} W^{-1}, \tag{51}$$

where W_F is the derivative of W (entry-wise) along the direction of F, and $J^{[2]}$ is the second compound matrix of the Jacobian $J(X) = DF(X)$. Let $m(P)$ be the Lozinskiĭ measure of P with respect to a matrix norm [13], i.e.,

$$m(P) = \lim_{h \to 0^+} \frac{|I + hP| - 1}{h}. \tag{52}$$

For a norm $\|\cdot\|$ on $\mathbb{R}^n$, it is established in [19] that the Lozinskiĭ measure of P associated with $\|\cdot\|$ can be evaluated as

$$m(P) = \inf\left\{c \;\middle|\; D_+\|Z\| \le c\|Z\| \text{ for all solutions of } Z' = PZ\right\} \tag{53}$$

where D_+ denotes the right-hand total derivative with respect to t. The following result is implicitly stated in [19]:

Theorem 10. *Assume that Ω is simply connected and the assumptions (H1) and (H2) hold. Then the unique equilibrium X^* of (50) is globally asymptotically stable in Ω if $m(P) < 0$.*

Based on Theorem 4, our system (1) has a unique endemic equilibrium when $\mathcal{R}_0 > 1$. Meanwhile, the uniform persistence (see Theorem 3) and the boundedness of the domain Δ imply that the system has a compact absorbing subset of Δ [6]. Hence, the assumptions (**H1**) and (H2) hold for the system (1). Below we verify the condition $m(P) < 0$.

The second additive compound matrix associated with the Jacobian of the system (1) is,

$$J^{[2]} = \begin{bmatrix} j_{11} & -\sigma HV & -\sigma QV & HS & QS & 0 \\ \sigma\left(\frac{EB}{\kappa+B} + HI\right) & j_{22} & Q(S+\sigma V) & 0 & 0 & QS \\ 0 & \xi & j_{33} & 0 & 0 & -HS \\ -\left(\frac{EB}{\kappa+B} + HI\right) & \phi & 0 & j_{44} & Q(S+\sigma V) & \sigma QV \\ 0 & 0 & \phi & \xi & j_{55} & -\sigma HV \\ 0 & 0 & \frac{EB}{\kappa+B} + HI & 0 & \sigma\left(\frac{EB}{\kappa+B} + HI\right) & j_{66} \end{bmatrix} \tag{54}$$

where $Q = \frac{E\kappa}{(\kappa+B)^2}$ and

$$j_{11} = -(1+\sigma)\left(\frac{EB}{\kappa+B} + HI\right) - 2\mu - \phi,$$

$$j_{22} = -\left(\frac{EB}{\kappa+B} + HI\right) - \phi - \mu + H(S+\sigma V) - T,$$

$$j_{33} = -\left(\frac{EB}{\kappa+B} + HI\right) - \phi - \mu - \delta - \nu,$$

$$j_{44} = -\sigma\left(\frac{EB}{\kappa+B} + HI\right) - \mu + H(S+\sigma V) - T,$$

$$j_{55} = -\sigma\left(\frac{EB}{\kappa+B} + HI\right) - \mu - \delta - \nu,$$

$$j_{66} = H(S+\sigma V) - T - \delta - \nu$$

Let

$$W = \begin{bmatrix} \frac{1}{I} & 0 & 0 & 0 & 0 & 0 \\ 0 & \frac{1}{I} & 0 & 0 & 0 & 0 \\ 0 & 0 & 0 & \frac{1}{I} & 0 & 0 \\ 0 & 0 & \frac{1}{B} & 0 & 0 & 0 \\ 0 & 0 & 0 & 0 & \frac{1}{B} & 0 \\ 0 & 0 & 0 & 0 & 0 & \frac{1}{B} \end{bmatrix}$$

Note that

$$W_F = \begin{bmatrix} \frac{-1}{I^2}\frac{dI}{dt} & 0 & 0 & 0 & 0 & 0 \\ 0 & \frac{-1}{I^2}\frac{dI}{dt} & 0 & 0 & 0 & 0 \\ 0 & 0 & 0 & \frac{-1}{I^2}\frac{dI}{dt} & 0 & 0 \\ 0 & 0 & \frac{-1}{B^2}\frac{dB}{dt} & 0 & 0 & 0 \\ 0 & 0 & 0 & 0 & \frac{-1}{B^2}\frac{dB}{dt} & 0 \\ 0 & 0 & 0 & 0 & 0 & \frac{-1}{B^2}\frac{dB}{dt} \end{bmatrix}$$

We have

$$W J^{[2]} W^{-1} = \begin{bmatrix} j_{11} & -\sigma HV & HS & -\sigma QV\frac{B}{I} & QS\frac{B}{I} & 0 \\ \sigma\left(\frac{EB}{\kappa+B} + HI\right) & j_{22} & 0 & Q(S+\sigma V)\frac{B}{I} & 0 & QS\frac{B}{I} \\ -\left(\frac{EB}{\kappa+B} + HI\right) & \phi & j_{44} & 0 & Q(S+\sigma V)\frac{B}{I} & \sigma QV\frac{B}{I} \\ 0 & \xi\frac{I}{B} & 0 & j_{33} & 0 & -HS \\ 0 & 0 & \xi\frac{I}{B} & \phi & j_{55} & -\sigma HV \\ 0 & 0 & 0 & \frac{EB}{\kappa+B} + HI & \sigma\left(\frac{EB}{\kappa+B} + HI\right) & j_{66} \end{bmatrix}$$

and

$$W_F W^{-1} = \begin{bmatrix} \frac{-1}{I}\frac{dI}{dt} & 0 & 0 & 0 & 0 & 0 \\ 0 & \frac{-1}{I}\frac{dI}{dt} & 0 & 0 & 0 & 0 \\ 0 & 0 & \frac{-1}{I}\frac{dI}{dt} & 0 & 0 & 0 \\ 0 & 0 & 0 & \frac{-1}{B}\frac{dB}{dt} & 0 & 0 \\ 0 & 0 & 0 & 0 & \frac{-1}{B}\frac{dB}{dt} & 0 \\ 0 & 0 & 0 & 0 & 0 & \frac{-1}{B}\frac{dB}{dt} \end{bmatrix}$$

Hence

$$P = W_F W^{-1} + W J^{[2]} W^{-1} = \begin{bmatrix} g_{11} & -\sigma HV & HS & -\sigma QV\frac{B}{I} & QS\frac{B}{I} & 0 \\ \sigma\left(\frac{EB}{\kappa+B} + HI\right) & g_{22} & 0 & Q(S+\sigma V)\frac{B}{I} & 0 & QS\frac{B}{I} \\ -\left(\frac{EB}{\kappa+B} + HI\right) & \phi & g_{33} & 0 & Q(S+\sigma V)\frac{B}{I} & \sigma QV\frac{B}{I} \\ 0 & \xi\frac{I}{B} & 0 & g_{44} & 0 & -HS \\ 0 & 0 & \xi\frac{I}{B} & \phi & g_{55} & -\sigma HV \\ 0 & 0 & 0 & \frac{EB}{\kappa+B} + HI & \sigma\left(\frac{EB}{\kappa+B} + HI\right) & g_{66} \end{bmatrix}$$

where

$$g_{11} = \frac{-E(S+\sigma V)}{\kappa+B}\frac{B}{I} - (1+\sigma)\left(\frac{EB}{\kappa+B} + HI\right) + T - H(S+\sigma V) - 2\mu - \phi$$

$$g_{22} = \frac{-E(S+\sigma V)}{\kappa+B}\frac{B}{I} - \left(\frac{EB}{\kappa+B} + HI\right) - \phi - \mu,$$

$$g_{33} = \frac{-E(S+\sigma V)}{\kappa+B}\frac{B}{I} - \sigma\left(\frac{EB}{\kappa+B} + HI\right) - \mu$$

$$g_{44} = -\xi\frac{I}{B} - \left(\frac{EB}{\kappa+B} + HI\right) - \phi - \mu,$$

$$g_{55} = -\xi\frac{I}{B} - \sigma\left(\frac{EB}{\kappa+B} + HI\right) - \mu$$

$$g_{66} = H(S+\sigma V) - T - \xi\frac{I}{B}$$

To proceed, we need to define a norm on $\mathbb{R}^6$. Here we use the one introduced in [19]:

$$\|z\| = \max\{U_1, U_2\},$$

where $x \in \mathbb{R}^6$, with components z_i, $1 \le i \le 6$. Also define

$$U_1(z_1, z_2, z_3) = \begin{cases} \max\{|z_1|, |z_2| + |z_3|\} & \text{if } \operatorname{sgn}(z_1) = \operatorname{sgn}(z_2) = \operatorname{sgn}(z_3) \\ \max\{|z_2|, |z_1| + |z_3|\} & \text{if } \operatorname{sgn}(z_1) = \operatorname{sgn}(z_2) = -\operatorname{sgn}(z_3) \\ \max\{|z_1|, |z_2|, |z_3|\} & \text{if } \operatorname{sgn}(z_1) = -\operatorname{sgn}(z_2) = \operatorname{sgn}(z_3) \\ \max\{|z_1|+|z_3|, |z_2| + |z_3|\} & \text{if } -\operatorname{sgn}(z_1) = \operatorname{sgn}(z_2) = \operatorname{sgn}(z_3) \end{cases}$$

$$U_2(z_4, z_5, z_6) = \begin{cases} |z_4| + |z_5| + |z_6| & \text{if } \operatorname{sgn}(z_4) = \operatorname{sgn}(z_5) = \operatorname{sgn}(z_6) \\ \max\{|z_4| + |z_5|, |z_4| + |z_6|\} & \text{if } \operatorname{sgn}(z_4) = \operatorname{sgn}(z_5) = -\operatorname{sgn}(z_6) \\ \max\{|z_5|, |z_4| + |z_6|\} & \text{if } \operatorname{sgn}(z_4) = -\operatorname{sgn}(z_5) = \operatorname{sgn}(z_6) \\ \max\{|z_4| + |z_6|, |z_5| + |z_6|\} & \text{if } -\operatorname{sgn}(z_4) = \operatorname{sgn}(z_5) = \operatorname{sgn}(z_6) \end{cases}$$

Consequently, there are 8 different cases for $\|z\|$. We discuss each case separately as follows.

Case 1: $U_1(z) > U_2(z)$ and $z_1, z_2, z_3 > 0$. Then $\|z\| = \max\{|z_1|, |z_2| + |z_3|\}$.

(i) $|z_1| > |z_2| + |z_3|$
Then $\|z\| = |z_1| = z_1$ and $U_2(z) < |z_1|$. Taking the right-hand derivative we obtain,

$$\begin{aligned} D_+\|z\| &= z_1' \\ &= g_{11}z_1 + g_{12}z_2 + g_{13}z_3 + g_{14}z_4 + g_{15}z_5 + g_{16}z_6 \\ &= \left(\frac{-E(S+\sigma V)}{\kappa+B}\frac{B}{I} - (1+\sigma)\left(\frac{EB}{\kappa+B} + HI\right) + T - H(S+\sigma V) - 2\mu - \phi\right) z_1 - \sigma HV z_2 + HS z_3 - \sigma QV\frac{B}{I}z_4 + QS\frac{B}{I}z_5 \\ &\le \left(\frac{-E(S+\sigma V)}{\kappa+B}\frac{B}{I} - (1+\sigma)\left(\frac{EB}{\kappa+B} + HI\right) + T - H(S+\sigma V) - 2\mu - \phi\right)|z_1| + HS(|z_2| + |z_3|) + Q(S+\sigma V)\frac{B}{I}(|z_4| + |z_5|) \\ &\le \left(\frac{-EB(S+\sigma V)}{(\kappa+B)^2}\frac{B}{I} - (1+\sigma)\left(\frac{EB}{\kappa+B} + HI\right) + T - \sigma HV - 2\mu - \phi\right)|z_1| \end{aligned}$$

which yields

$$D_+\|z\| \le (T - 2\mu - \phi)\|z\| \tag{55}$$

(ii) $|z_1| < |z_2| + |z_3|$
Then $\|z\| = |z_2| + |z_3|$ and $U_2(z) < |z_2| + |z_3|$. Taking the right-hand derivative we obtain,

$$\begin{aligned} D_+\|z\| &= z_2' + z_3' \\ &= (g_{21} + g_{31})z_1 + (g_{22} + g_{32})z_2 + (g_{23} + g_{33})z_3 + (g_{24} + g_{34})z_4 + (g_{25} + g_{35})z_5 + (g_{26} + g_{36})z_6 \\ &= -(1-\sigma)\left(\frac{EB}{\kappa+B} + HI\right)z_1 + \left(\frac{-E(S+\sigma V)}{\kappa+B}\frac{B}{I} - \left(\frac{EB}{\kappa+B} + HI\right) - \mu\right)z_2 + \left(\frac{-E(S+\sigma V)}{\kappa+B}\frac{B}{I} - \sigma\left(\frac{EB}{\kappa+B} + HI\right) - \mu\right)z_3 + Q(S+\sigma V)\frac{B}{I}(z_4 + z_5 + z_6) \\ &\le -(1-\sigma)\left(\frac{EB}{\kappa+B} + HI\right)|z_1| + \left(\frac{-E(S+\sigma V)}{\kappa+B}\frac{B}{I} - \sigma\left(\frac{EB}{\kappa+B} + HI\right) - \mu\right)(|z_2| + |z_3|) - (1-\sigma)\left(\frac{EB}{\kappa+B} + HI\right)|z_2| + Q(S+\sigma V)\frac{B}{I}|z_4 + z_5 + z_6| \\ &\le \left(\frac{-EB(S+\sigma V)}{(\kappa+B)^2}\frac{B}{I} - \left(\frac{EB}{\kappa+B} + HI\right) - \mu\right)(|z_2| + |z_3|) \end{aligned}$$

Hence,

$$D_+\|z\| \le -\mu\|z\| \tag{56}$$

Case 2: $U_1(z) > U_2(z)$ and $z_3 < 0 < z_1, z_2$. Then $\|z\| = \max\{|z_2|, |z_1| + |z_3|\}$.

(i) $|z_2| > |z_1| + |z_3|$
Then $\|z\| = |z_2| = z_2$ and $U_2(z) < |z_2|$. Taking the right-hand derivative we obtain,

$$\begin{aligned} D_+\|z\| &= z_2' \\ &= g_{21}z_1 + g_{22}z_2 + g_{23}z_3 + g_{24}z_4 + g_{25}z_5 + g_{26}z_6 \\ &= \sigma\left(\frac{EB}{\kappa+B} + HI\right)z_1 + \left(\frac{-E(S+\sigma V)}{\kappa+B}\frac{B}{I} - \left(\frac{EB}{\kappa+B} + HI\right) - \phi - \mu\right)z_2 + Q(S+\sigma V)\frac{B}{I}z_4 + QS\frac{B}{I}z_6 \\ &\le \sigma\left(\frac{EB}{\kappa+B} + HI\right)|z_1| + \left(\frac{-E(S+\sigma V)}{\kappa+B}\frac{B}{I} - \left(\frac{EB}{\kappa+B} + HI\right) - \phi - \mu\right)|z_2| + Q(S+\sigma V)\frac{B}{I}(|z_4| + |z_6|) \\ &\le \left(\frac{-EB(S+\sigma V)}{(\kappa+B)^2}\frac{B}{I} - (1-\sigma)\left(\frac{EB}{\kappa+B} + HI\right) - \phi - \mu\right)|z_2| \end{aligned}$$

Hence,

$$D_+\|z\| \le -\mu\|z\| \tag{57}$$

(ii) $|z_2| < |z_1| + |z_3|$
Then $\|z\| = |z_1| + |z_3| = z_1 - z_3$ and $U_2(z) < |z_1| + |z_3|$. Taking the right-hand derivative we obtain,

$$\begin{aligned} D_+\|z\| &= z_1' - z_3' \\ &= (g_{11} - g_{31})z_1 + (g_{12} - g_{32})z_2 + (g_{13} - g_{33})z_3 + (g_{14} - g_{34})z_4 + (g_{15} - g_{35})z_5 + (g_{16} - g_{36})z_6 \\ &= \left(\frac{-E(S+\sigma V)}{\kappa+B}\frac{B}{I} - \sigma\left(\frac{EB}{\kappa+B} + HI\right) + T - H(S+\sigma V) - 2\mu - \phi\right)z_1 - (\sigma HV + \phi)z_2 + \left(HS + \frac{E(S+\sigma V)}{\kappa+B}\frac{B}{I} + \sigma\left(\frac{EB}{\kappa+B} + HI\right) + \mu\right)z_3 - \sigma QV\frac{B}{I}(z_4 + z_5 + z_6) \\ &\le \left(\frac{-E(S+\sigma V)}{\kappa+B}\frac{B}{I} - \sigma\left(\frac{EB}{\kappa+B} + HI\right) + T - H(S+\sigma V) - 2\mu - \phi\right)|z_1| - (\sigma HV + \phi)|z_2| - \left(HS + \frac{E(S+\sigma V)}{\kappa+B}\frac{B}{I} + \sigma\left(\frac{EB}{\kappa+B} + HI\right) + \mu\right)|z_3| + Q(S+\sigma V)\frac{B}{I}|z_4 + z_5 + z_6| \\ &\le \left(\frac{-EB(S+\sigma V)}{(\kappa+B)^2}\frac{B}{I} - \sigma\left(\frac{EB}{\kappa+B} + HI\right) - HS - \mu\right)(|z_1| + |z_3|) + (T - \sigma HV - \mu - \phi)|z_1| \\ &\le \max\{-\mu, T - 2\mu - \phi\}(|z_1| + |z_3|) \end{aligned}$$

Hence,

$$D_+\|z\| \le \max\{-\mu, T - 2\mu - \phi\}\|z\| \tag{58}$$

Case 3: $U_1(z) > U_2(z)$ and $z_2 < 0 < z_1, z_3$. Then $\|z\| = \max\{|z_1|, |z_2|, |z_3|\}$.

(i) $|z_1| > |z_2|, |z_3|$

Then $\|z\| = |z_1| = z_1$ and $U_2(z) < |z_1|$. Taking the right-hand derivative we obtain,

$$\begin{aligned}
D_+\|z\| &= z_1' \\
&= g_{11}z_1 + g_{12}z_2 + g_{13}z_3 + g_{14}z_4 + g_{15}z_5 + g_{16}z_6 \\
&= \left(\frac{-E(S+\sigma V)}{\kappa+B}\frac{B}{I} - (1+\sigma)\left(\frac{EB}{\kappa+B}+HI\right)\right. \\
&\quad \left. +T - H(S+\sigma V) - 2\mu - \phi\right) z_1 \\
&\quad -\sigma HVz_2 + HSz_3 - \sigma QV\frac{B}{I}z_4 + QS\frac{B}{I}z_5 \\
&\le \left(\frac{-E(S+\sigma V)}{\kappa+B}\frac{B}{I} - (1+\sigma)\left(\frac{EB}{\kappa+B}+HI\right)\right. \\
&\quad \left. +T - H(S+\sigma V) - 2\mu - \phi\right) |z_1| \\
&\quad +\sigma HV|z_2| + HS|z_3| + Q(S+\sigma V)\frac{B}{I}(|z_4|+|z_5|) \\
&\le \left(\frac{-EB(S+\sigma V)}{(\kappa+B)^2}\frac{B}{I} - (1+\sigma)\left(\frac{EB}{\kappa+B}+HI\right)\right. \\
&\quad \left. +T - 2\mu - \phi\right) |z_1|
\end{aligned}$$

Hence,

$$D_+\|z\| \le (T - 2\mu - \phi)\|z\| \tag{59}$$

(ii) $|z_2| > |z_1|, |z_3|$
Then $\|z\| = |z_2| = -z_2$ and $U_2(z) < |z_2|$. Taking the right-hand derivative we obtain,

$$\begin{aligned}
D_+\|z\| &= -z_2' \\
&= -g_{21}z_1 - g_{22}z_2 - g_{23}z_3 - g_{24}z_4 - g_{25}z_5 - g_{26}z_6 \\
&= -\sigma\left(\frac{EB}{\kappa+B}+HI\right) z_1 \\
&\quad -\left(\frac{-E(S+\sigma V)}{\kappa+B}\frac{B}{I} - \left(\frac{EB}{\kappa+B}+HI\right) - \phi - \mu\right) z_2 \\
&\quad -Q(S+\sigma V)\frac{B}{I}z_4 - QS\frac{B}{I}z_6 \\
&\le -\sigma\left(\frac{EB}{\kappa+B}+HI\right)|z_1| \\
&\quad +\left(\frac{-E(S+\sigma V)}{\kappa+B}\frac{B}{I} - \left(\frac{EB}{\kappa+B}+HI\right) - \phi - \mu\right)|z_2| \\
&\quad +Q(S+\sigma V)\frac{B}{I}(|z_4|+|z_6|) \\
&\le \left(\frac{-EB(S+\sigma V)}{(\kappa+B)^2}\frac{B}{I} - \left(\frac{EB}{\kappa+B}+HI\right) - \phi - \mu\right)|z_2|
\end{aligned}$$

Hence,

$$D_+\|z\| \le -\mu\|z\| \tag{60}$$

(iii) $|z_3| > |z_1|, |z_2|$
Then $\|z\| = |z_3| = z_3$ and $U_2(z) < |z_3|$. Taking the right-hand derivative we obtain,

$$\begin{aligned}
D_+\|z\| &= z_3' \\
&= g_{31}z_1 + g_{32}z_2 + g_{33}z_3 + g_{34}z_4 + g_{35}z_5 + g_{36}z_6 \\
&= -\left(\frac{EB}{\kappa+B}+HI\right) z_1 + \phi z_2 \\
&\quad +\left(\frac{-E(S+\sigma V)}{\kappa+B}\frac{B}{I} - \sigma\left(\frac{EB}{\kappa+B}+HI\right) - \mu\right) z_3 \\
&\quad +Q(S+\sigma V)\frac{B}{I}z_5 + \sigma QV\frac{B}{I}z_6 \\
&\le -\left(\frac{EB}{\kappa+B}+HI\right)|z_1| - \phi|z_2| \\
&\quad +\left(\frac{-E(S+\sigma V)}{\kappa+B}\frac{B}{I} - \sigma\left(\frac{EB}{\kappa+B}+HI\right) - \mu\right)|z_3| \\
&\quad +Q(S+\sigma V)\frac{B}{I}(|z_5|+|z_6|) \\
&\le \left(\frac{-EB(S+\sigma V)}{(\kappa+B)^2}\frac{B}{I} - \sigma\left(\frac{EB}{\kappa+B}+HI\right) - \mu\right)|z_3|
\end{aligned}$$

Hence,

$$D_+\|z\| \le -\mu\|z\| \tag{61}$$

Case 4: $U_1(z) > U_2(z)$ and $z_1 < 0 < z_2, z_3$. Then $\|z\| = \max\{|z_1| + |z_3|, |z_2| + |z_3|\}$.

(i) $|z_1| > |z_2|$
Then $\|z\| = |z_1| + |z_3| = -z_1 + z_3$ and $U_2(z) < |z_1| + |z_3|$. Taking the right-hand derivative we obtain,

$$\begin{aligned}
D_+\|z\| &= -z_1' + z_3' \\
&= (g_{31} - g_{11})z_1 + (g_{32} - g_{12})z_2 + (g_{33} - g_{13})z_3 \\
&\quad +(g_{34} - g_{14})z_4 + (g_{35} - g_{15})z_5 + (g_{36} - g_{16})z_6 \\
&= \left(\frac{E(S+\sigma V)}{\kappa+B}\frac{B}{I} + \sigma\left(\frac{\sigma EB}{\kappa+B}+HI\right) - T + H(S+\sigma V) + 2\mu + \phi\right) z_1 \\
&\quad +(\sigma HV + \phi)z_2 + \left(\frac{-E(S+\sigma V)}{\kappa+B}\frac{B}{I} - \sigma\left(\frac{EB}{\kappa+B}+HI\right) - HS - \mu\right) z_3 \\
&\quad +\sigma QV\frac{B}{I}(z_4 + z_5 + z_6) \\
&\le -\left(\frac{E(S+\sigma V)}{\kappa+B}\frac{B}{I} + \sigma\left(\frac{\sigma EB}{\kappa+B}+HI\right) - T + H(S+\sigma V) + 2\mu + \phi\right)|z_1| \\
&\quad +(\sigma HV + \phi)|z_2| + \left(\frac{-E(S+\sigma V)}{\kappa+B}\frac{B}{I} - \sigma\left(\frac{EB}{\kappa+B}+HI\right) - HS - \mu\right)|z_3| \\
&\quad +Q(S+\sigma V)\frac{B}{I}|z_4 + z_5 + z_6| \\
&\le \left(\frac{-EB(S+\sigma V)}{(\kappa+B)^2}\frac{B}{I} - \sigma\left(\frac{EB}{\kappa+B}+HI\right) - HS - \mu\right)(|z_1| + |z_3|) \\
&\quad +(T - \sigma HV - \mu - \phi)|z_1| + (\sigma HV + \phi)|z_2| \\
&\le \left(\frac{-EB(S+\sigma V)}{(\kappa+B)^2}\frac{B}{I} - \sigma\left(\frac{EB}{\kappa+B}+HI\right) - HS - \mu\right)(|z_1| + |z_3|) \\
&\quad +(T - \mu)|z_1| \\
&\le \left(\frac{-EB(S+\sigma V)}{(\kappa+B)^2}\frac{B}{I} - \sigma\left(\frac{EB}{\kappa+B}+HI\right) + T - HS - 2\mu\right)(|z_1| + |z_3|)
\end{aligned}$$

Hence,

$$D_+\|z\| \le (T - 2\mu)\|z\| \tag{62}$$

(ii) $|z_1| < |z_2|$
Then $\|z\| = |z_2| + |z_3| = z_2 + z_3$ and $U_2(z) < |z_2| + |z_3|$. Taking the right-hand derivative we obtain,

$$\begin{aligned}
D_+\|z\| &= z_2' + z_3' \\
&= (g_{21} + g_{31})z_1 + (g_{22} + g_{32})z_2 + (g_{23} + g_{33})z_3 \\
&\quad +(g_{24} + g_{34})z_4 + (g_{25} + g_{35})z_5 + (g_{26} + g_{36})z_6 \\
&= -(1-\sigma)\left(\frac{EB}{\kappa+B}+HI\right) z_1 \\
&\quad +\left(\frac{-E(S+\sigma V)}{\kappa+B}\frac{B}{I} - \left(\frac{EB}{\kappa+B}+HI\right) - \mu\right) z_2 \\
&\quad +\left(\frac{-E(S+\sigma V)}{\kappa+B}\frac{B}{I} - \sigma\left(\frac{EB}{\kappa+B}+HI\right) - \mu\right) z_3 \\
&\quad +Q(S+\sigma V)\frac{B}{I}(z_4 + z_5 + z_6) \\
&\le (1-\sigma)\left(\frac{EB}{\kappa+B}+HI\right)|z_1| \\
&\quad +\left(\frac{-E(S+\sigma V)}{\kappa+B}\frac{B}{I} - \left(\frac{EB}{\kappa+B}+HI\right) - \mu\right)|z_2| \\
&\quad +\left(\frac{-E(S+\sigma V)}{\kappa+B}\frac{B}{I} - \sigma\left(\frac{EB}{\kappa+B}+HI\right) - \mu\right)|z_3| \\
&\quad +Q(S+\sigma V)\frac{B}{I}|z_4 + z_5 + z_6| \\
&\le (1-\sigma)\left(\frac{EB}{\kappa+B}+HI\right)|z_1|
\end{aligned}$$

$$+\left(\frac{-EB(S+\sigma V)}{(\kappa+B)^2}\frac{B}{I}-\sigma\left(\frac{EB}{\kappa+B}+HI\right)-\mu\right)(|z_2|+|z_3|)$$
$$-(1-\sigma)\left(\frac{EB}{\kappa+B}+HI\right)|z_2|$$
$$\le\left(\frac{-EB(S+\sigma V)}{(\kappa+B)^2}\frac{B}{I}-\sigma\left(\frac{EB}{\kappa+B}+HI\right)-\mu\right)(|z_2|+|z_3|)$$

Hence,

$$D_+\|z\| \le -\mu\|z\| \tag{63}$$

Case 5: $U_2(z) > U_1(z)$ and $z_4, z_5, z_6 > 0$.
Then $\|z\| = |z_4| + |z_5| + |z_6| = z_4 + z_5 + z_6$ and $U_1(z) < |z_4| + |z_5| + |z_6|$. Taking the right-hand derivative we obtain,

$$\begin{aligned}D_+\|z\| &= z_4' + z_5' + z_6'\\ &= (g_{41}+g_{51}+g_{61})z_1 + (g_{42}+g_{52}+g_{62})z_2\\ &\quad +(g_{43}+g_{53}+g_{63})z_3 + (g_{44}+g_{54}+g_{64})z_4\\ &\quad +(g_{45}+g_{55}+g_{65})z_5 + (g_{46}+g_{56}+g_{66})z_6\\ &= \xi\frac{I}{B}(z_2+z_3) + \left(-\xi\frac{I}{B}-\mu\right)z_4\\ &\quad +\left(-\xi\frac{I}{B}-\mu\right)z_5 + \left(-T-\xi\frac{I}{B}\right)z_6\\ &\le \xi\frac{I}{B}|z_2+z_3| + \left(-\xi\frac{I}{B}-\mu\right)(|z_4|+|z_5|) + \left(-T-\xi\frac{I}{B}\right)|z_6|\\ &\le -\mu(|z_4|+|z_5|) - T|z_6|\\ &\le -\mu(|z_4|+|z_5|+|z_6|)\end{aligned}$$

Hence,

$$D_+\|z\| \le -\mu\|z\| \tag{64}$$

Case 6: $U_2(z) > U_1(z)$ and $z_6 < 0 < z_4, z_5$. Then $\|z\| = \max\{|z_4| + |z_5|, |z_4| + |z_6|\}$.

(i) $|z_5| > |z_6|$
Then $\|z\| = |z_4| + |z_5| = z_4 + z_5$ and $U_1(z) < |z_4| + |z_5|$. Taking the right-hand derivative to obtain,

$$\begin{aligned}D_+\|z\| &= z_4' + z_5'\\ &= (g_{41}+g_{51})z_1 + (g_{42}+g_{52})z_2 + (g_{43}+g_{53})z_3\\ &\quad +(g_{44}+g_{54})z_4 + (g_{45}+g_{55})z_5 + (g_{46}+g_{56})z_6\\ &= \xi\frac{I}{B}(z_2+z_3) + \left(-\xi\frac{I}{B}-\left(\frac{EB}{\kappa+B}+HI\right)-\mu\right)z_4\\ &\quad +\left(-\xi\frac{I}{B}-\sigma\left(\frac{EB}{\kappa+B}+HI\right)-\mu\right)z_5 - H(S+\sigma V)z_6\\ &\le \xi\frac{I}{B}|z_2+z_3| + \left(-\xi\frac{I}{B}-\sigma\left(\frac{EB}{\kappa+B}+HI\right)-\mu\right)(|z_4|+|z_5|)\\ &\quad -(1-\sigma)\left(\frac{EB}{\kappa+B}+HI\right)|z_4| + H(S+\sigma V)|z_6|\\ &\le \left(-\sigma\left(\frac{EB}{\kappa+B}+HI\right)+H(S+\sigma V)-\mu\right)(|z_4|+|z_5|)\end{aligned}$$

Noting that $\sigma \le 1$ and $S + \sigma V \le N$, we thus have

$$D_+\|z\| \le (H(S+\sigma V)-\mu)\|z\| \le (HN-\mu)\|z\| \tag{65}$$

(ii) $|z_5| < |z_6|$
Then $\|z\| = |z_4| + |z_6| = z_4 - z_6$ and $U_1(z) < |z_4| + |z_6|$. Taking the right-hand derivative we obtain,

$$\begin{aligned}D_+\|z\| &= z_4' - z_6'\\ &= (g_{41}-g_{61})z_1 + (g_{42}-g_{62})z_2 + (g_{43}-g_{63})z_3\\ &\quad +(g_{44}-g_{64})z_4 + (g_{45}-g_{65})z_5 + (g_{46}-g_{66})z_6\\ &= \xi\frac{I}{B}z_2 + \left(-\xi\frac{I}{B}-2\left(\frac{EB}{\kappa+B}+HI\right)-\phi-\mu\right)z_4\\ &\quad -\sigma\left(\frac{EB}{\kappa+b}+HI\right)z_5 - \left(HS+H(S+\sigma V)-T-\xi\frac{I}{B}\right)z_6\\ &\le \xi\frac{I}{B}|z_2| + \left(-\xi\frac{I}{B}-2\left(\frac{EB}{\kappa+B}+HI\right)-\phi-\mu\right)|z_4|\\ &\quad -\sigma\left(\frac{EB}{\kappa+b}+HI\right)|z_5| + \left(HS+H(S+\sigma V)-T-\xi\frac{I}{B}\right)|z_6|\\ &\le \left(-2\left(\frac{EB}{\kappa+B}+HI\right)-\phi-\mu\right)|z_4|\\ &\quad -\sigma\left(\frac{EB}{\kappa+b}+HI\right)|z_5| + (HS+H(S+\sigma V)-T)|z_6|\\ &\le \max\{-\mu, HS+H(S+\sigma V)-T\}(|z_4|+|z_6|)\end{aligned}$$

Hence,

$$\begin{aligned}D_+\|z\| &\le \max\{-\mu, HS+H(S+\sigma V)-T\}\|z\|\\ &\le \max\{-\mu, 2HN-T\}\|z\|\end{aligned} \tag{66}$$

Case 7: $U_2(z) > U_1(z)$ and $z_5 < 0 < z_4, z_6$. Then $\|z\| = \max\{|z_5|, |z_4| + |z_6|\}$.

(i) $|z_5| > |z_4| + |z_6|$
Then $\|z\| = |z_5| = -z_5$ and $U_1(z) < |z_5|$. Taking the right-hand derivative we obtain,

$$\begin{aligned}D_+\|z\| &= -z_5'\\ &= -g_{51}z_1 - g_{52}z_2 - g_{53}z_3 - g_{54}z_4 - g_{55}z_5 - g_{56}z_6\\ &= -\xi\frac{I}{B}z_3 - \phi z_4 - \left(-\xi\frac{I}{B}-\sigma\left(\frac{EB}{\kappa+B}+HI\right)-\mu\right)z_5\\ &\quad +\sigma HVz_6\\ &\le \xi\frac{I}{B}|z_3| - \phi|z_4| + \left(-\xi\frac{I}{B}-\sigma\left(\frac{EB}{\kappa+B}+HI\right)-\mu\right)|z_5|\\ &\quad +\sigma HV|z_6|\\ &\le \sigma HV(|z_4|+|z_6|) + \left(-\sigma\left(\frac{EB}{\kappa+B}+HI\right)-\mu\right)|z_5|\\ &\le \left(-\sigma\left(\frac{EB}{\kappa+B}+HI\right)+\sigma HV-\mu\right)|z_5|\end{aligned}$$

Hence,

$$D_+\|z\| \le (\sigma HV-\mu)\|z\| \le (HN-\mu)\|z\| \tag{67}$$

(ii) $|z_5| < |z_4| + |z_6|$
Then $\|z\| = |z_4| + |z_6| = z_4 + z_6$ and $U_1(z) < |z_4| + |z_6|$. Taking the right-hand derivative we obtain,

$$\begin{aligned}D_+\|z\| &= z_4' + z_6'\\ &= (g_{41}+g_{61})z_1 + (g_{42}+g_{62})z_2 + (g_{43}+g_{63})z_3\\ &\quad +(g_{44}+g_{64})z_4 + (g_{45}+g_{65})z_5 + (g_{46}+g_{66})z_6\\ &= \xi\frac{I}{B}z_2 + \left(-\xi\frac{I}{B}-\phi-\mu\right)z_4 + \sigma\left(\frac{EB}{\kappa+B}+HI\right)z_5\\ &\quad +\left(\sigma HV-T-\xi\frac{I}{B}\right)z_6\\ &\le \xi\frac{I}{B}|z_2| + \left(-\xi\frac{I}{B}-\phi-\mu\right)|z_4| - \sigma\left(\frac{EB}{\kappa+B}+HI\right)|z_5|\\ &\quad +\left(\sigma HV-T-\xi\frac{I}{B}\right)|z_6|\end{aligned}$$

$$\leq (-\phi-\mu)|z_4| - \sigma\left(\frac{EB}{\kappa+B}+HI\right)|z_5| + (\sigma HV - T)|z_6|$$
$$\leq \max\{-\mu, \sigma HV - T\}(|z_4| + |z_6|)$$

Hence,

$$D_+\|z\| \leq \max\{-\mu, \sigma HV - T\}\|z\| \leq \max\{-\mu, HN - T\}\|z\| \tag{68}$$

Case 8: $U_2(z) > U_1(z)$ and $z_4 < 0 < z_5, z_6$. Then $\|z\| = \max\{|z_4| + |z_6|, |z_5| + |z_6|\}$.

(i) $|z_4| > |z_5|$

Then $\|z\| = |z_4| + |z_6| = -z_4 + z_6$ and $U_1(z) < |z_4| + |z_6|$. Taking the right-hand derivative we obtain,

$$\begin{aligned}
D_+\|z\| &= -z_4' + z_6' \\
&= (g_{61} - g_{41})z_1 + (g_{62} - g_{42})z_2 + (g_{63} - g_{43})z_3 \\
&\quad + (g_{64} - g_{44})z_4 + (g_{65} - g_{45})z_5 + (g_{66} - g_{46})z_6 \\
&= -\xi\frac{I}{B}z_2 - \left(-\xi\frac{I}{B} - 2\left(\frac{EB}{\kappa+B}+HI\right) - \phi - \mu\right)z_4 \\
&\quad + \sigma\left(\frac{EB}{\kappa+B}+HI\right)z_5 + \left(HS + H(S+\sigma V) - T - \xi\frac{I}{B}\right)z_6 \\
&\leq \xi\frac{I}{B}|z_2| + \left(-\xi\frac{I}{B} - 2\left(\frac{EB}{\kappa+B}+HI\right) - \phi - \mu\right)|z_4| \\
&\quad + \sigma\left(\frac{EB}{\kappa+B}+HI\right)|z_5| \\
&\quad + \left(HS + H(S+\sigma V) - T - \xi\frac{I}{B}\right)|z_6| \\
&\leq \left(-2\left(\frac{EB}{\kappa+B}+HI\right) - \phi - \mu\right)|z_4| \\
&\quad + \sigma\left(\frac{EB}{\kappa+B}+HI\right)|z_5| + (HS + H(S+\sigma V) - T)|z_6| \\
&\leq \left((-2+\sigma)\left(\frac{EB}{\kappa+B}+HI\right) - \phi - \mu\right)|z_4| \\
&\quad + (HS + H(S+\sigma V) - T)|z_6| \\
&\leq \max\{-\mu, HS + H(S+\sigma V) - T\}(|z_4| + |z_6|)
\end{aligned}$$

Hence,

$$\begin{aligned}
D_+\|z\| &\leq \max\{-\mu, HS + H(S+\sigma V) - T\}\|z\| \\
&\leq \max\{-\mu, 2HN - T\}\|z\|
\end{aligned} \tag{69}$$

(ii) $|z_4| < |z_5|$

Then $\|z\| = |z_5| + |z_6| = z_5 + z_6$ and $U_1(z) < |z_5| + |z_6|$. Taking the right-hand derivative we obtain,

$$\begin{aligned}
D_+\|z\| &= z_5' + z_6' \\
&= (g_{51} + g_{61})z_1 + (g_{52} + g_{62})z_2 + (g_{53} + g_{63})z_3 \\
&\quad + (g_{54} + g_{64})z_4 + (g_{55} + g_{65})z_5 + (g_{56} + g_{66})z_6 \\
&= \xi\frac{I}{B}z_3 + \left(\phi + \left(\frac{EB}{\kappa+B}+HI\right)\right)z_4 + \left(-\xi\frac{I}{B} - \mu\right)z_5 \\
&\quad + \left(HS - T - \xi\frac{I}{B}\right)z_6 \\
&\leq \xi\frac{I}{B}|z_3| - \left(\phi + \left(\frac{EB}{\kappa+B}+HI\right)\right)|z_4| \\
&\quad + \left(-\xi\frac{I}{B} - \mu\right)|z_5| + (HS - T - \xi\frac{I}{B})|z_6| \\
&\leq -\left(\phi + \left(\frac{EB}{\kappa+B}+HI\right)\right)|z_4| - \mu|z_5| + (HS - T)|z_6| \\
&\leq -\mu|z_5| + (HS - T)|z_6| \\
&\leq \max\{-\mu, HS - T\}(|z_5| + |z_6|)
\end{aligned}$$

Hence,

$$D_+\|z\| \leq \max\{-\mu, HS - T\}\|z\| \leq \max\{-\mu, HN - T\}\|z\| \tag{70}$$

We now summarize our results from the analysis above. To ensure $m(P) < 0$, from Cases 1–5 we need

$$T - 2\mu < 0; \tag{71}$$

and from Cases 6–8 we need

$$HN - \mu < 0 \quad \text{and} \quad 2HN - T < 0 \tag{72}$$

Using the condition (71), the inequalities in (72) yield

$$N < \min\left\{\frac{T}{2H}, \frac{\mu}{H}\right\} = \frac{T}{2H} \tag{73}$$

Hence, we conclude from Theorem 10 that under the conditions (71) and (73), the endemic equilibrium of the model (1) with constant controls is globally asymptotically stable when $\mathcal{R}_0 > 1$.

References

[1] J.R. Andrews, S. Basu, Transmission dynamics and control of cholera in haiti: an epidemic model, Lancet 377 (2011) 1248–1255.
[2] E. Asano, L.J. Gross, S. Lenhart, L.A. Real, Optimal control of vaccine distribution in a rabies metapopulation model, Math. Biosci. Eng. 5 (2008) 219–238.
[3] E. Bertuzzo, et al., Prediction of the spatial evolution and effects of control measures for the unfolding haiti cholera outbreak, Geophys. Res. Lett. 38 (2011) L06403.
[4] S.M. Blower, H. Dowlatabadi, Sensitivity and uncertainty analysis of complex models of disease transmission: an hiv model, as an example, Int. Stat. Rev. 62 (1994) 229–243.
[5] B. Buonomo, A simple analysis of vaccination strategies for rubella, Math. Biosci. Eng. 8 (2011) 677–687.
[6] G.J. Butler, P. Waltman, Persistence in dynamical systems, Proc. Am. Math. Soc. 96 (1986) 425–430.
[7] V. Capasso, S.L. Paveri-Fontana, A mathematical model for the 1973 cholera epidemic in the european mediterranean region, Rev. Dépidémol. Publ. 27 (1979) 121–132.
[8] C. Castillo-Chavez, Z. Feng, W. Huang, On the computation of $\mathcal{R}_0$ and its role on global stability, Mathematical Approaches for Emerging and\ Reemerging Infectious Diseases: An Introduction, IMA vol. 125, Springer-Verlag, 2002.
[9] C. Castillo-Chavez, B. Song, Dynamical models of tuberculosis and their applications, Math. Biosci. Eng. 1 (2004) 361–404.
[10] D.L. Chao, M.E. Halloran, I.M. Longini, Vaccination strategies for epidemic cholera in haiti with implications for the developing world, Proc. Natl. Acad. Sci. U.S.A. 108 (2011) 7081–7085.
[11] Cholera vaccines: who position paper, WKly Epidemiol. Rec. 85 (117–128) (2010).
[12] C.T. Codeço, Endemic and epidemic dynamics of cholera: the role of the aquatic reservoir, BMC Infect. Dis. 1 (2001) 1.
[13] W.A. Coppel, Stability and Asymptotic Behavior of Differential Equations, Heath Mathematical Monographs, DC Heath, Boston, 1965.
[14] S. Cumberland, An old enemy returns, Bull. World Health Organ. 87 (2009) 85–86.
[15] K.A. Date, et al., Consideration for oral cholera vaccine use during outbreak after earthquake in haiti, 2010–2011, Emerg. Infect. Dis. 17 (11) (2011).
[16] K.R. Fister, S. Lenhart, J.S. McNally, Optimizing chemotheapy in an hiv model, Electron. J. Differ. Equ. 32 (1998) 1–12.
[17] W.H. Fleming, R.W. Rishel, Deterministic and Stochastic Optimal Control, Springer, New York, 1975.
[18] H.I. Freedman, S. Ruan, M. Tang, Uniform persistence and flows near a closed positively invariant set, J. Dyn. Differ. Eq. 6 (1994) 583–600.
[19] A.B. Gumel, C.C. McCluskey, J. Watmough, An SVEIR model assessing potential impact of an imperfect anti-SARS vaccine, Math. Biosci. Eng. 3 (2006) 485–512.
[20] D.M. Hartley, J.G. Morris, D.L. Smith, Hyperinfectivity: a critical element in the ability of v. cholerae to cause epidemics? PLoS Med. 3 (2006) 0063–0069.
[21] C.M. Kribs-Zaleta, J.X. Velasco-Hernandez, A simple vaccination model with multiple endemic states, Math. Biosci. 164 (2000) 183–201.
[22] R.I. Joh, H. Wang, H. Weiss, J.S. Weitz, Dynamics of indirectly transmitted infectious diseases with immunological threshold, Bull. Math. Biol. 71 (2009) 845–862.
[23] H.R. Joshi, Optimal control of an hiv immunology model, Optim. Control Appl. Methods 23 (2002) 199–213.
[24] E. Jung, S. Lenhart, Z. Feng, Optimal control of treatments in a two-strain tuberculosis model, Discrete Contin. Dyn. Syst., Ser. B 2 (4) (2002) 473–482.
[25] D. Kirschner, G.F. Webb, A model for treatment strategy in the chemotherapy of aids, Bull. Math. Biol. 58 (2) (1996) 367–390.
[26] S. S. Lenhart, J. Workman, Optimal control applied to biological models, Chapman Hall/CRC, 2007.
[27] M.Y. Li, J.R. Graef, L. Wang, J. Karsai, Global dynamics of a seir model with varying total population size, Math. Biosci. 160 (1999) 191–213.
[28] M.Y. Li, J.S. Muldowney, A geometirc approach to global-stability problems, SIAM J. Mathe. Anal. 27 (1996) 1070–1083.
[29] M.Y. Li, H.L. Smith, L. Wang, Global dynamics of an seir epidemic model with vertical transmission, SIAM J. Math. Anal. 62 (2001) 58–69.
[30] S. Liao, J. Wang, Stability analysis and application of a mathematical cholera model, Math. Biosci. Eng. 8 (2011) 733–752.
[31] P.R. Mason, Zimbabwe experiences the worst epidemic of cholera in africa, J. Infect. Dev. Ctries. 3 (2009) 148–151.

[32] D.S. Merrell, et al., Host-induced epidemic spread of the cholera bacterium, Nature 417 (2002) 642–645.
[33] J.G. Morris Jr., Cholera: modern pandemic disease of ancient lineage, Emerg. Infect. Dis. 17 (11) (2011).
[34] Z. Mukandavire, S. Liao, J. Wang, H. Gaff, D.L. Smith, J.G. Morris, Estimating the reproductive numbers for the 2008-2009 cholera outbreaks in zimbabwe, Proc. Nat. Acad. Sci. U.S.A. 108 (2011) 8767–8772.
[35] S. Marino, I. Hogue, C.J. Ray, D.E. Kirschner, A methodology for performing global uncertainty and sensitivity analysis in system biology, J. Theor. Biol. 254 (2008) 178–196.
[36] G.B. Nair, et al., New variants of Vibrio cholerae O1 biotype El Tor with attributes of the classical biotype from hospitalized patients with acute diarrhea in bangladesh, J. Clin. Microbiol. 40 (2002) 3296–3299.
[37] R.L.M. Neilan, E. Schaefer, H. Gaff, K.R. Fister, S. Lenhart, Modeling optimal intervention strategies for cholera, Bull. Math. Biol. 72 (2010) 2004–2018.
[38] E.J. Nelson, J.B. Harris, J.G. Morris, S.B. Calderwood, A. Camilli, Cholera transmission: the host, pathogen and bacteriophage dynamics, Nat. Rev.: Microbiol. 7 (2009) 693–702.
[39] L.S. Pontryagin, V.G. Boltyanski, R.V. Gamkrelize, E.F. Mishchenko, The Mathematical Theory of Optimal Processes, Wiley, New York, 1967.
[40] A. Safa, G.B. Nair, R.Y.C. Kong, Evolution of new variants of Vibrio cholerae O1, Trends Microbiol. 18 (2010) 46–54.
[41] S. Shin, S.N. Desai, B.K. Sah, J.D. Clemence, Oral vaccines against cholera, Clin. Infect. Dis. 52 (11) (2011) 1343–1349.
[42] Z. Shuai, J.H. Tien, P. van den Driessche, Cholera models with hyperinfectivity and temporary immunity, Bull. Math. Biol 74 (2012) 2423–2445.
[43] Z. Shuai, P. van den Driessche, Global dynamics of cholera models with differential infectivity, Math. Biosci. 234 (2011) 118–126.
[44] Z. Shuai, P. van den Driessche, Global stability of infectious disease models using lyapunov functions, SIAM J. Appl. Math. 73 (2013) 1513–1532.
[45] J.P. Tian, J. Wang, Global stability for cholera epidemic models, Math. Biosci. 232 (2011) 31–41.
[46] J.H. Tien, D.J.D. Earn, Multiple transmission pathways and disease dynamics in a waterborne pathogen model, Bull. Math. Biol. 72 (2010) 1502–1533.
[47] A.L. Tuite, et al., Cholera epidemic in haiti, 2010: Using a transmission model to explain spatial spread of disease and identify optimal control interventions, Ann. Intern. Med. 154 (2011) 293–302.
[48] P. van den Driessche, J. Watmough, Reproduction numbers and sub-threshold endemic equilibria for compartmental models of disease transmission, Math. Biosci. 180 (2002) 29–48.
[49] J. Wang, S. Liao, A generalized cholera model and epidemic-endemic analysis, J. Biol. Dyn. 6 (2) (2012) 568–589.
[50] X. Zhou, J. Cui, Z. Zhang, Global results for a cholera model with imperfect vaccination, J. Franklin Int. 349 (2012) 770–791.
[51] Center for Disease Control and Prevention, web page: www.cdc.gov.
[52] World Health Organization (WHO), web page: www.who.org.
[53] WHO Cholera-fact sheet number 107: February 2014. http://www.who.int/mediacentre/factsheets/fs107/en/.
[54] WHO report on global surveillance of epidemic-prone infectious diseases, 2000, pp. 39–54. http://www.who.int/csr/resources/publications/surveillance/WHO_Report_Infectious_Diseases.pdf.

กองกลาง สำนักงานอธิการบดี
เลขรับ 16997
วันที่ 12 ต.ค. 2558
เวลา 15.52

R2557C095

บันทึกข้อความ

คณะวิทยาศาสตร์ มหาวิทยาลัยนเรศวร
เลขรับ 12491
วันที่ 28 ก.ย. 2558
เวลา 15.12

ส่วนราชการ คณะวิทยาศาสตร์ ภาควิชา คณิตศาสตร์ โทร. 3202
ที่ ศธ 0527. 04.01(7)/ 887 วันที่ 28 กันยายน 2558
เรื่อง ขอปิดโครงการวิจัยและส่งผลงานตามตัวชี้วัด

กองบริหารการวิจัย
รับที่ 5212
วันที่ 29 ก.ย. 2558
เวลา 16:12น.

(1) เรียน อธิการบดี

ตามที่ มหาวิทยาลัยอนุมัติให้ทุนอุดหนุนการวิจัยจากงบงบประมาณรายได้ กองทุนวิจัยมหาวิทยาลัยนเรศวร ประจำปีงบประมาณ พ.ศ. 2557 สัญญาเลขที่ R2557C095 เรื่อง แบบจำลองคณิตศาสตร์สำหรับโรคอหิวา และการศึกษาการควบคุมการแพร่ระบาด ในวงเงิน 180,000.00 บาท (หนึ่งแสนแปดหมื่นบาทถ้วน) โดยมี ดร.ชัยรัตน์ มดนาค สังกัดคณะ คณะวิทยาศาสตร์ เป็นหัวหน้าโครงการ นั้น

ขณะนี้ได้ดำเนินการมาเป็นระยะเวลา 1 ปี 6 เดือน และมีผลงานวิจัยตามตัวชี้วัดความสำเร็จของโครงการวิจัย (รายละเอียดดังเอกสารที่แนบมาพร้อมนี้) และเพื่อให้ผลงานทางวิชาการของข้าพเจ้าเป็นประโยชน์ต่อการศึกษาและสาธารณชน ข้าพเจ้าอนุญาตให้กองบริหารการวิจัยและสำนักหอสมุดเผยแพร่ผลงานวิจัยฉบับสมบูรณ์และบทคัดย่อ ในระบบสารสนเทศ ดังนี้

☑ ระบบผลงานวิจัยฉบับสมบูรณ์ (http://dra-is.research.nu.ac.th/dra-elibrary/)
☑ ฐานข้อมูล NU Digital Repository (http://obj.lib.nu.ac.th/media)
☐ ไม่ยินยอม เนื่องจาก.....

ดังนั้นผู้วิจัยจึงขอปิดโครงการวิจัยดังกล่าว และหากมีผลงานวิจัยเกิดขึ้นภายหลังจักนำแจ้งให้มหาวิทยาลัยทราบทันที

จึงเรียนมาเพื่อโปรดพิจารณาอนุมัติ

งานธุรการ (หน่วยสัญญา)
☑ ตรวจสอบและคุมยอด - 9 ต.ค. 2558
☐ ระบบบริหารโครงการวิจัย 15 ต.ค. 2558
☐ ระบบ NRPM.....

.....
ดร.ชัยรัตน์ มดนาค
หัวหน้าโครงการวิจัย

(2) เรียน อธิการบดี
เห็นควรอนุมัติ และให้ดำเนินการบันทึกข้อมูล

ลงชื่อ .....
(นางสาวสุชีลา พุ่มอยู่)
หัวหน้างานวิจัยและบริการวิชาการ
ผู้ประสานงานวิจัยคณะ
(วันที่ 28 ก.ย. 2558

(4) เรียน อธิการบดี
(/) เห็นควรอนุมัติ ( ) เห็นควรไม่อนุมัติ

ลงชื่อ .....
(นางสาวสิริกร ชูแก้ว)
ผอ.กองบริหารการวิจัย
(วันที่ 12 ต.ค. 2558

- 9 ต.ค. 2558
12 ต.ค. 2558